Item marked with *** have to be changed later. It is a reference where the article is in press and final volume is not known.

Glaciation or not? An analytic review of features of glaciation and sediment gravity flows: introducing a methodology for field research

Mats O. Molén

Umeå FoU AB, Vallmov 61, S-903 52 Umeå, Sweden

Table of contents

ABSTRACT

For more than 150 years, geological features claimed to be evidence for pre-Pleistocene glaciations have been debated. Advancements in recent decades, in understanding features generated by glacial and mass flow processes, are here reviewed. It is timely to make renewed comparisons and to re-visit the interpretations of data used to support pre-Pleistocene glaciations. Similarities and differences of Quaternary glaciogenic and sediment gravity flow features, which are most often referred to as proxies and evidence of ancient glaciations, are documented, discussed and closely examined, in order to uncover the origin of more ancient deposits. It is necessary to use multiple proxies to develop a correct interpretation of ancient strata.

Analyses and evaluation of data are from a) Quaternary glaciations and glaciers, b) formations which have been assigned to pre-Pleistocene glaciations, and c) formations with comparable features associated with mass-flow deposition (and occasionally tectonics). The aim is not to reinterpret specific formations and past climate changes, but to enable data to be evaluated using a broader and more inclusive conceptual framework. To achieve this goal, detailed descriptions of field evidences are documented from papers that may suggest different interpretations of these data. This is not in an intention to present revised interpretations of these papers, but to collect data and develop a foundation for enhanced analysis of geologic processes and features.

Regularly occurring features interpreted to be glaciogenic and are contemporaneous with pre-Pleistocene diamictites which have been interpreted to be tillites, have often been shown to have few or no Quaternary glaciogenic equivalents. These same features commonly form by sediment gravity flows or other non-glacial processes, which may have led to misinterpretations of ancient deposits. These features include, for example, appearances and documented data from the extent and thickness of diamictite deposits, environmental and depositional affinity of fossils in close connection to diamictites, grading and bedding of

diamictites, fabrics, size of erratics, polished and striated clasts and surfaces ("pavements"), boulder pavements, lineations, valleys, glaciofluvial deposits, dropstones, laminated sediments, glaciomarine sediments, periglacial structures, soft sediment tectonics, and surface microtextures. The analysis of these features provide detailed documentation that may be used to help identify the origin for many pre-Pleistocene diamictites. Recent decades of progress in research relating to glacial and sediment gravity flow processes has resulted in proposals by geologists, based on more detailed field data, more often of an origin by mass movements and tectonism than glaciation. The most coherent data of this review, i.e. appearances of features produced by glaciation, sediment gravity flows and a few other geological processes, are summarized in a Diamict Origin Table.

Keywords:
tillite
sediment gravity flow (SGF)
striation
groove
dropstone
paleoclimate
fossil vegetation
glaciogenic proxies
surface microtexture
Late Paleozoic Ice Age

Terminology

Dropstone and lonestone: Dropstone is a genetic label for a clast that has been dropped into

water from ice. This label may also be used for clasts dropped by other agents, like from floating vegetation. In the current paper the label dropstone will refer to any outsized clasts which have been interpreted in the literature to be dropped from ice, even if that interpretation may not be valid. A non-genetic term for outsized clasts is lonestone. This term would be better to use than dropstone, but as lonestones are commonly interpreted to be dropstones and the terms sometimes even are used interchangeable, the label dropstone is used whenever it has been done so by earlier researchers. Otherwise, the interpretation of the origin has to be discussed for every clast that is referred to.

Groove: Commonly defined in width as >10 mm up to a few meters or more. Marine geologists may label any large linear erosional (V-shaped) forms as grooves (Nwoko et al., 2020a), even if they are kilometers in width, but in the current paper the definition is used for erosion by tools.

Striation: Commonly defined as <10 mm in width. Marine geologists may label large erosional (wide and flat-bottomed) channels made by megaclasts on the sea bottom as striations (Nwoko et al., 2020a), but that definition is not used in the current paper.

Tillite and"tillite": This label is a genetic term, and by definition a lithified till. Any ancient diamictite which has been classified as tillite by former researchers, even if the evidence from recent geological research indicates a non-glacial origin of the deposit, will here also be labeled tillite. If the word diamictite should be used instead of tillite, then the current or most common interpretation of the deposit will be missed. Therefore, for the discussions concerning the interpretation of the origin of a deposit, the term will be marked within quotation marks, i.e. “tillite,” independent of the most recent interpretation.

1. Introduction

1.1. Structure of the current paper

The basic assumption for the current paper is that the recent is better known than the past. This is an actualistic approach, i.e., the principle that the same processes and natural laws applied in the past are the same as those active today. By not using models or longstanding interpretations, but recent field studies and experiments, this actualistic approach is followed. Recent progress in studies of sediment gravity flow (SGF) (used interchangably with mass flow), glaciogenic and a few other processes which may be relevant, are applied when documenting the origin of ancient deposits. Where there is a lack of published data, documentation is compiled or otherwise acknowledged as missing. It may be questioned that mainly Quaternary examples of geologic features are used in comparison to features from the much longer pre-Quaternary time scales, but as it is assumed that natural laws have not changed, this will not be much of a problem.

Diamictites are often interpreted to have been formed in a cold climate environment based on the general structure of the deposits, associated geologic features, and polar wander paths. Geochemical data may be used to strengthen the interpretation of glaciation, but these display apparent shortcomings (Frimmel, 2010; Bahlburg and Dobrzinski, 2011; Garzanti and Resentini, 2016; Macdonald, 2020; Caetano-Filho et al., 2021; Mikhailova et al., 2021; Rogov et al., 2021; Scotese et al., 2021; Retallack et al., 2021). Similarities in outcrop of most of the features of glaciation may, however, be produced by different geologic processes (Isbell et al., 2021), mainly SGFs, and therefore more detailed criteria are needed for interpretation. The current paper analyzes and reviews a broad range of such geologic features. The intention is to design questions for field research, rather than to present solutions to all problems of interpretation. Only the appearance of geologic features which are described in great detail will be documented, and former general inferred interpretations of glaciation may not be followed. Different processes which may create similar features are documented in a way of using process-related or “process-sedimentological” principles “to consider alternative hypotheses” (Shanmugam, 2012). Relevant field data is summed up in a

Diamict Origin Table, as a guide to the interpretation of the geologic features which have been documented and discussed (Appendix).

Even if there is an awareness of the importance of gathering data from different research disciplines, it may be difficult to evaluate what data shall be used while constructing and interpreting models. Areas which have been described to have formed by ancient glaciations have to be discussed from data compilation from many research disciplines. It may also be insufficient to use interpretations from different research disciplines or articles as facts, if the research data may be better described from a different geological and climatological aspect than is currently done.

The current paper concentrates on features which are most often reported and also documented in detail in association with "tillites," and these are compared to similar features from Quaternary glaciations and SGFs that mimic (or are) these features. Therefore, unintentionally, this work may have become controversial, not because of the compilation of research data, but because of longstanding interpretations of many ancient deposits. The documentation is to a large part biased by reference to well documented and extensive outcrops. The main exception is the documentation of outsized clasts, because lonestones are often interpreted to be dropstones and therefore are commonly suggested to be evidence for glaciation (e.g., Rodríguez-López et al., 2016; López-Gamundí et al., 2021; Le Heron et al., 2021a; Bronikowska et al., 2021).

1.2. Historical sketch

Ever since diamictites were first interpreted to be pre-Pleistocene ice age deposits, by Ramsay in 1855 for some Permian boulder deposits in England (Harland and Herod, 1975; Hoffman, 2011), there has been much controversy over their interpretation. The first steps of SGF

191 research can be said to have started in 1827, with the introduction of the term flysch (Studer,
192 1827). The first mention of a submarine fan was in 1955 (Menard, 1955), and the first
193 mention of a turbidite-fan link in ancient fans was in 1962 (Bouma, 1962; Shanmugam,
194 2016). The importance of SGFs in the geologic record has often been underestimated
195 (Shanmugam, 2016, 2020, 2021b), even if SGF deposits have often been documented in
196 papers concerning diamictites. Lately, hyperpycnal flows have been recognized to transform,
197 after deposition, into a full spectrum of SGF deposits, including cohesive debris flows and
198 rhythmites, which adds one more dimension to this research area (Zavala and Arcuri, 2016;
199 Shanmugam, 2019, 2021b; Zavala, 2019, 2020).

200 Since the early 1970s, starting with an earlier paper by Crowell (1957), it has been recognized
201 that many “ice-age remains” have been deposited by different kinds of SGFs, for example by
202 turbidity currents but especially by cohesive debris flows. For example, in the Tertiary of
203 Alaska, twelve major glaciations were reinterpreted as formed largely by SGFs (Plafker et al.,
204 1977; Eyles and Eyles, 1989). Schermerhorn published a comprehensive review which
205 documented the evidence for a SGF origin of ancient diamictites, shown in his classic work
206 on Late Precambrian diamictites (Schermerhorn, 1974a, 1976a, 1976b, 1977). The current
207 paper is partly inspired by the work of Schermerhorn, but is also influenced by published
208 work on fan deposits and SGFs (Shanmugam, 2016; Peakall et al., 2020). Many researchers
209 in addition to Schermerhorn have compared tills, glaciomarine sediments and different kinds
210 of SGFs, but the work may have been hampered by the assumption that outcrops with
211 equivocal origin are ice-age deposits (Hambrey and Harland, 1981; Boulton and Deynoux,
212 1981; Anderson, 1983; Wright et al., 1983; Eyles, 1993). The documentation in
213 Schermerhorn´s classic paper (1974a) has to a large part gone unnoticed, even though this
214 article may be referred to in passing (e.g., Le Heron et al., 2017). Eyles (1993) wrote: “ ...
215 unfortunately, the inclusion of strata that were indisputable of a glacial origin weakened the
216 essential correctness of Schermerhorn´s argument.”

Pre-Pleistocene formations which are, or have been, interpreted to have formed by glaciations are documented from the Archean, the Paleoproterozoic, the Neoproterozoic, and during all periods of the Phanerozoic (Hambrey and Harland, 1981; Caputo and Santos, 2020; Youbi et al., 2021) sometimes even in the tropics and indicating low elevations (Soreghan et al., 2014), including during five different episodes of the Cretaceous (Alley et al., 2020). The most accepted and geologically important glaciations are in the Paleoproterozoic, the Neoproterozoic, the Upper Ordovician, and the Late Paleozoic Ice Age (LPIA; recently dated to 372-259 million years; Pauls et al., 2021) (Hambrey and Harland, 1981).

1.3. Bias in diamictite research

Glaciogenic proxies are documented in order to find stratigraphic intervals displaying glaciations, as there, on the basis of uniformitarianism, had been many glaciations throughout earth history (e.g., Williams, 2005). The current interpretation of a stratigraphic interval commonly biases the research questions and which observations and measurements are made, and frequently it is mainly data supposed to be relevant for the current interpretation that are reported. These circumstances have resulted in that alternative interpretations were not always fully investigated. Therefore the features which are described in the literature often contain too few details to establish if the deposits have originated from glacial action, SGF or by any other means. For example, a clast or a surface with striations is often reported to have been glacially striated if present in connection to a diamictite (Atkins, 2003). In other words, features which may be formed in different environments are reported, but diagnostic features may not be documented or discussed. Single or even groups of features which display appearances partly similar to and interpreted to be glaciogenic features, may subsequently be shown to be very different from Pleistocene and more recent glaciogenic features. In short, the question of the origin of diamictites has become a part of a scientific paradigm (Kuhn, 1970; Shanmugam, 2016) connected to long-term climatic correlations (Young, 2013; Shields

et al., 2022).

As recent research uncovers growing evidence of non-glacial transport, diamictites worldwide have more often been interpreted as glaciomarine and often considered as parts of interglacial periods. This includes approximately 95% of all "glaciogenic" deposits, i.e. sediments which may contain an abundance of marine fossils, and to a large part are made up of SGF deposits (Eyles 1993; González and Glasser, 2008; Isbell et al., 2016; López-Gamundí et al., 2016, 2021; Assine et al., 2018; Vesely et al., 2018; Rosa et al., 2019; Sterren et al., 2021; Isbell et al., 2021; Molén and Smit, 2022). These interpretations make it more difficult to discover if the deposits had been produced primarily by glaciation or are non-glacial marine. In this case often the only "unequivocal" evidence for glacial influence is considered to be dropstones, especially if outsized clasts occur in rhythmites, but also if SGF deposits or stratified diamictites display outsized clasts (e.g., Ezpeleta et al., 2020). Apart from dropstones, striated clasts and surfaces ("pavements") are commonly referred to as evidence for glaciation without discussing alternative interpretations in depth (e.g., different examples in Molnia, 1983a; Miall, 1983, 1985; Eyles, 1993; Hoffman et al., 1998; Carto and Eyles, 2012a; Rodríguez-López et al., 2016; Le Heron et al., 2017; Le Heron and Vandyk, 2019).

1.4. Geologic features produced by sediment gravity flows

Gravity-induced slope processes include variations of rock fall, slides, slumps, debris flows and turbidites. In some outcrops there is an almost complete visible sectioned sequence, horizontally and/or vertically, which shows how mass movements have changed from e.g., slides, to debris flows, and finally to turbidity currents (Ogata et al., 2019; Rodrigues et al., 2020; Kennedy and Eyles, 2021). Sedimentary and erosional features which commonly form from such processes, especially those originating from cohesive debris flows, share many similarities in appearance to glaciogenic features and are present in many diamictites which

had been interpreted to be glaciogenic (e.g., Molén, 2017, 2021). Another process which shows similarities to slope processes are land derived hyperpycnal flows. Such flows can in some cases last for months. Even though they have a different origin from slope processes, they display similarities in the sedimentation process and the deposits may be reworked and transform into a full spectrum of SGFs (Zavala and Arcuri, 2016; Shanmugam, 2019, 2021b; Zavala, 2019, 2020). Hyperpycnal flow deposits are therefore included here in what is commonly described as SGF deposits.

Below is a list of features that commonly originate by especially cohesive debris flows, but which also may originate from other slope processes like turbidites and slides that commonly co-occur with debris flows. These geologic features are important to acknowledge as there are differences between features of glaciation and SGFs which will be outlined herein. The features below are well known in the geologic community within the discipline of slope processes, but the details are often not well known outside of this community. All the features listed have to be acknowledged. An assemblage of these are commonly present in close connection to diamictites, i.e. they are parts of ancient diamictites and other erosional and depositional features which have been interpreted to be glaciogenic, and are by definition also present in areas displaying non-glacial SGF deposits. If the features in the list below are studied more in detail, it may be possible to demonstrate if an area or outcrop was formed mainly by SGFs or by glaciation. A subsample of references from a complete research discipline, which may be the most important from the discipline of SGF research, which all document many of the features in the list below, are Middleton and Hampton (1976), Shanmugam et al. (1994), Schneider and Fisher (1998), Major et al. (2005), Moscardelli et al. (2006), Talling et al. (2007, 2012, 2015), Watt et al. (2012), Dakin et al. (2013), Pickering and Hiscott (2015), Shanmugam (2016, 2020, 2021), Peakall et al. (2020), Cardona et al. (2020), Baas et al. (2021); Dufresne et al. (2021).

a) diamict texture, but deposits often may be in streaks and display some sorting and grading,

b) grooves and striations on clasts and surfaces/pavements, especially below debris flows that may hold clasts in fixed positions,

c) lonestones which may be interpreted as dropstones,

d) sharp and irregular fronts,

e) a great degree of scatter and variable thickness of the deposits,

f) variable erosion and depth of deformation of the underlying substratum (e.g, sharp, undulating, interdigitating, ripple-type, grooved),

g) deposition in or at the end of channels,

h) reworking at the top of the deposits by bottom currents,

I) conformably draping by mass flow beds of rapid deposition (mainly turbidites),

j) soft sediment structures, like load casts, clastic dykes, boudinage, folds and convolute bedding,

k) scour and fill structures,

l) rhythmites,

m) climbing ripples,

n) contorted rip-up soft slabs of sandstone or other sediments,

o) mud-flakes or clasts which have often been pressed down into the underlying sediments from above, and therefore the beds also display holes or depressions below debrites, where embedded clasts have been eroded out,

p) a thickness-to-width ratio commonly thicker than 1:50,

q) more than 3-5% clay, or otherwise may transform distally into hyperconcentrated flow or sediment-laden floods,

r) an appearance of crossbedding,

s) a basement which has been rounded with a superficial appearance of having been glaciated, e.g. displaying bedrock forms similar to roches moutonnées, even with evidence of plucking,

t) brecciation of the substratum, which may also display cataclasis,

u) a thin basal layer of debris, i.e. a traction carpet or liquefied sandstone,

v) rip up soft sedimentary megaclasts with intact stratigraphy,

x) entrainment of sediments, including processes that may be defined as plucking, during the complete path of movement,

y) laminar behavior,

z) uphill movement,

za) no or rare evidence of fossils,

zb) an upper hummocky terrain,

zc) drop formed landforms which are erosional remnants.

2. Similarities and differences between glaciogenic and other geologic features

Ancient outcrops commonly are visually restricted, and therefore it may be difficult to document appearances of features from the action of glaciers or any other processes. Many different geological features which may be misinterpreted in restricted outcrops, are documented below. Some researchers state that it may be impossible to confidently identify a specific environment of deposition by macroscopically features and textural criteria (Kilfeather et al., 2010), but as is documented in the current paper there are more unequivocal critera than is usually recognized.

If there is glaciogenic material which has never been processed by but only transported by a glacier, such as supraglacial till, it will not acquire many of the characteristics imposed by glacial forces. The same holds for flow tills, if they are supraglacial mass flows that have never been covered by a glacier. This may also hold for some aspects of squeezed flow till (Hicock, 1991; Hicock and Dreimanis, 1992b). Flow tills are in any case difficult to differentiate from non-glaciogenic mass flows, especially if they are formed subaqueously (Evenson et al., 1977). Englacial till which has been deposited as melt-out till also may not acquire many glaciogenic features. However, all material that is deposited in a subglacial

environment will display evidence of this process (Mahaney, 2002; Molén, 2014). Furthermore, supraglacial tills and other tills that have not been transported at the base of a glacier are usually a minor part of glaciogenic sediments, and they are easily removed by later erosion, in contrast to basal till.

Many features which are interpreted to be evidence of glaciation form in a wide range of environments (e.g., Eyles, 1993; Eyles and Boyce, 1998; Atkins, 2003; Thompson, 2009). If clasts from one environment are incorporated by a new process, e.g., tectonic material that is mixed with finer material and beach/slope material in a debris flow, the origin of the deposit may be difficult to uncover (e.g., Festa et al., 2019). This mixing of different materials is common in SGFs, and up to 50% of the material may be entrained through erosion from the substrate along the path of the flow (e.g., Thompson, 2009; Carto and Eyles, 2012a, 2012b; Ortiz-Karpf et al., 2017; Ogata et al., 2019; Nugraha et al., 2020; Rodrigues et al., 2020). Eyles and Eyles (2000) described a “cement-mixer-model” of how different sediments could mix.

Each of the features reviewed in the sections 2.1.-2.18. is commonly referred to when exploring evidence of glaciation. There is, however, an increasing understanding that similar features, which more or less mimic the typical glacial features, also can originate as a consequence of different kinds of SGFs and other non-glacial processes. In addition, there are many geologic features from “ancient ice-ages” which have rarely or never been formed by Pleistocene or younger glaciers. These features may be at odds with a glaciogenic interpretation, but often at the same time indicate a SGF or/and tectonic origin. Also, there are some general problems in regard to “tillites” that do not apply to SGFs, e.g. climate and correlations, which are also discussed below.

2.1. Geographical extent, dating, climate and fossils

367 *2.1.1. Geographical extent*

368 SGFs occur worldwide, independent of latitude, and are therefore present in the same areas as
369 the more geographically restricted glaciers. Mountain glaciers are areally restricted, but are
370 present worldwide if above the equilibrium-line altitude (e.g., Mahaney, 1990).

371 The geographic extents of deposits from "ancient ice-ages" are often comparatively small and
372 "tillites" are often dispersed as separate outcrops (e.g., Lindsay, 1966; Finkl and Fairbridge,
373 1979; Fairbridge and Finkl, 1980; Deynoux and Trompette, 1981b; Le Heron et al., 2018a).
374 There are two exceptions. The first is the Ordovician deposits in northern Africa which cover
375 between 8 x 10^6 (Biju-Duval et al., 1981) and 20 x 10^6 km^2 (Fairbridge, 1979). The size
376 difference depends on whether the Arabian diamictites are included or not. If the lesser
377 Ordovician outcrops in South Africa, Europe and South America are included, the maximum
378 hypothetical glaciated area is c. 40 x 10^6 km^2 (Le Heron et al., 2005, 2018a; Ghienne et al.,
379 2007). The second exception is the LPIA outcrops which cover maybe 30 x 10^6 km^2 if
380 deposits from separate basins in South America, Antarctica, Australia, India, South Africa,
381 Congo and Madagascar are included (Gravenor, 1979). Parts of the Arabic Peninsula,
382 Ethiopia, Chad and a few other areas may also be included in the LPIA (e.g., Bussert, 2010,
383 2014; Le Heron, 2018). The LPIA has lately been alternatively interpreted as many smaller
384 glaciations, to a large part marine and including SGFs, and parts of the area have even been
385 described as formed in a large glacial lake (Horan, 2015; Dietrich et al., 2019; Fedorchuk et
386 al., 2019; López-Gamundí et al., 2021; Isbell et al., 2021; Ives and Isbell, 2021).

387 Neoproterozoic diamictites are commonly present in downwarping or deep basins, otherwise
388 close to rifts, and rarely on stable bedrock (Schermerhorn, 1974a; Eyles, 1993; Arnaud, 2008;
389 Frimmel, 2018; Kennedy and Eyles, 2019, 2021), and many Precambrian "tillites" can be
390 correlated with tectonic movements apparently connected to continental breakup (Eyles,

1993; Williams, 2005; Carto and Eyles, 2012a, 2012b; Delpomdor et al., 2016; Gómez-Peral et al., 2017; Kennedy and Eyles, 2019, 2021; Molén 2021). Recent active areas of tectonism/volcanism may display similar geologic features as in Precambrian “tillites” (Carto and Eyles, 2012a). Peperites are mixed with Neoproterozoic diamictites in Argentina and Paleoproterozoic diamictites in Canada, indicating that volcanism was the triggering process for the origin of some diamictites (Young et al., 2004b; Pazos et al., 2008). Deposits from Phanerozoic ice-ages have accumulated on more stable bedrock than during the Precambrian (Schermerhorn, 1974a), but the LPIA formations in both southern Africa and South America, have been deposited in tectonically controlled former sinking basins or close to areas of tectonic movements (Johnson et al., 1997; Barbolini et al., 2018; Hansen et al., 2019; Dietrich and Hofmann, 2019; Fedorchuk et al., 2019; Limarino and López-Gamundí, 2021; Creixell et al., 2021; Veroslavsky, 2021; Molén and Smit, 2022). The overall geological framework of the Ordovician glaciated area was a continuous transgression over a slowly subsiding cratonic platform (Ghienne, 2003), and there is evidence of recurrent magmatic activity in the area from the Precambrian to the Holocene (Ghuma and Rogers, 1978; El-Makhrouf, 1988; Young et al., 2004a; Permenter and Oppenheimer, 2007; Liégeois, 2006). Consequently, even the Paleozoic glaciations may in some aspects be connected to tectonism. Quaternary glaciations commonly were and are on more stable bedrock.

Many ancient sedimentary deposits which are interpreted to be glacially influenced are hundreds of meters to many kilometers thick (Volkheimer, 1969; Schermerhorn, 1974a; Woolfe, 1994: Visser, 1989a; Vesely and Assine, 2014; Ali et al., 2018; Kennedy and Eyles, 2019; Rosa et al., 2019), as are mass flow deposits (Kuenen, 1964; Komar, 1970). As an example, a median thickness value for 197 mass flows (mainly Pliocene and younger) is 66 m, but thicknesses of hundreds of meters are common and there are examples of kilometers (Moscardelli and Wood, 2016; Ogata et al., 2019; Alves and Gamboa, 2020). Large mass movements may even generate isostatic uplift or downwarping of the lithosphere (Kneller et

al, 2016). Sedimentation will in general be more massive in areas where there is rapid subsidence in tectonically active basins (Kennedy and Eyles, 2021). SGF deposits may be complex, multi-layered units which may have been deposited during an event or a very short time period (e.g., Shanmugam, 2012, 2021b).

Even though the examples below are mostly from sediments deposited on oceanic crust, marine fossils are present almost worldwide, from former transgressions, and marine fossils are present next to geologic features which are interpreted to be glaciogenic (see examples in sections 2.1., 2.13, 2.15). Massive debris flows may travel 200 km without depositing any sediment (Talling et al., 2007), and therefore the resulting deposits may appear to be isolated "tillite" mounds. Many SGFs travel long distances, e.g., 900-2000 km outside off the coast of northwestern Africa (Georgiopoulou et al., 2010; Moscardelli and Wood, 2016), and there have been suggestions of 4000 km for less dense turbidity currents (Pickering and Hiscott, 2015). Such flows affected extensive areas, e.g., 95 000 km^2 for the Storegga Slide (Haflidason et al., 2004) and 132 000 km^2 in the Canada Basin (Moscardelli and Wood, 2016). The largest known Late Pleistocene debris flow influenced an area of 45 000 km^2 (Embley, 1982) and the largest known recent turbidity current influenced an area of 500 000 km^2 (Heezen and Hollister, 1971), but SGFs are usually much more restricted in areal extent than these two deposits, with a median value less than 100 km^2 (Moscardelli and Wood, 2016).

In contrast to "tillites" and SGF deposits, separate till beds, with characteristic structure and mineral content, can be traced over hundreds of kilometers and are often less than five meters thick (Schermerhorn, 1974a). Most layers are less than 100 m and usually not more than 10 m thick. In Canada the thickness of the till is 2-10 m (Eyles et al., 1983), in Norway the mean till layer is 5 m (Haldorsen, 1983), in Finland 2-3 m and in Sweden 5-15 m (Flint, 1971). At the southern limit of the North American inland ice sheet, separate till beds are superposed

and in total often thicker, e.g., from 10 to 52 m in a 300 km wide band (Flint, 1971), but in Europe the tills often thin out at the southern limits (Piotrowski et al., 2001). The thickest known accumulation of till beds from the Pleistocene is 400 m (Flint, 1971; Schermerhorn, 1974a).

The late Cenozoic exceptions, which exhibit thick glacial sequences, are in places with glaciomarine sedimentation, at the continental shelf of Antarctica and the Yakataga Formation of the Gulf of Alaska (Anderson, 1983). Most of these deposits have originated by SGFs but under the influence of nearby glaciers (Eyles and Lagoe, 1998).

Valley glaciers commonly merge into larger glaciers. Similarly "glacial" paleo-flows may be in one main direction and a few smaller merging valley flow directions (Visser, 1981). This is similar to what may take place during large slides/SGFs (e.g., Haflidason et al., 2004). Also, SGFs may diverge, bend and split into many smaller flows (Moscardelli et al., 2006; Sobiesiak et al., 2018; Kumar et al., 2021), somewhat similar to what may take place if a glacier is spreading out over a more planar surface.

Erosion has reduced the extent of many Pleistocene glaciogenic deposits. This explanation must not, however, be used only to defy the small and discontinuous extent of ancient deposits without documentation of evidence of erosion subsequent to a glacial period.

2.1.2. Correlations and dating

In general, there are always intricate problems with correlations, especially if these are long distance (Blauw, 2012; Gaucher et al., 2015). Commonly diamictites do not contain material that may be isotopically dated. Diamictites and "glaciogenic features" have therefore sometimes been interpreted to be glacial, only if they are of the "correct" age. Furthermore,

diamictites which commonly are regarded as glaciogenic today have earlier been regarded as not glaciogenic, because they have been considered to have been in the wrong paleogeographic area (Caputo and Santos, 2020). In some cases, diamictites have been redated, even four times, in order to correlate these to other deposits which have been interpreted to be glaciogenic. There are examples of redating from the Neoproterozoic throughout the Phanerozoic and occasionally even into the Pleistocene (Dow et al., 1971; Schenk, 1972; Schermerhorn, 1974a; McClure, 1980; Rehmer, 1981; Carto and Eyles, 2012b; de Wit, 2016a, 2016b; Moxness et al., 2018; Caputo and Santos, 2020; Hore et al., 2020). All these reinterpretations show that there are many difficulties and unknowns in the studies of diamictites and other geologic features which have been referred to as being glaciogenic.

2.1.3. Fossil vegetation

Fossil vegetation, including coal deposits, is often present adjacent to or in between deposits from "ancient ice-ages" (e.g., Plumstead, 1964; Lindsay, 1970a; Finkl and Fairbridge, 1979; Rocha-Campos and Santos, 1981; Gravenor and Rocha-Campos, 1983; Gravenor et al., 1984; Stavrakis and Smyth, 1991; Woolfe, 1994; Fedorchuk et al., 2019; Kent and Muttoni, 2020). Even if the time scales are long, these sedimentary proximities are so common that they have to be discussed.

Plants are better climatic indicators than rocks and would indicate any deviation from a polar climate. However, the ecology of plants often is interpreted from geology and not from plant physiology or ecology, which may be circular reasoning. For example, old editions of books may describe the Glossopteris flora as subtropical or tropical, but not so in more recent editions (e.g., Dott and Batten, 1976, compared to e.g., Prothero and Dott, 2003).

Current experiments and observations show different levels of ^{13}C and ^{12}C in living plants,

depending on e.g. latitude, temperature, precipitation and species (Cernusak et al., 2008; Kohn, 2010; White, 2015; Porter et al., 2017; Stein et al., 2021). Furthermore, there are different sensitivities to pCO_2 and other environmental factors for different plants (Klein and Ramon, 2019; Wilson et al., 2020; Stein et al., 2021), and many plants are insensitive to environmental drivers for isotope discrimination including pCO_2, water and temperature (Stein et al., 2021). Some researchers have even sampled data only from plant studies that show isotope discrimination, to calculate former pCO_2 (Stein et al., 2021). All these different data make ancient pCO_2 model calculations based on plant fossil carbon-isotope data suspicious.

2.1.3.1. Association between vegetation and glaciogenic sediments

Macrofossils are rarely found in diamictites. However, in the LPIA of South Africa, fossils of plants of Gangamopteris of the Glossopteris flora have been found within the diamictites and squeezed in between the Dwyka “tillite” and the underlying “ice-polished bedrock” (du Toit, 1926; Sandberg, 1928). Coalified plant fragments occur within massive “tillites,” and coal seams are often present on or between “tillites” (du Toit, 1926; Sandberg, 1928; Adie, 1975; Anderson and McLachlan, 1976; John, 1979; Bond, 1981a, 1981b; Le Blanc Smith and Eriksson, 1979; Visser, 1983a, 1989a; Stavrakis, 1986; Stavrakis and Smyth, 1991; Von Brunn, 1994; Hancox and Götz, 2014; Caputo and Santos, 2020). Coal seams that may be interbedded with “glaciogenic” diamictites have in many instances coalesced with other coal seams to form one thick coal seam (Stavrakis and Smyth, 1991). Interlayering of diamictite and coal beds is often considered to be a result of reworking of diamictites (Hancox and Götz, 2014), but that explanation does not hold well for plant fossils within massive diamictites and coalesced strata. Geologic evidence of long time periods are commonly missing. Coal seams that are interbedded between diamictites are often thin, and complete sequences may appear to be a kind of debrites (Hancox and Götz, 2014).

In the LPIA of Antarctica, diamictites intrude strata upward as diapirs (nearest plant fossils are c. 0.5 m above the “tillite”; Cuneo et al. , 1993), and boulders and conglomerates from the upper strata protrude downward into the diamictite. Furthermore, “glaciotectonic structures” are present both in the “tillite” and the lower part of the coal bearing strata (mainly sandstones and conglomerates; Isbell, 2010). In some places the boundary between the beds are gradational, and in other places the deposits are interfingering (Cuneo et al. , 1993; Isbell, 2010). Considered as a whole, these evidences indicate a short time period. Isbell (2010) concluded that the evidence suggested “temperate glacial conditions.”

Deposits containing fossil plants close to diamictites may be considered to be hyperpycnites, i.e. deposits formed by dense water flows laden with sediment and large plant parts. These may be sorted into dense and diluted parts, with or without plant material, but plant material may also be transported with turbidities, cyclones and tsunamis (Zavala and Arcuri, 2016; Shanmugam, 2019, 2021b; Zavala, 2019, 2020; Dou et al., 2021). Plant parts have been transported into deep marine basins at estimated paleodepths of approximately 400-600 m (Pickering and Corregidor, 2005).

The evidence from the absence of plant fossils within most Paleozoic diamictite deposits may be an indication of water depth or transport distance, i.e. in deeper water, or during longer transport, plant material and other organisms may be sorted out. The $\delta^{13}C_{carb}$ in the Dwyka Group diamictites appear to be of primarily algal origin, which may be an indication of water depth (Scheffler et al., 2003). Fossils are seldom reported from within debris flow deposits. On the other hand, Holocene glaciogenic deposits may hold an abundance of trees and other plants, if forests have grown nearby (Ryder and Thomson, 1986; Fleisher et al., 2006). This would not be considered to be uncommon in areas with Alpine glaciation or at the southernmost parts of continental glaciers, but less common if there was polar climate.

2.1.3.2. Ecology

The vegetation present next to "glaciogenic" facies of the LPIA deposits does not include typical cold-climate plants (Anderson and McLachlan, 1976; McLoughlin, 2011; Hancox and Götz, 2014; Caputo and Santos, 2020). The LPIA fossil plants, i.e. the Glossopteris flora, do not display any typical appearances of cold climate peats or other cold climate environments, and no indication that they could have thrived in polar climates (Srivastava and Agnihotri, 2010; McLoughlin, 2011; Isbell et al., 2016; Götz et al., 2018; Gastaldo et al., 2020a, 2020b; Mays et al., 2020; Tripathy et al., 2021). The main argument for a cold climate adaptation of the vegetation (if this question even is raised) is the close connection to sedimentary deposits which are regarded to be from an ice age. Similar plant fossils are present even at a paleolatitude of 75-85°S, even if there are not always diamictites close by, and the estimated range of productivity of these far southern forests is similar to that of modern forests (Cuneo et al., 1993; Isbell et al., 2016; Miller et al., 2016; Decombeix et al., 2021). There also are indications that at least some plants were evergreen (Gulbranson et al., 2014), and no evidence of frost rings (Taylor et al., 1992). But growth rings would be expected from a shift from light to dark seasons, or amount of precipitation (e.g., Glock, et al., 1960; LaMarche, 1969; McLoughlin, 2011). Even if all these fossil plants are not close to diamictites in time or space, they are in a paleopolar area. It would seem as reasonable to argue that because there are temperate or possible subtropical plant fossils present close to many diamictites, as these are also present where there is no diamictites, such deposits cannot be glaciogenic and might instead be SGF deposits. Although the Glossopteris flora species are gymnosperms, and not angiosperms which have been better studied, leaf size and appearance may be an indicator of paleoclimate. Hence, the physiology of the fossil plants, displaying complete (non-toothed) and also large sized leaves, suggests that the Glossopteris flora of Gondwana could even be considered to be evidence for a tropical or subtropical climate zone (e.g., Gastaldo et al., 2020a; DeVore and Pigg, 2020).

The Paleozoic ferns, gymnosperms and other plants are present in many climatic zones. The same genus or even species of plants that are present next to Paleozoic “tillites,” are also present in many places with non-glacial climate (e.g., compare Gateway to the Paleobiology Database, 2020, to Barbolini, 2014). For example, Glossopteris flora, which is present over most of Gondwana (McLoughlin, 2011), have been discovered in the Late Permian of Jordan, i.e. in the northern, tropical/subtropical part of Gondwana (Blomenkemper et al., 2020), in Mongolia (Naugolnykh and Uranbileg, 2018), and also in deposits at the Permian-Triassic border of Pakistan which are considered to have been laid down during a greenhouse climate (Schneebeli-Hermann et al., 2015). Meyerhoff et al. (1996), Srivastava and Agnihotri (2010), McLoughlin (2011), and Mays et al. (2020) describe more examples of Glossopteris flora outside of the Gondwana area, but there is skepticism whether all these fossils really are Glossopteris (Mays et al., 2020). Coal-forming plants showing affinities to plants which are present in North America and Europe and are interpreted to be from tropical or subtropical areas, are also present in Gondwana, but these fossils have not been clearly described or are reassigned to other species, which may make the interpretation of paleoclimate from these fossils at least equivocal (Charrier, 1986; Spiekermann et al., 2020). However, well documented Sigillaria is present in northern Gondwana (Seward, 1932) and lepidodendroid lycopsids (Lepidodendrales) in the Devonian of Australia (Peyrot, et al., 2019).

From the evidence of the vegetation, it may be possible that the climate during the LPIA was similar to the Middle/Late Permian, Mesozoic and early Cenozoic “near-tropical” “Greenhouse World” climate, the latter displaying no large glaciers and mean annual temperatures from maybe +5°C to +20°C (or at least no long periods of time with temperatures below the freezing point) close to the poles (Leonard et al., 1981; Sloan and Barron, 1990; Bickert and Heinrich, 2011; Rose et al., 2013; Mori et al., 2016; Bernardi et al., 2018; Decombeix et al., 2021), with e.g., dinosaurs (Mori et al., 2016; Fiorillo et al., 2019; Takasaki et al., 2019) and subtropical and temperate forests growing close to the poles

588 (Wolfe, 1977; Morris, 1985; Francis, 1990; Kerr, 1993, 2008; Wilf et al., 2009; Cerda et al.,
589 2012). There is a lack of evidence of continuous glaciation in Gondwana during the LPIA,
590 even if the South Pole was situated close by from the Late Proterozoic until the Early Triassic
591 (e.g., Horan, 2015). And there are very few and no unequivocal evidences of glaciation in the
592 northern hemisphere during the LPIA (Isbell et al., 2012, 2013, 2016; Montañez and Poulsen,
593 2013; Craddock et al., 2019; Griffis et al., 2019; Fedorchuk et al., 2019, 2021; Rosa and
594 Isbell, 2021). The LPIA is immediately followed by a period of "Triassic Hothouse extremes"
595 (Götz et al., 2018). Even during the Neogene the Antarctic continental mean summer
596 temperatures were +5°C, i.e. possible 30°C warmer than today (Rees-Owen et al., 2018).

597 All the evidence from fossils show that there is no need to ascribe a polar climate to polar
598 areas, as may be done when referring to polar wander paths and also to the recent climate at
599 the poles.

600 *2.2. Till structure*

601 In many aspects SGF deposits may be indistinguishable from subglacial tills (section 1.4. and
602 e.g., Mountjoy et al., 1972; Schermerhorn, 1974a; Kurtz and Anderson, 1979; Lowe, 1982;
603 Visser, 1983a; Wright et al., 1983).

604 Transverse and irregular moraine forms are not common in diamictites, but are regularly
605 present in Pleistocene and younger tills. However, compressional transverse ridges,
606 hummocky terrain, and flow lines similar to those on the surfaces of some glaciers, are
607 formed by SGFs (e.g., Haflidason et al., 2004; Pickering and Hiscott, 2015; Nugraha et al.,
608 2020; Dufresne et al., 2021; Procter et al., 2021).

609 *2.2.1. More mass flows and marine sediments than basal glaciogenic sediments*

610 "Tillites," in comparison to glaciogenic depoits from the Holocene and Pleistocene, more
611 often have been disturbed by SGFs, or have been interpreted to be deposited mainly by glacial
612 marine sedimentation (i.e. 95%, section 1.3.), and, therefore, it is especially difficult to
613 distinguish such deposits from non-glaciogenic SGF deposits (e.g., Aalto, 1971; Martin,
614 1981a; Von Brunn and Stratten, 1981; Gravenor et al., 1984; Molén and Smit, 2022). The
615 natural explanation for this – erosion of higher lying terrestrial source areas – has not been
616 substantiated by reports concerning possible evidence of erosion of "tillites," and there may
617 still be much sedimentary material close to the central areas of "glaciation" (Biju-Duval et al.,
618 1981; Gravenor and Rocha-Campos, 1983; Visser, 1988, 1989a; Le Heron et al., 2010).

619 Often ancient basal "tillites"/diamictites are overlain and/or underlain by SGF deposits or
620 marine strata (e.g., Banerjee, 1966; Visser, 1983b; González and Glasser, 2008; Caputo and
621 Santos, 2020) – a less common observation in Pleistocene deposits. Slides, slumps and debris
622 flows often trigger turbidity flows that will retain some coarse sediment and will be deposited
623 on top of, or downslope from, the denser flow (Hampton, 1972; Middleton and Hampton,
624 1976; Embley, 1980, Lowe. 1982). This can explain why diamictites often are surrounded by,
625 or draped with, shale or rhythmites with lonestones (e.g., Molén, 2017, 2021; Rampino, 2017;
626 López-Gamundí et al., 2021).

627 *2.2.2. No rock flour and density of deposits*

628 Till contains a large component of rock flour, i.e. material with a grain size <2 μm, as
629 opposed to many "tillites" (Frakes, 1979; Molén, 2017). For example, the Saharan and Saudi
630 Arabian Ordovician diamictites which are interpreted to be glaciogenic are composed of
631 similar sized material as the underlying sandstones, i.e. sand/silt and no (or very little)
632 grinded rock flour (Le Heron et al., 2005, 2006; Yassin and Abdullatif, 2017). Diamictites in
633 China also are sandy to silty (Chen et al., 2021).

Deposits formed by direct sedimentation from dense suspension are among the most loosely packed natural sediments (Lowe, 1982), i.e. different from subglacially deposited material. However, SGF deposits appear to consolidate quickly, which may mimic compression of sediments by glaciers in tills (Moscardelli et al., 2006). Also, as diamictites are lithified, the cementing agent might obscure indices of the former ratio of pore spaces.

2.2.3. Correlation between clast size and thickness of strata

The largest boulders in "tillites" are often present in the thickest sedimentary horizons (Schermerhorn, 1974a; Martin et al., 1985; Eyles and Januszczak, 2007). This indicates transport by SGFs (Dott, 1963; Kuenen, 1964; Larsen and Steel, 1978; Derbyshire, 1979; Lowe, 1982; Walton and Palmer, 1988; Middleton and Neal, 1989; Eyles and Januszczak, 2007; Kennedy and Eyles, 2021). Ice distribute boulders more randomly.

2.2.4. Grading in sediments

There is much grading in diamictites which have been or are interpreted to be "tillites," including lodgement/basal "tillites," i.e. a) graded bedding, upwards fining, or the largest boulders deposited at the bottom of the sequences (Kulling, 1951; Lindsay, 1968; Bowen, 1969; Schermerhorn, 1975; Visser and Kingsley, 1982; Visser, 1982; Deynoux, 1985b; Gravenor and Von Brunn, 1987; Le Heron et al., 2018b, Le Heron et al., 2021b), b) "tillites" grading upwards to shales, dropstone bearing shales or fluvial sediment (Dow et al., 1971; Frakes and Crowell, 1969; Visser et al., 1987; Mustard and Donaldson, 1987b; López-Gamundí, 2010), c) reverse grading from "sandstone with rounded dropstones" to "clast-rich diamictite" (Hoffman et al., 2021), and d) conglomerates or breccias grade upwards to, or are directly overlain, by diamictites which have been interpreted to be "tillites" or SGFs (Kulling, 1951; Lindsay, 1966, 1970; Lindsey, 1969; Cahen and Lepersonne, 1981;

Deynoux and Trompette, 1981b; Visser, 1981, 1983b, 1997; Mustard and Donaldson, 1987a, 1987b; Isbell et al., 2008; Festa et al., 2016; Kennedy and Eyles, 2021; Molén, 2021).

The occurrence of breccias might indicate that the process of movement was triggered by tectonism, or that the bedrock broke to pieces by the impact of a SGF (Dakin et al., 2013; Molén, 2021). Grading is an indication of transportation by SGFs (section 1.4; Cecioni, 1957; Eriksson, 1991), but may be present in glacogenic deposits. Even if there is not any evidence of grading in all stratigraphic successions, many pre-Pleistocene "glaciogenic" and also SGF deposits display a general sequence, with a few or many of the following facies, starting from the bottom: breccia, conglomerate or clast supported diamictite, massive diamictite, stratified diamictite, sand or siltstone, and rhythmites with finer material displaying lonestones (e.g., Molén, 2017, 2021; Le Heron et al., 2021b López-Gamundí et al., 2021; Molén and Smit, 2022). Furthermore, massive diamictites which have been studied in more detail, have been shown to be stratified, and may indicate a non-glacial origin (Stavrakis, 1986; Stavrakis and Smyth, 1991; Von Brunn, 1994; Visser, 1997; Visser et al. 1997; Huber et al. 2001; Haldorsen et al. 2001; Isbell et al., 2008; Dietrich and Hofmann, 2019; pers. commun., Johan N. J. Visser, 2020; Molén and Smit, 2022).

2.2.5. Bedding and amalgamation

Sandstones which have been interpreted to be "tillites" may be faintly bedded and display structures similar to dish structures (Biju-Duval et al., 1981; Gravenor and Rocha-Campos, 1983; Deynoux 1985b), which might indicate deposition by debris flows (Middleton and Hampton, 1976; Lowe, 1982; Visser, 1983a). But, fissility textures in tills, and dewatering of two component glaciomarine facies, may occasionally display an appearance similar to dish structures.

Ancient diamictites often display amalgamation of debris flow deposits (Kennedy and Eyles, 2021), which Domack and Hoffman (2011) interpreted as amalgamation of tillites. The number of "tillite" beds also had been interpreted as the number of glaciations (Ali et al., 2018).

2.2.6. Presence of soft sediment structures

In SGFs, large rip-up contorted slabs of soft sediments are commonly transported (Crowell, 1957; Lindsay, 1966; Lowe, 1979; Shanmugam, 2012, 2021b; Vesely et al., 2018; Rosa et al., 2019; Rodrigues et al., 2020; Isbell et al., 2021), but sometimes such "clasts" have been taken as evidence for glaciation (Deynoux and Trompette, 1981b; Runkel et al., 2010). Even though soft-sediment rafted material may occasionally be transported by and not become shattered by glaciers, "tillites" often contain contorted transported sheets of sediment, thus indicating a more probable transport by SGFs (Lindsay, 1966; Bowen, 1969; Frakes et al., 1969; Visser, 1983b; Deynoux, 1985b; Molén, 2017; Kennedy and Eyles, 2019, 2021).

Other structures which are commonly present in SGF deposits, but also in a lesser amount in what is or have been considered to be glaciogenic sediments/tillites are: rotational structures, necking structures (squeezing of material between clasts), wisps, flame structures, sediment diapirs, load casts, intra-clasts of diamictite (not to confuse with intra-tills; Evans et al., 2006), and dykes (e.g., Shanmugam, 2012, 2017b, 2021b; Isbell et al., 2016; Moxness et al., 2018; Molén, 2021; Kennedy and Eyles, 2019; Caputo and Santos, 2020; Molén and Smit, 2022).

2.2.7. Clasts pressed into underlying surface

Clasts in "tillites" have been pressed down into the underlying surface, which actually is not

always considered to had been soft (Lindsay, 1970a, 1970b; Hambrey, 1983; Caputo and Santos, 2020). This can be better explained by a SGF over unconsolidated sediment than a glacial origin (Molén, 2017).

2.2.8. Channels below or next to "tillites"

In the sedimentary strata just below or next to "tillites" there are occasionally erosional channels (Lindsay, 1970a; Biju-Duval et al., 1981; Schatz et al., 2011; Molén, 2017). These structures indicate that water, debris flows or slides eroded the underlying sediments before deposition took place, but these may not be incompatible with a glaciogenic origin (Mountjoy et al., 1972; Karlsrud and Edgers, 1982; Walton and Palmer, 1988; Eyles and Eyles, 1989; Eyles 1990; Eriksson, 1991; Talling et al., 2007; Dakin et al., 2013; Shanmugam, 2016; Baas et al., 2021).

2.2.9. Fabrics

The long axes of pebbles in Pleistocene tills often show a 10-20° dip in the direction of the ice movement, but there may also be a transverse fabric present (Lindsay, 1968, 1970a, 1970b; van der Meer et al., 2003; Evans et al., 2016).

In SGFs the fabric of outsized clasts can be similar to a till fabric, including a bimodal fabric and transverse oriented clasts, but it also display differences changing with the height in the sedimentary sequence (Lindsay, 1968; Best, 1992; Kim et al., 1995; Major, 1998; Kennedy and Eyles, 2019). In many SGF deposits the fabric is planar or sub-parallel to bedding (Evenson et al., 1977; Hill et al., 1982; Gravenor, 1986; Eriksson, 1991; Rodrigues et al., 2020), but it may be (sub)vertical, in places displaying protruding large clasts, or, about 30% of the clasts have a dip in excess of 20º (Lawson, 1979; Visser, 1996; Dasgupta, 2003; Liu et

al., 2021). The variation of the fabric sometimes makes it possible to find support for an origin by SGF. It is more difficult to provide conclusive evidence for a glacial origin of a diamictite only from fabrics, if the deposits are not in widespread horizons, even if doubts about the origin may not be strong (Lindsay, 1968; Lawson, 1979; Hicock and Dreimanis, 1992b; Piotrowski et al., 2001, 2002).

Pre-Pleistocene “tillite” fabrics typically display no systematic patterns and appearances which are indicative of tills, i.e. there are many varied directions and dips (Bigarella et al., 1967; Lindsey, 1969; Lindsay, 1970a, 1970b; Lindsay et al., 1970; Rehmer, 1981; Young, 1981a; Gravenor and Rocha-Campos, 1983; Miall, 1983; Deynoux, 1983, 1985b; Visser et al., 1987, 1997; Visser 1996). Many “tillite” fabrics seem to be more or less planar, but sometimes the dips are not reported (Visser, 1983b).

2.2.10. Flutes

Flutes may be formed behind obstacles in any environment. In glacial environments, obstacles are commonly at least 0.3-0.5 m higher than a lodged till surface, the flute is commonly lower and thinner than the obstacle, and the length may be many kilometers (Woodworth-Lynas, 1996). These are different from flutes described from areas which are interpreted to have been produced by glaciation, e.g. different appearance next to obstacles or no evidence of obstacles (e.g., Rosa et al., 2019; Le Heron et al., 2019).

2.2.11. Impact structures, meteorites

Deformed en echelon-fractures, hinged and crushed stones, which are followed by brittle fracture, such as so-called “bread-cut-to-slices”structures are typical for impact-cratering events (Oberbeck et al., 1993a, 1993b, 1994; Rampino, 2017). Such evidence has been

746 proxies to reinterpret “tillites” as originating by impact-generated debris flows (Rampino,
747 1994, 2017). Other criteria for impacts are shocked clast and minerals, and distinctive surface
748 microtextures on quartz grains (Rampino, 1994, 2017; Mahaney, 2002).

749 *2.3. Erratics*

750 *2.3.1. Erratics, transport and inclinations – similarities*

751 Except for by glaciation, erratics can be transported by e.g. mass flows, tsunamis and
752 cyclones (Carter, 1975; Malahoff et al., 1979; Elfström, 1987; Shanmugam, 2012, 2021b;
753 Lascelles and Lowe, 2021). The largest clasts transported by tsunamis are 40x27x6 m
754 (Lascelles and Lowe, 2021; see also Shanmugam, 2012, 2021b). Probably the largest known
755 erratics in “tillites” are 40 m, 100 m, and 320 m long, respectively, and the structures in the
756 surrounding diamictites indicate that these clasts have been transported by SGFs
757 (Schermerhorn, 1975; Molén, 2017). Large clasts are often deposited at the margin of mass
758 flow deposits (Ortiz-Karpf et al., 2017).

759 Large slide blocks are often more than one kilometer long and hundreds of meters high. The
760 largest known blocks are hundreds of square kilometers in area. Some of these have been
761 moved many tens to hundreds of kilometers (Maxwell, 1959; Wilson, 1969; Mountjoy et al.,
762 1972; Schermerhorn, 1975; Moore et al., 1989, 1995; Alves, 2015; Ortiz-Karpf et al., 2017;
763 Hodgson et al., 2018; Sobiesiak et al., 2018; Soutter et al., 2018; Alves and Gamboa, 2020;
764 Nwoko et al., 2020a, 2020b; Puga Bernabéu et al., 2020; Kennedy and Eyles, 2021; Kumar et
765 al., 2021). This long distance transport of material, whether debris flows or slides, is possible
766 because of processes labeled hydroplaning, shear wetting or substrate liquefaction (de Blasio,
767 2006; Moscardelli et al., 2006; Sobiesiak et al. 2016, 2018; Alves and Gamboa, 2020).

768 Turbidity currents and other mass flows have transported debris many hundreds (Wilson,
769 1969; Komar, 1970; Embley, 1976; Embley and Morley, 1980; Wright et al., 1983;
770 Middleton and Neal, 1989; Stoopes and Sheridan, 1992; Shanmugam, 2016) to thousands
771 (Kuenen, 1964; Stevenson et al., 2014) of kilometers. Far-transported clasts may become
772 incorporated in existing sediments, whereafter the deposits turn unstable and move as dense
773 SGFs, which after deposition displays characteristics similar to tills (Crowell, 1957; Jansa
774 and Carozzi, 1970; Walton and Palmer, 1988; Eyles 1990).

775 Slopes beneath Pleistocene and younger glaciers may vary, but often it is close to zero over
776 large areas, i.e. close to 0.001°. Slopes recorded for coarse grained turbidity flows (containing
777 gravel sized clasts) are commonly as low as 0.02-0.05° (Kuenen, 1964; Komar, 1970; Wright
778 et al., 1983; Stevenson et al., 2014; Sobiesiak et al., 2018). For debris flows the angle
779 commonly is below 1° but in places less than 0.1° (Mountjoy, 1972; Carter, 1975; Middleton
780 and Hampton, 1976; Embley, 1976, 1982; Shanmugam, 2021b), but even debris flows may
781 move over an area with lower slopes than 0.05° (Stevenson et al., 2014). Subaqueous
782 landslides have been recorded to travel on slopes of approximately 1° for almost 1000 km
783 (Yincan et al., 2017). If these slopes are compared with those in ancient "tillites," some of the
784 gentler slopes in "tillites" are steeper than for glaciers, thus indicating a possibility of SGF
785 transport, for example, in the Ordovician in Sahara 1° (Fairbridge, 1971), and in different
786 places in South America 0.25-1° (Caputo and Crowell, 1985).

787 Even though all researchers may not be aware of how common this is (de Wit, 2016a, 2016b),
788 SGFs and slides may climb upwards (e.g., Pickering and Hiscott, 2015; Nugraha et al., 2020),
789 sometimes for horizontal distances of more than 100 km (Stevenson et al., 2014). A recent
790 slide started from above the sea surface, then moved submerged for 1.5 km down to a depth
791 of 80-90 m below sea level, before it re-emerged on land and was deposited at a height of 15
792 m above sea level (Dufresne et al., 2018). A submarine slide moved uphill 500 m against a

16° slope (Tucholke, 1992), and another travelled upwards for 140 km to a height of 300 m (Moore et al., 1989). One slide (or "debris avalanche") traveled uphill to a height of 100 m at a velocity of approximately 52 m/s (Watt et al., 2012). Submarine hills and overbank levee sites which are covered by turbidites may be more than 180 m above the surrounding bottom of the sea (Abbot and Embley, 1982; Mountjoy et al., 2018), but heights between 5-120 m are commonly recorded (some covers may just by because of the thickness of the flows), and for debris flows 20 m uphill flow has been documented (Stevenson et al., 2014).

2.3.2. Erratics, transport and inclinations – differences

2.3.2.1. Size dependence

In glaciers there is no clear maximum size for transported clasts, as the competence of ice sheets is almost limitless. The Pleistocene glaciers transported scores of large clasts (both sedimentary and magmatic, e.g., Bukhari et al., 2021; Fig. 1). Even if there has been no large systematic study, Quaternary glaciations have accumulated innumerable quantities of large clasts in boulder size, which are evident almost everywhere. The accumulation of large boulders in Fig. 1D, in this single spot (which is not exceptional, but common), is more abundant than the total number of boulders present in many "tillites" covering large areas. Both in "tillites" and SGFs boulders are rarer (e.g., Molén, 2021). In Pleistocene deposits great areas are covered with thousands upon thousands of boulders even with diameters larger than one meter (Fig. 1). Erratics with diameters larger than 5-10 m are not rare, and some erratics are hundreds of meters (Embleton and King, 1968) and even many kilometers in length (Stalker, 1975, 1976). The largest known block, which might have been transported with glacier ice, measures 4000x2000x120 m (Sugden and John, 1982).

In all deposits from ancient "ice-ages" the erratics are usually not larger than a few meters in

diameter, and even erratics one meter in diameter are rare (e.g., Kulling, 1951; Flint, 1961; Schwarzbach, 1961; Hambrey and Harland, 1981; Visser and Kingsley, 1982; Visser, 1982, 1983b; Caputo and Crowell, 1983; Martin et al., 1985; Deynoux, 1985b; Haldorsen et al., 2001; Zimmerman et al., 2011; Bechstädt et al., 2018; Vesely et al., 2021). Blocks larger than five meters in diameter have rarely been reported. A common maximum clast size is 1.5-2 m, but often the largest erratics have a diameter less than 25-50 cm, and over large areas the size is only around 5 cm (e.g., Von Brunn and Stratten 1981; Le Blanc Smith and Eriksson, 1979; Visser, 1983b; Chen et al., 2020, 2021; Le Heron et al., 2021b; Vesely et al., 2021; Molén 2021).

In beds from the same area, which have been deposited by verified SGFs, or at least showing indication of quick deposition, the clast size is often larger than in supposed “tillites” or other glaciogenic material which has not been deposited by SGF processes (Molén, 2021). When these differences are documented, which is not often done, there is a clear systematic trend. For example, in LPIA deposits in South America, the “glaciogenic” beds commonly carry clasts of cobble size, while gravity or water flow deposits carry boulders of many meters in size (Rosa et al., 2019; López-Gamundí et al., 2021). And in the Neoproterozoic Namibian deposits the largest clast, many meters in size, are in massive debris flows or slides, even though these clasts at the same time had been interpreted to be dropstones (Domack and Hoffman, 2011). This systematic difference is opposite to what is expected, because glaciers can in general transport larger clasts than SGFs, without showing any evidence of flow structures.

If a SGF moves at a low velocity, if there is less water and less turbulent movement involved, and if the SGF is denser, i.e. a high-strength cohesive debris flow, then the final deposit ought to display an appearance more similar to a till than deposits from other mass movements. This might be the explanation of why deposits from “ancient ice-ages” do not contain many large

841 erratics. If a deposit from a dense SGF should not exhibit easily recognizable and extensive
842 evidence of turbulence, SGF currents and tectonic slide and slip structures, it might be that a
843 size of 1-3 m in diameter is most often the maximum size of the clasts that can be transported
844 (Komar, 1970; Clark, 1991; Talling et al., 2012; Dakin et al., 2013; Peakall et al., 2020). This
845 size of clasts is often the maximum size that has been observed moving with slow (Shepard
846 and Dill, 1966; Carter, 1975; Middleton and Hampton, 1976) and fast (Elfström, 1987) SGFs.
847 When the clasts are larger, a stronger current and/or higher buoyancy in the matrix is
848 necessary, and the sedimentary structures (e.g., fluvial, bedding and different kinds of slide
849 and load structures) will more clearly indicate that there has been a SGF, and the difference
850 between the deposit and a till is clear cut.

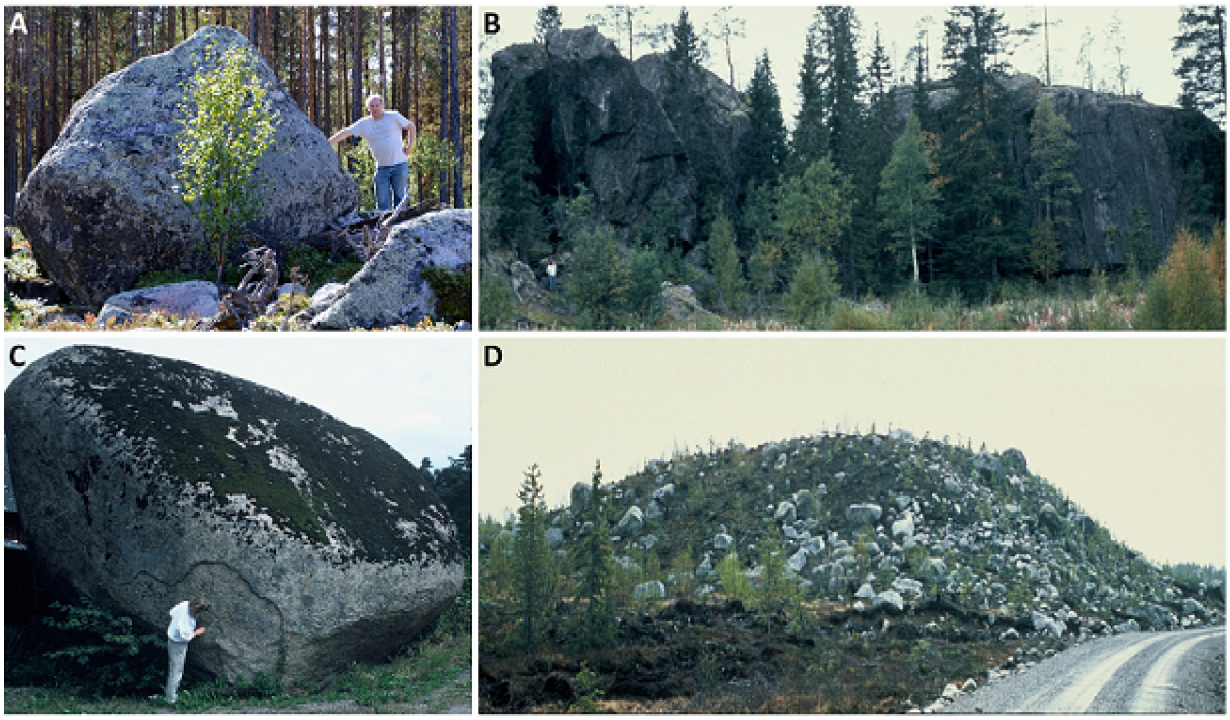

851 Fig. 1. This is the common appearance of tills and other glaciogenic material in most parts of
852 Sweden, i.e. there are innumerable large boulders everywhere. A. Clast in the jökulhaup or
853 sandur of Mettjaur, Västerbotten county, Sweden. This size of clasts is common. B. The
854 probably largest erratic clast in Europe, the Botsmark rock (split into pieces probably by a
855 local postglacial earthquake; Mörner, 2008). There is till under this piece of a mountain, so it

has not only been transported on top of the underlying bedrock. (See person in white shirt for scale.) C. Large boulder in southern Sweden, Scania. D. A Blattnick moraine, a special kind of Rogen moraine, displaying large boulders (Markgren and Lassila, 1980).

2.3.2.2. Jigsaw puzzle texture

A jigsaw-puzzle texture, where sediment has been pressed in between separate pieces of fractured clasts, are often present in mass flow deposits (Costa, 1984; Scott, 1988b; Stoopes and Sheridan, 1992; Schneider and Fisher, 1998; Legros et al., 2000; Capra and Macias, 2002; Thompson, 2009: Thompson et al., 2010; Dufresne et al., 2018, 2021). These have also been documented from "tillites" that display SGF facies (Harker and Giegengack, 1989; Bose et al., 1992; Harker, 1993; Arnaud and Eyles, 2006; Ali et al., 2018; Molén, 2021). Jigsaw-puzzle textures have not been reported from basal tills (Ui, 1989; Thompson, 2009). In stony tills clasts have been single fractured with pieces still nearly in place, and soft or weathered clasts have been transported with glaciers, but these do not display a typical jigsaw-puzzle texture (Broster and Seaman, 1991; Piotrowski et al., 2004).

In areas that may be interpreted to be subglacial, the basal unconformity below diamictites may be highly irregular and heterogenous, with areas of sediment injections into sedimentary bedrock, and "elongated boulders" of sediment displaying jigsaw-puzzle texture, but all these features are common in SGFs (Dufresne et al., 2021; Molén 2021; Le Heron et al., 2021b).

*2.4. Polished, faceted and striated clast*s

It is often assumed that glacially transported clasts exhibit more striations than clasts that have been transported by SGFs. This assumption is not well documented as there is a great

difference in the frequency of striated clasts reported from different kinds of environments (Table S1, Supplementary material).

Polished, faceted and striated clasts can form by different kinds of mass movements and by tectonic movements including by folding (Crowell, 1957; Flint, 1961; Schermerhorn and Stanton, 1963; Winterer, 1964; Schermerhorn, 1974a; Doré, 1981; Eisbacher, 1981; Rehmer, 1981; Hambrey, 1983; Martin et al., 1985; Eyles and Boyce, 1998; Atkins, 2003; Dakin et al., 2013). In SGFs there may be more striated clasts where there are more clasts (Kennedy and Eyles, 2021). Even hard quartzite can be striated in SGFs (Van Houten, 1957; Schermerhorn 1974a; Eyles, 1993), but usually most striations are exhibited by sedimentary clasts (Winterer, 1964). Clasts formed under these circumstances may be impossible to distinguish from clasts polished, faceted and striated by the action of ice-movement.

In the LPIA "tillites" of South Africa the shapes and sizes of clasts exhibit a very complex pattern which do not give any independent support to a glaciogenic origin (Hall and Visser, 1984). "Glacially shaped" so-called flat-iron clasts in the Gowganda Formation are slightly concave or convex "para-flat" with many small protuberances which shows that they cannot have been shaped by ice, and the deposits having an appearance more like a breccia that has been transported a short distance (Miall, 1985; Molén, 2021).

Even if there may be differences between striations on clasts from different environments, there are many similarities, and not all environments have been compared (Atkins, 2003, 2004). Striations on clasts in SGFs may be random and also curve around corners. Striations on glacially striated clasts may display one or more sub-parallel, or parallel, directions, usually on a flat side of the clast. But, glacially transported clasts may display striations that turn around edges or curvatures (Hicock, 1991; Hicock and Dreimanis, 1992a). Clasts that are tectonically scratched usually display strictly parallel striations, and occasionally in more than

one direction (Frakes, 1979; Kennedy et al., 2019). Photographs and reports on striated clasts in SGFs reveal that they usually have random but frequently parallel to sub-parallel striations (Winterer, 1964; Lindsay, 1966; Winterer and von der Borch, 1968; Atkins, 2004) similar to clasts from "tillites" which have striations that are random (Kulling, 1951), bend around corners (Frakes, 1979; Deynoux, 1985b) display single parallel (du Toit, 1926; Deynoux and Trompette, 1981b), and crossing parallel and sub-parallel striations (Deynoux, 1985b). Occasionally clasts in "tillites" display both tectonic and "glacial" striations so the evidence is equivocal (Aitken, 1991).

Occasionally clasts displaying "glaciogenic" climate features, like einkanter, "flutes" and ventifacts, may be described from conglomerates and interpreted to have been formed at an earlier time by glaciers (Williams, 2005). The internal structure of clasts may display an appearance of being striated, some clasts appear to be faceted after having been cleaved in flat planes, including bullet shaped clasts, and as a result, mistakes have been made in the interpretation of ancient deposits as "tillites" (Vellutini and Vicat, 1983; Rowe and Backeberg, 2011). Stoss and lee-forms on clasts may be formed in different environments where there is mechanical erosion, but in lodgement tills clasts may have double stoss-lee forms (Krüger, 1984, Benn and Evans, 1996). Double stoss-lee forms on clasts may be the only unequivocal criteria for glaciation (Krüger, 1984).

In "tillites" soft sedimentary clasts may be subangular, fresh and commonly striated, while harder basement clasts are rounded, commonly weathered and rarely striated (Schermerhorn, 1976b; Deynoux and Trompette, 1981b; Eisbacher, 1981; Deynoux, 1985b). This may be an indication for SGFs which transport older pre-weathered and pre-rounded basement clasts together with newly ripped up sedimentary clasts.

2.5. Striated, grooved and polished surfaces/pavements

925 *2.5.1. Presence of striated, grooved and polished surfaces/pavements*

926 Pavements/striated surfaces can form by many different processes, including by glaciers, sea
927 ice (Hume and Schalk, 1964; Flint, 1971; Hoppe, 1981), icebergs (section 2.7), mass
928 transport and tectonism (Sandberg, 1928; Flint, 1961; Schermerhorn and Stanton, 1963;
929 Frakes et al., 1969; Hambrey, 1983; Iverson, 1991; Eyles and Boyce, 1998; Legros et al.,
930 2000; Vandyk et al., 2021). Subaqueous flow tills may generate tool marks, but these would
931 be very restricted (Evenson et al., 1977). There are many similarities displayed by surfaces
932 produced by these diverse processes. There are also many differences in appearance which
933 usually, if they are thoroughly documented, may be sufficient to reveal the origin of various
934 striated/grooved surfaces.

935 Erosional marks are almost always formed beneath glaciers, but it is not always recognized
936 how commonly these form by different kinds of mass flows (e.g., Scott, 1988b; Dakin et al.,
937 2013; Peakall et al., 2020). Striated, grooved and polished bedrock, including chevron
938 structures/crescentic gouges/chattermarks, grooves, nailhead striae (which may be labeled
939 prod marks by SGF researchers), and deposition of fluted ridges, form as a result of different
940 kinds of mass movements. These have been documented in both ancient and recent
941 formations, including from debris flows, volcanic flows, avalanches, earth slides, tectonism
942 and other kinds of mass movements (Pettijohn and Potter, 1964; Glicken, 1996; Shepard and
943 Dill, 1966; Enos, 1969; Wilson, 1969; Harrington, 1971; Daily et al., 1973; Allen, 1984;
944 Scott, 1988b; Waitt, 1989; Blatt, 1992; Schneider and Fisher, 1998; Eyles and Boyce, 1998;
945 Atkins, 2003; Draganits et al., 2008; Dakin et al., 2013; Hu and McSaveney, 2018; Sobiesiak
946 et al., 2018; Peakall et al., 2020; Vandyk et al., 2021). Cohesive SGFs may move plastically,
947 sometimes almost like a glacier, and therefore striations, grooves and polishing will appear
948 more similar to erosion by glacier ice, at least on a local scale. This may also happen from
949 pure tectonic movements, i.e. slickensides or fault grooves which locally may display an

apperance very similar to glaciogenic striated and abraded formations including presence of crescentic fractures, flute ridges, nail head striations and striated clasts (Eyles and Boyce, 1998; Atkins, 2003; Vandyk et al., 2021). The most common tools producing marks in soft sediment, including striations and grooves, appear to be shale clasts (Hampton, 1972; Middleton and Hampton, 1976; Lowe, 1979; Clark, 1991; Peakall et al., 2020).

Debris flows may overlie grooved surfaces that are tens of kilometers long, 15 m deep and 25 m wide (Posamentier and Kolla, 2003; Peakall et al., 2020). Detailed studies of grooves formed by SGFs, have documented flows covering distances in excess of 40 km and areas of c. 300 km^2 (Peakall et al., 2020). That may explain why most pre-Pleistocene pavements are in soft sediments (e.g., Le Heron et al., 2020), as opposite to the Pleistocene and Holocene.

Examples of misidentified pavements include several meters long grooves and striations in the Triassic of Australia, which are clearly non-glacial (Gore and Taylor, 2003). On the island of Svalbard 2-3 m long striations and “ice-polished bedrock” (sandstone and shale) have been formed under the action of sea-ice and waves (Hoppe, 1981). Other “glaciogenic” surfaces exhibiting nail-head striae and “possible” crescentic gouges (Schenk, 1965) have been reinterpreted as tectonic in origin (e.g., Miall, 1985). In certain cases pavements are mentioned as evidence of glaciation, but upon investigation the descriptions appear to be erroneous and there are not even any indications of pavements (Dey et al., 2020).

2.5.2. Formation of striated, grooved and polished surfaces/pavements

Striations formed by clasts frozen to the bottom of glaciers consist of sub-parallel sets, commonly accompanied by chattermarks and/or nailhead striae (Anderson, 1983). Similar striations can, however, also be formed by SGFs, and be both parallel/sub-parallel and somewhat curved and show crosscutting to 90° but commonly < 40°, both on rock surfaces

and on soft sediment (Pettijohn and Potter, 1964; Enos, 1969; Harrington, 1971; Middleton and Hampton, 1976; Allen, 1984; Ricci Lucchi, 1995; Hu and McSaveney, 2018; Peakall et al., 2020). Tectonic striations will mostly be parallel. Soft sediment slickensides may form internally in tills (Evans et al., 2006), but commonly the appearance of slickensides is very different from striations and grooves.

At the sole of warm-based glaciers clasts gradually reorient, horizontally and vertically, such that striations and grooves will always change their appearances (Iverson, 1991). There is a debate concerning whether cold-based glaciers move, but a clast at the bottom of a glacier is never frozen with no internal movement within the ice and striations are varied in appearance (Atkins, 2004, 2013). Glacial striations of Pleistocene age, on sedimentary bedrock may display a superficial appearance similar to striated surfaces below SGFs, as they are parallell and straight for short distances (Fig. 2A). But such glaciogenic striations bear evidence of sideways horizontal and vertical movements (Iverson, 1991), and commonly are short (e.g., 0.05-1 m; Sokołowski and Wysota, 2020), even if the features are not incompatible with some mass flow striations.

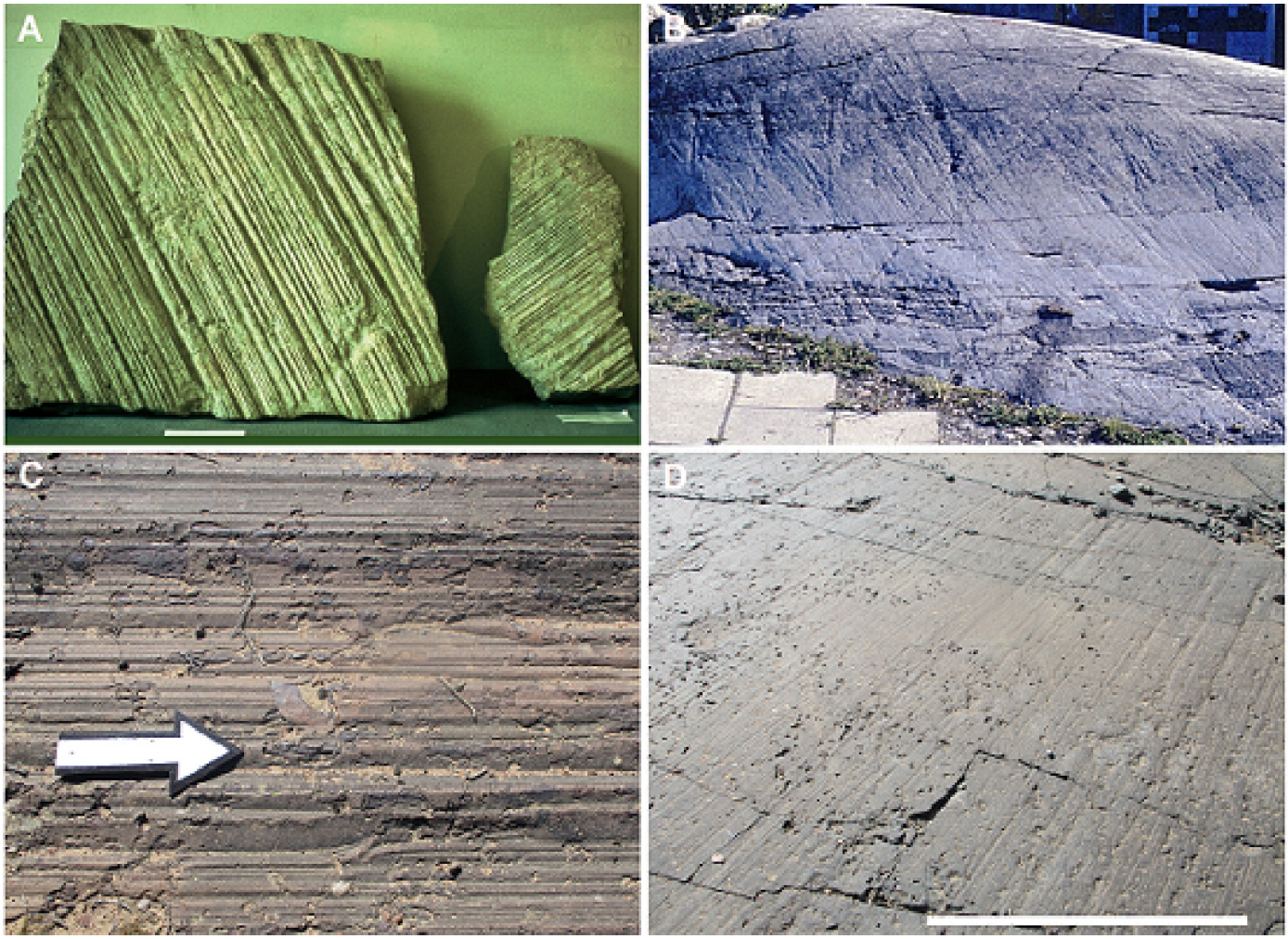

Fig. 2. Pavements. A and B are Pleistocene (Weichselian), C and D are LPIA. A. Glacial striations in Silurian limestone (Gotland, Sweden). The striations in the limestone show superficial similarities to some striations from SGFs in soft sediments. But, the evidence of horizontal and vertical wobbles of the clasts from within the glacier is clearly apparent, if only looking a little bit more in detail on the picture. (Gotlands Museum, 1986. Pieces of paper are c. 10 cm.) B. Glacial striations on the stoss side of a roche moutonée in magmatic bedrock (University of Stockholm, Sweden). At the roche moutonée the striations and grooves are short, irregular, and subparallel. C. Soft sediment LPIA “glaciogenic” striations which are perfectly similar to those formed by SGFs, i.e. straight an parallell and no or little evidence of vertical or sideways wobbles of the tools making the striations and grooves (Oorlogskloof, South Africa, arrow is 25 cm) (Draganits et al., 2008; Peakall et al., 2020; Molén and Smit, 2022). D. LPIA striations on Precambrian andesitic lava (marker is c. 1 m) (Douglas, South Africa). The striations are almost exactly parallel for a distance of more than

50 m (variation is reported as approximately 1° by Stratten and Humphreys, 1974).

2.5.3. Differences displayed by striated, grooved and polished surfaces/pavements

SGFs and slides generate a number of features on surfaces, including different grooves and striations, which are seldom or never generated with similar appearances below glaciers. Striated and grooved surfaces displaying such appearances, i.e. those that are generated by mass flows, are common in areas where there are pre-Pleistocene "tillites." For example, during the Paleozoic the majority of "subglacially formed pavements" are in unlithified sand (Le Heron et al., 2020; Fig. 2C), whereas similar surfaces are very rare or non-existent in Pleistocene and more recent deposits. A number of the appearances of striated surfaces displayed by SGFs are documented in the list below. Most of these appearances are documented by Peakall et al. (2020) and Baas et al. (2021).

a) SGFs commonly display straight movements, often for hundreds of meters or more, and extensive striated and grooved surfaces may be generated in time periods of only seconds or minutes (Piper et al., 1999; Peakall et al., 2020; Baas et al., 2021). Debris flows have traveled at a speed of 500 km/h (Shanmugam, 2002).

b) Grooves are often parallel, display constant rounding, depth and width, may display parallel internal striae, and occasionally raised lateral ridges (Peakall et al., 2020, Baas et al., 2021).

c) SGFs may pass areas without leaving much traces. This is shown by the presence of bypass zones, which can be tens of kilometers, where there is no erosion (Moscardelli et al., 2006; Georgiopoulou et al., 2010; Talling et al., 2012; Stevenson et al., 2014; Cardona et al., 2020; Peakall et al., 2020; Baas et al., 2021).

d) Stacked striated surfaces are common in SGFs, with more or less vertical and horizontal distance between these surfaces, i.e. in some areas the striated surfaces even shift

stratigraphic position and move up and down through the beds as a result of different movements during deposition (Enos, 1969; Petit and Laville, 1987; Draganits et al., 2008; Le Heron et al., 2014; Peakall et al., 2020). (Fig. 3.) Similar stacked striated surfaces are not observed from Pleistocene or more recent deposits where it is known that glaciers were the depositional agent (Trosdtorf et al., 2005a). Stacked striated/grooved surfaces commonly display similarities to what has been labeled “tectonic hydroplastic slickensides” or “internal grooves and striations” in SGFs that form in soft sand (Enos, 1969; Petit and Laville, 1987; Deynoux and Ghienne, 2004, 2005; Le Heron et al., 2005, 2014), while some are stacked slickensided (or slickenlined) clay or mud (Simms, 2007; Cesta, 2015; Rodrigues et al., 2020). Woodworth-Lynas and Dowdeswell (1994), Vesely and Assine (2014), and Rosa et al. (2019) interpreted single and stacked soft sediment surfaces as evidence for ice-keel scouring by icebergs. Such an interpretation was not accepted for “glaciogenic” striated surfaces in the Ordovician of northern Africa, that was interpreted as hydroplastic and formed simultaneously by tectonics and pressure from below thick glaciers (Deynoux and Ghienne, 2004, 2005; Le Heron et al., 2005, 2014). (Iceberg keel grooves are discussed in section 2.7.)

e) Traction carpet sediments are common between striated surfaces and superposed diamictite debrites. The sediments may be striated, and may be a stratigraphic plane where clasts commonly glide (Moscardelli et al., 2006; Georgiopoulou et al., 2010; Talling et al., 2012; Dakin et al., 2013; Cardona et al., 2020; Peakall et al., 2020; Molén and Smit, 2022). Thin basal layers of sediment are not present between Quaternary tills and pavements, even if a process for the origin of such sediments could be hypothesized during special circumstances in rare and confined environments.

f) Contacts below “tillites” may display overhanging walls (Miall, 1985; Molén 2021) or channels (Moncrieff and Hambrey, 1988) which may exhibit striations (Frakes and Crowell, 1970; Armentrout, 1983). This may result from erosion by SGFs rather than from glaciation, with or without striations (Scott, 1966; Shepard and Dill, 1966; section 1.4.).

Table S2 (Supplementary material) lists striated surfaces which display similar appearances as mass flows, from striated surfaces/pavements which had been interpreted to have formed by glacial ice. Even though all appearances of pre-Pleistocene striated surfaces have not been observed in recent deposits, and some are difficult to fully explain, the evidence documented in Table S2 display similarities to striated surfaces which have a mass transport or a tectonic origin, rather than a glaciogenic origin. In conclusion, similar pavement features commonly do not form, or have never formed, by Pleistocene or younger glaciers, and therefore these "pavements" are better explained by a mass transport origin rather than by glaciation.

Fig. 3. Four soft sediment stacked sandstone striated surfaces, LPIA, Dwyka Group, Oorlogskloof, South Africa. These surfaces are perfectly similar to those made by SGFs (Draganits et al., 2008; Peakall et al., 2020). The regular appearance of the grooves show no similarity with glaciogenic surfaces.

2.6. Striated, grooved and polished surfaces, rock polish

Mechanically abraded rock surfaces formed beneath glaciers may display a thin glossy coating layer. Such glacial polish is typically a few micrometers thick, consisting of minute transported clasts and mineral fragments in a fine-grained amorphous matrix of nano-sized phyllosilicates. The observations suggest bending and fracturing of the uppermost part of the original bedrock, followed by smearing of clast fragments and amorphous material on top of the bedrock surfaces (Siman-Tov et al., 2017). Variants of such surfaces may also be generated in fault zones. Except for formation by mechanical shearing, an appearance of rock polish may result from purely chemical precipitation (Bussert, 2010; Molén, 2017).

Striated and grooved surfaces below Neoproterozoic diamictites, commonly interpreted to be "tillites," have been shown to be at least partly formed by post-depositional chemical modification, and there is "polish" even on striations with rugged surfaces (Molén, 2017). Surfaces on Ordovician "glaciogenic" soft sandstone surfaces display cataclasis of mineral grains, but not amorphization and smearing of clast fragments (Denis et al., 2010). Ichno-fossil Tigillites burrows at this striated surface remains undeformed, which would be quite exceptional if a glacier would have passed the soft sediment area (Denis et al., 2010). In Chinese Ediacarian-Cambrian sediments "glaciogenic" polish is mentioned to occur on apparently soft sediment surfaces, where striations also have been formed inside the diamictite, above a surface displaying perfectly straight striations in two directions, but occasionally curvilinear (Le Heron et al., 2018b). None of these polished surfaces displays more than superficial similarities to polish on Quaternary pavements.

A recent rock avalanche in China, initially moving as a "water-saturated, dense grain flow," passing over dolomitic black shale, formed a surface "highly reminiscent of a classical striated rock pavement from beneath a glacier," displaying polish and chemical precipitation (Hu and McSaveney, 2018). Polish, melting and precipitation are formed in realistic mechanical experiments and from landslides (Legros et al., 2000; Hu and McSaveney, 2018).

Heat is always produced by friction, and large mass flows or slides could under certain circumstances probably generate high temperatures, capable of creating polish and lithifying the underlying surface (compare to a pavement where temperatures of c. 1000°C have been suggested below an outcrop commonly interpreted to have been deposited below glaciers; Bestmann et al., 2006; Molén, 2017).

2.7. Striated, grooved and polished surfaces, iceberg keel scour marks

Ice scour marks form when keels of icebergs and sea or lake ice press up ridges and plough through unconsolidated sediments. Some of the pre-Pleistocene soft sediment surfaces which have been interpreted to be formed by glaciers, had been interpreted to be from icebergs or sea ice (Woodworth-Lynas, 1992; Woodworth-Lynas and Dowdeswell, 1994; Vesely and Assine, 2014, who reinterpreted 17 soft sediment surfaces as generated by icebergs; Rodríguez-López et al., 2021: Table S2, Supplementary material) while others refrain from such an interpretation (Deynoux and Ghienne, 2004, 2005; Le Heron et al., 2005, 2014, 2020). Similarities between SGFs, single moving clasts, and iceberg scours, include cases where the underlying sediments become depressed. Similarities also include berms that may be pushed up next to iceberg scours, in size from a few centimeters to many meters high, and similar linear ridges which may form by SGFs next to single clasts which are moving at the bottom, and even sometimes by running water. Non-glacial push up and sedimentary linear structures may be labeled lateral ridges, flowbands, or sometimes levees (e.g., Dufresne and Davies, 2009; Kneller et al., 2016; Peakall et al., 2020; Procter et al., 2021).

Quaternary ice keel scour marks may be more than 20 km long, depth may be 80 m, and they may be up to 1 km wide. They may form at depths of more than 600 m, but are more common at depths of 60-400 m or less (Woodworth-Lynas, 1992; Woodworth-Lynas and Dowdeswell, 1994; Dowdeswell and Hogan, 2016). In SGFs isolated outrunner blocks, up to many

hundreds of square meters in size, are common, and have traveled many kilometers over very low gradients e.g., 0.3-0.4°, and have made long glide tracks and scour marks in the sea bottom (Prior et al., 1982; Nissen et al., 1999; Ilstad et al., 2004; Moscardelli et al., 2006; Festa et al., 2016, Nwoko et al, 2020b, Kumar et al., 2021). Larger outrunner blocks, in kilometer-sizes, have outrun the main slide deposits for c. 10 km and have excavated megascours that, including the basal erosion within the main slide deposit, are 1 km wide, 150 m deep and 70 km long (Soutter et al., 2018). SGFs may make deep scours that turn through about 45°, and then split into many smaller <10 m deep scours (Moscardelli et al., 2006). There may therefore by at least superficial similarities between ice keel scour marks and mass flow processes, and in at least one case they are known to have formed in a non-glacial turbidity current environment (Scott, 1966). “Iceberg grooves”in the Paleoproterozoic of India were only between 1.2-7.8 cm wide, and 9.2-13.1 cm deep, and pointing in the direction of 66-68° from the surface (instead of close to 90°) (Rodríguez-López et al., 2021). This gives them an appearance of small fractures induced only by short sediment movement, and these were later (quickly) filled with sandy laminated sediments.

In a few instances grooves below “tillites” are curved (Bryan, 1983), up to an angle of 90° in one meter (Fairbridge, 1979), and they may still be parallel after they changed direction (Allen, 1975). This is believed to result from overturning of iceblocks, or from changed wind or current direction that diverted icebergs with clasts frozen to their bottom. However, from different mechanisms, SGFs may turn, at occasions even 180°, and therefore the direction of sole structures also will change (Enos, 1969; Kneller et al., 1991; Pickering et al., 1992; Butler and Tavarnelli, 2006; Draganits et al., 2008; Peakall et al., 2020).

Woodworth-Lynas (1996) published a detailed list of features generated by icebergs, and an update of a few of the more important of these which can be readily studied in ancient lithified restricted outcrops in the field, are mentioned below:

a) In the Quaternary there is an abundance of ice-keel scours generated by icebergs over a total approximate area of $10x10^6$ km^2 (Woodworth-Lynas and Dowdeswell, 1994). The complete bottom surface may be covered by a network of ice-scour marks, occasionally displaying straight directions but commonly curvilinear and often in many different directions (Woodworth-Lynas, 1992; Woodworth-Lynas and Dowdeswell, 1994; Batchelor et al., 2020). Because of e.g. tides, there are examples of looped or spiralling iceberg scour marks (Woodworth-Lynas et al., 1985; Newton et al., 2016). Different from Quaternary sediments, large grooves which have been interpreted as ice scour marks in pre-Pleistocene environments (commonly in sand) are often single, but if many soft sediment surfaces are superposed or next to each other they are pointing in the same direction (different from stacked soft striated surfaces in recent tidal mud sediments; Woodworth-Lynas, 1996), and they often display exactly parallel grooves and striations within the scour.

b) There may be grooves and striations within ice-scour marks (Batchelor et al., 2020), and if so these are subparallel, i.e. different to parallel grooves and striations commonly generated beneath SGFs (section 2.5.).

c) Commonly pre-Pleistocene surfaces which have been interpreted to be iceberg keel scours, are horizontal, while more recent marks may be undulous in cross-section and display small scale faults induced by iceberg loading (Thomas and Connell, 1985; Woodworth-Lynas and Guigné, 1990). Wave action and diurnal tides are documented from ice-berg keel scour marks in Quaternary sediments (Woodworth-Lynas and Guigné, 1990; Bennett and Bullard, 1991), and there should be evidence of constant changing vertical movements below icebergs. There is also documentation of up to 2 m high and 20-40 m wide orthogonal or perpendicular ridges, asymmetric in cross-profile, that are interpreted to have been produced from tides during the Quaternary (Dowdeswell and Hogan, 2016; Batchelor et al., 2020).

d) Ring structures, a few decimeters high and wide, made from up to 50 m large chunks of shore ice, are formed today in Canada (Dionne, 1992). Similar forms produced by icebergs, i.e. grounding pits, may be 10 m deep and 50 m in diameter (Dowdeswell and Ottesen, 2013;

Batchelor et al., 2020). Similar structures have not been reported from the pre-Pleistocene.
e) There are micromorphological criteria for iceberg keel scours (Linch and Dowdeswell, 2016) which have been used to interpret the origin of a pre-Pleistocene soft-sediment striated pavement as not formed by icebergs but by a grounded icemass (Le Heron et al., 2020).
f) There are grounding-zone wedges showing clear evidence of still-stands or re-advances of glaciers, up to 15 m high, which have not been registered from the pre-Pleistocene (Batchelor et al., 2020).
g) Large areas (kilometers) display up to 2 m high asymmetric or sinuous corrugation ridges that are transverse to the strike of the glaciers, which are easily explained by tide-water fluctuations during glacial retreat (Batchelor et al., 2020). Similar structures have not been documented in the pre-Pleistocene.

In conclusion, if there is evidence of a series of vertical and sideway movements, from tides, waves wind or currents, and subparallel grooves/striations, an iceberg keel origin of scour marks may be a better option of interpretation than other processes. Other data may be of help, as mentioned above, but the evidence from movement is diagnostic.

2.8. Boulder pavements

There are many boulder accumulations with a more or less flat upper surface which geologists have described as boulder pavements. Hansom (1983) described boulder pavements which probably originated by winnowing out of fine material from glacial till on beaches. Close to the continental shelf/continental slope boundary (Boulton, 1990), or anywhere below sea level where there is net erosion, the fine material will be winnowed out and leave the boulders. In other places, pavements originated where sea ice had forced boulders into the underlying substrate (Hansom, 1983). Hara and Thorn (1982) described fluvial boulder beds which had been modified by periglacial processes as “subnival boulder pavements,” and frost

heaved boulders that display “flat” tops because of gravity but not paving. During drainage of dammed lakes, boulders can accumulate to form a deposit exhibiting a flat upper surface, called a boulder delta (Elfström, 1987). The Mount St. Helens eruption generated a lahar that cut volcanic boulders and produced “... a surface similar to a glacial pavement cut in conglomerate” (Scott, 1988a), and more or less planar boulder accumulations are present in other SGF deposits (Best, 1992). What appears to be boulder or pebble trains (which may be described as boulder pavements) may be formed by SGFs, but are often present in “tillites” (Bussert, 2014; Kennedy and Eyles, 2019).

The Pleistocene “classical” inter- and intra-till boulder pavements are usually only one layer thick (Clark, 1991; Hicock, 1991). These have been suggested to originate possible by a process slightly similar to debris flows, where boulders sink down into fine-grained till and after that deforms by overriding glaciers (Clark, 1991; Hicock, 1991). It would therefore be difficult to differentiate this kind of pavement from boulders that have accumulated from debris flows (Lowe, 1979, 1982).

Boulder pavements are common in pre-Pleistocene “tillites” (e.g., Lindsay, 1970a; Gravenor, 1979; Rocha-Campos and Santos, 1981; Martin, 1981a; Von Brunn and Stratten, 1981; Visser, 1983b; Caputo and Crowell, 1985; Visser and Hall, 1985, López-Gamundí et al., 2016). but are more seldom reported from the Pleistocene (Derbyshire, 1979).

Pre-Pleistocene boulder pavements are often located at the base or top of “tillites.” Boulder pavements have been a) traced back to channel deposits (Lindsay, 1970a), b) described as bevelled dropstones (Moncrieff and Hambrey, 1988), c) formed by a local fault and covered by calcite (González and Glasser, 2008), and d) described as boulders lined up after each other, with a decrease in size both upstream and downstream, thus showing affinities to pebble trains in streams (Dal Cin, 1968). Boulder pavements are most common in the Dwyka

Group in South Africa, and display many different appearances. The basal “tillite” in the southern part of the Dwyka Group commonly is capped with a bed of boulder “tillite” at the top of an upwards coarsening sequence (Visser and Loock, 1982), and boulder accumulations may grade upwards into conglomerates labeled boulder rudites. One boulder pavement displays single imbricated beds (Visser and Hall, 1985) more typical of debris flow, tsunami or cyclone deposits (Shanmugam, 2012, 2021b). Boulder beds may be up to 12 m thick, and display moderate sorting (Visser and Hall, 1985). In places boulders have accumulated on the lee side of an obstacle (Visser and Loock, 1988) or are described as a lag deposit of a single layer of boulders at the base of sandstones (Visser et al., 1987).

An origin of boulder pavements by SGFs seems at least as possible as an origin beneath a glacier, by winnowing out of material, by reversed grading, or simply by the common upwards movement of large clasts which takes place in SGFs (section 2.13.1.1.). The differences between ancient and Pleistocene inter/intra-till boulder pavements may be considerable.

2.9. Erosional landforms, lineations

There will always be superficial similarities between landforms generated by different processes, including at the boundary layer in different environments (Stokes, 2018), whether it be glaciers, running water or mass movements. The direction of movement and the cohesiveness or plasticity of the moving medium will generate features which may display different appearances.

Commonly sea bottoms are sculptured and grooved over large areas by SGFs or slides. Ice streams mold large areas into streamlined landforms, i.e. lineations, sediment into drumlin-like forms, and through erosion of bedrock they produce linear landforms (Eyles et al., 2018).

Lucchitta (2001) studied subaqueous (glaciogenic) lineations at the Antarctic shelf, and concluded that they were similar to glaciogenic lineations on Mars. However, the lineations on Mars, including gigantic outflow channels, are probably formed by catastrophic water release from subsurface groundwater reservoirs, i.e. large scale tectonism and fissures releasing water, and not by glaciers (Baker and Milton, 1974; Baker and Kochel, 1979; Burr et al., 2002; Plescia, 2003; Rodriguez, 2005; Leask et al., 2007). Similar lineations were produced by catastrophic release of water and debris flows triggered by the failure of Mount St Helens stratocone (Major et al., 2005), the formation of the English Channel and the Channeled Scablands in Washington (Plescia, 2003; Gupta, 2007; Gupta et al., 2007, 2017). Other landforms in unconsolidated sediments or bedrock, heading in different directions, formed subaqueously or subaerially, including 60 km long channels/megascours and lineations with dimensions of up to many tens of km long, 6-8 km wide, and 600 m deep, from SGFs, and in places they are U-shaped (Best, 1992; Moscardelli et al., 2006; Robinson et al., 2017; Ortiz-Karpf et al., 2017; Nwoko et al., 2020a, 2020b). Lineations, tens of kilometers long, up to 10 m high, and with wavelengths of 100 m, also are formed by density-driven sediment and water movement, during seasonal weather conditions (Canals et al., 2006). A slide generated c. 30-120 km long, 100-600 m wide and 10-30 m deep grooves (Gee et al., 2007), which may be labeled lineations, but such forms may be labeled striations by marine geologists (e.g., de Blasio, 2006; Gee et al., 2007; Nwoko et al., 2020a). Smaller lineations, e.g., only 0.4-1.5 m high and spaced at 5-7 m, may also be formed by SGFs (Piper et al., 1999).

In the Quaternary, there are megalineations that excessively outnumber those that are interpreted from the Paleozoic, both in areal size and evidence of large-scale energy impact during geological processing. These cover extensive areas, both subaqueously and subaerially, with both soft (drumlinised sediment) and hard (rock drumlinoid) forms (Margold et al., 2015; Dowdeswell et al., 2016a, 2016b; Eyles et al., 2018; Stokes, 2018;

Bukhari et al., 2021), contrasting with Paleozoic surfaces which are interpreted to be megalineations. In some areas there are also numerous, up to kilometers long and wide, transverse ridges (Stokes, 2018; Batchelor et al., 2020). The present author knows of no transverse ridges on lineations interpreted from the pre-Pleistocene. Pre-Pleistocene ice streams and lineations appear to be more sinuous, partly anastomosing or amalgamated, follow an outline similar to a SGF where they also change direction, are often parallel to the strike of the underlying bedrock, and are shorter and wider (see figures and descriptions in Andrews et al., 2019). Similar structures form by SGFs and slides, but may be labeled striations (Gee et al., 2005, 2007; Macdonald et al., 2011). Other areas displaying megalineations interpreted from Google Earth from sandstone plateaus in Chad (Le Heron, 2018), display many different surface structures when investigated at greater detail including an underlying "dipping substrate" (Le Heron, 2018), rather than ice streams.

Single linear landforms, including those which are drop formed, which display similarities to landforms that are interpreted to be glaciogenic (Assine et al., 2018), form by catastrophic outbursts of water which may or may not have any connection to glaciation (Burr et al., 2002; Plescia, 2003; Gupta, 2007; Gupta et al., 2007, 2017; Robinson et al., 2017), and also from SGFs (Dufresne and Davies, 2009), and may be labeled "whaleback bars" (Scott, 1988a) or "shadow remnants" (Moscardelli et al., 2006).

Pre-Pleistocene roches moutonnées have often been reported, but these often display steep stoss sides and gentle lee sides (e.g., Frakes and Crowell, 1970; Visser and Loock, 1988; Bussert, 2010; Assine et al., 2018), as opposed to Pleistocene roches moutonnées. They may therefore be interpreted to be whalebacks or rock drumlins. Some "roches moutonnées" seem to have their stoss side undercut by erosion (Frakes and Crowell, 1970, their Fig. 6C) – a more likely phenomenon to take place below a SGF or in running water than below a glacier. Others have been shown to be a product of tectonics and fluvial erosion on structurally

controlled bedrock features (Vandyk et al., 2021). There is a large difference between the number of "roches moutonnées" and other small scale erosional landforms in pre-Pleistocene formations compared to younger formations, as they are almost all-present in Pleistocene and Holocene glaciogenic formations.

Bedrock forms, especially those in magmatic rocks, should be better preserved than sediments in the rock record, but there is no extensive record evident from ancient "tillites."

2.10. Erosional landforms – plucking

A process similar to glacial plucking may be caused by SGFs and fluvial action, including on the surface of magmatic bedrock (Dill, 1964, 1966; Shepard and Dill, 1966; Carter, 1975; Tinkler, 1993; Whipple et al., 2000; Stock and Dietrich, 2006; Dakin et al., 2013; Lamb et al., 2014; Hodgson et al., 2018; Vandyk et al., 2021). So-called p-forms (or s-forms) may be formed by non-glacial fluvial currents (Tinkler, 1993, Vandyk et al., 2021), even though they often are interpreted to be formed subglacially (Le Heron et al., 2019a; Chen et al., 2020; Vandyk et al., 2021). Additionally, there is a debate whether fluvial landforms which are similar to glaciofluvial landforms, have been produced by tsunamis or storm waves (Bryant and Young 1996; Burgeois, 2009; Shanmugam, 2012; Lascelles and Lowe, 2021). Cavitation may be one process responsible for plucking (Falvey, 1990). Another process that display slight similarities to glacial plucking is more like delamination, i.e. detachment of soft sediments or clasts and entrainment into SGFs (e.g., Butler and Tavarnelli, 2006; Clark and Stanbrook, 2009; Butler and McCaffrey, 2010; Dykstra et al., 2011; Fonnesu et al., 2016; Sobiesiak et al., 2016; Eggenhuisen et al., 2011; Hodgson et al., 2018; Ogata et al., 2019; Cardona et al., 2020; Kennedy and Eyles, 2021), and where the delaminated sediments have later been lithified (which is what commonly takes place, as can be seen almost everywhere in the complete geologic rock record). If plucking leaves a jagged and uneven surface, and no

later polishing (Miall, 1985), this indicate plucking by SGFs and not by glaciers (Molén, 2021).

2.11. Glacial and non-glacial valleys and fjords

2.11.1. Glacial and non-glacial valleys – general appearance

Many processes create valleys. Steep incisions hundreds of meters deep may be consistent both with glacial action and fluvial erosion driven by pure tectonic rift uplift (Vandyk et al., 2021). Hanging valleys are surprisingly common in non-glaciated areas, including in magmatic and metamorphic rocks, both subaqueously and subaerially (Dill, 1964; Sheppard and Dill, 1966; Erginal and Ertek, 2002; Mitchell, 2006; Wobus et al., 2006; Crosby et al., 2007; Lamb, 2008; Amblas et al., 2011; Harris et al., 2014; Normandeau et al., 2015). Such valleys could be the equivalent of "glacial" hanging valleys that have been interpreted from the Dwyka Group in South Africa (Visser, 1982; Hancox and Götz, 2014). "Glacial valleys" an basins in the LPIA of Namibia and Brazil, are "pre-glacial" in places including with examples of streamlined and striated landforms that are interpreted to be e.g. roches moutonnées (Martin, 1981b, Santos et al., 1996; Dietrich et al., 2021; Rosa et al., 2021).

Submarine canyons are preferentially eroded in "resistant bedrock" (i.e., metamorphic, igneous and lithified sedimentary bedrock; Moosdorf et al., 2018) and next to the coast, and c. 1000 canyons are present at the Last Glacial Maxium and later shorelines (Bernhardt and Schwanghart, 2021). Isostatic movements could have elevated pre-Pleistocene submarine canyons above the present sea surface, giving these an appearance of having been carved by glaciers.

Approximately a thousand non-glacial channels or scours, on slopes as low as 0.02°, which

are up to kilometers in depth and many kilometers in width and length, have been documented, and this is only from the northeast Atlantic margin (Macdonald et al., 2011). Channels are common in mass transport deposits (Kneller et al., 2016; sections 2.2.8, 2.7.-2.9.). Smaller channels are common on fan deposits (Shanmugam, 2016). Initial V-shaped grooves or "megalineaments" up to tens of kilometers long, 6-8 km wide and 600 m deep, formed by mass flow transport, may turn into larger U-shaped valleys during movement (pictures in Ortiz-Karpf et al., 2017). Megascours, up to 1 km wide, 150 m deep and 70 km in length, some with a basal slide surface of 7000 km^2 and moving down slopes of c. 1.1° for 290 km, some formerly interpreted as submarine channels, some with extremely irregular basal boundary geometry, had originated by erosion from debris flows and slides (Dakin et al., 2013; Sobiesiak et al., 2018; Soutter et al., 2018).

All this variation and similarities need to acknowledged when the origin of ancient valleys is the question for study.

2.11.2. Glacial and non-glacial valleys – shape

Glaciated valleys are commonly U-shaped, and fluvial valleys are commonly V-shaped (Montgomery, 2002; Prasicek et al., 2014). But glaciogenic tunnel valleys may be both V-shaped and U-shaped (van der Vegt et al., 2012). And U-shaped valleys are produced by many non-glacial processes and in different environments, i.e. in pull-apart basins (Gürbüz, 2010; Fedorchuk et al., 2019), by slides, rivers and SGFs (Woolfe, 1994; Ebert, 1996; Lamb, 2008; Giddings et al., 2010; Amblas et al., 2011; Macdonald et al., 2011; Clarke et al, 2012; He et al., 2013; Vachtman et al., 2013; Coles, 2014; Ortiz-Karpf et al., 2017; Pauls et al., 2019; Isbell et al., 2021), in submarine canyons (Imbo et al., 2003; He et al., 2013; Gales et al., 2014; Pehlivan, 2019; Puga Bernabéu et al., 2020; see also Kumar et al., 2021), and by lowering of the sea level (compare descriptions in Germs and Gaucher, 2012 to Sial et al.,

2015; and also Giddings et al., 2010 to Bechstädt et al., 2018). Coles (2014) wrote: “In fact fluvial valleys occupied a wide range of valley shapes, not simply the V-shape referred to in previous, particularly glacial orientated, literature. This means these idealized forms cannot be solely used to distinguish between glacial and fluvial valleys.”

2.11.3. Glacial and non-glacial valleys – fjords

Fjords are distinctive overdeepened narrow valleys. They are most shallow at the outlet where there is a “sill” or ridge of any material, but commonly bedrock (Fig. 4), which can be more than 1 km higher than the deepest parts of the fjords (Mangerud et al., 2019). Fjords are very common in the Pleistocene and Holocene, almost 1800 are recorded (Syvitski and Shaw, 1995), and these would easily be preserved in the rock record. However, there is a very poor record of ancient fjords. The few examples reported in the literature mainly document sedimentary infill of valleys, they do not display the typical fjord appearance with e.g., a ridge at the outlet, and may display uneven and irregular floors (Bowen, 1969; Visser, 1987; Kneller et al., 2004; Bussert, 2010; Alonso-Muruaga et al., 2018; Bechstädt et al., 2018; Moxness et al., 2018; Fedorchuk et al., 2019; Dietrich et al., 2021; Vesely et al., 2021). Landforms interpreted as fjords/glaciated valleys, including documented striated and abraded landforms, may have been formed by tectonics combined with SGFs and fluvial erosion (sections 2.5, 2.9-2.11.1).

Fig. 4. The smallest fjord observed by the present author, Vassdalsvatnet, Lofoten Peninsula, Norway. The length of this fjord is around 400 m, but it has the same appearance as all other fjords, i.e. it is deepest in the middle and displays a ridge at the outlet. There are actually two ridges in this fjord, similar to what may be present in some larger fjords. One is next to the road and another one is sticking up through the ice as a small island (in the middle of the picture). In the same area there are more small fjords with slightly greater lengths and depths.

2.12. Glaciofluvial deposits

Any strong water currents produce similar features, e.g., compare González and Glasser (2008) to Lamb et al. (2014). Lang et al. (2020) described bedforms in glaciogenic settings generated by "supercritical" currents and wrote: "individual bedform types are generally not indicative of any specific depositional environment." Further, they stated that glaciogenic "upper-flow regime bedforms" are rare in pre-Pleistocene deposits, and provided only five examples from pre-Pleistocene environments and all from Upper Ordovician "glaciogenic"

sandstone areas (Lang et al., 2020).

Only when water flow is restricted by ice, and no other obstacles are present, there may be differences. All kinds of glaciofluvial deposits where ice restricted the flow of water, e.g., in kames (Fig. 5B), englacial and supraglacial eskers, lateral channels, crevasse fillings, etc., are missing from ancient deposits. These structures ought to be the more diagnostic features, as opposed to the often documented "glaciofluvial" or fluvial outwash and channel sandstones which can form in a wide variety of environments.

2.12.1. Eskers

Pleistocene eskers are commonly well sorted, often large boulders at the bottom center, then followed by finer clasts and sand (Fig. 5A). Their appearance is like linear conglomerates, but mostly sand higher up in the stratigraphic sequence. This general and most important structural configuration of eskers is the most significant difference compared to pre-Pleistocene linear landforms which are interpreted to be eskers. Furthermore, there are no reports of erratics on top of or close to the top of pre-Pleistocene "eskers," which is a common phenomenon for Pleistocene eskers (Frakes, 1979). Only a few reports mention "glacial" tectonic disturbances in pre-Pleistocene "eskers" or "tunnel valleys," similar to ice-push structures, ice-block load structures and lateral slump and slide structures displayed by Pleistocene eskers (Allen, 1975; Biju-Duval et al., 1981).

Sediments which are interpreted to be pre-Pleistocene eskers are rarely reported (Vesely et al., 2021). There are, however, sandstone channels in many places which show superficial similarities to eskers. These are mainly present in the Upper Ordovician and many may have been reinterpreted to be tunnel valleys (see below). LPIA linear sandstone bodies in South America which had been interpreted to be eskers are commonly short but may be up to 100 m

long and display about the same width (1.5-2 m) as height (1-2.5 m) (González and Glasser, 2008), while common width/depth ratios for eskers lie between 2 and 20 (Vesely et al., 2021). These “eskers” display occasional thin layers of pebbles, and are covered by “tillite” (González and Glasser, 2008). There are also debris-filled (e.g., conglomerates) channels in the same area which earlier had been interpreted to be eskers (González and Glasser, 2008).

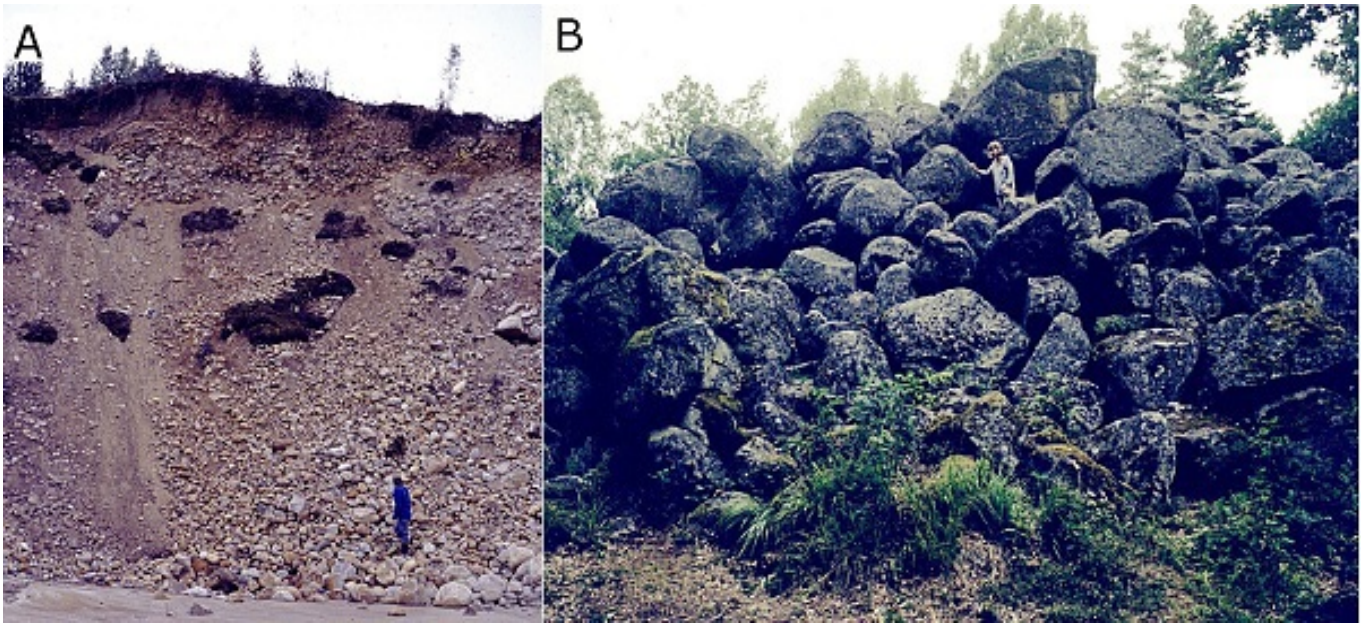

Fig. 5. A. Esker in Västerbotten county, Sweden. Boulders of different sizes and sand are sorted into different zones. Upper zone is winnowed out (below highest coastline). Commonly eskers consist of more sand and smaller boulders than the esker in the picture. B. A kame, i.e. a “short esker hill.” This one is exceptional as it mainly consists of very large boulders. Antamåla rör, Småland county, Sweden (Lundqvist, 1979).

2.12.2. Tunnel valleys

Ordovician and LPIA geologic features which have been interpreted as tunnel valleys (but sometimes may be interpreted as ice stream valleys) are commonly made up of sandstone.

These may be tens of kilometers long, tens of meters to occasionally more than 300 m deep, more than 1 km wide, linear or slightly sinuous, and may display amalgamation or an anastomosing network (Le Heron et al., 2004; Le Heron. 2010; Vesely et al., 2021). These tunnel valleys display many similarities to other types of valleys with which they can be confused. They are in many respects similar to fluvially eroded valleys (e.g., Baker and Milton, 1974; Gupta et al., 2017; Zaki et al., 2018, 2020, 2021). In some ways, they are similar to quickly formed slump-generated recent megachannels, but the sedimentary material is almost only sand in the Paleozoic valleys but richer in clay in recent valleys which may explain structural differences in appearance (Eyles and Lagoe, 1998). Tunnel valleys also resemble tidal channels (except for depth, up to 60 km long, 3 km wide and 22 m deep; Aliotta and Perillo, 1987), non-glacial sandstone channels (lacustrine or marine, tens of kilometers long, tens of meters deep, more than 1 km wide, linear or slightly sinuous and often amalgamated, but if exhumed may show up as positive landforms; e.g., Bell et al., 2020; Dou et al., 2021), and submarine channels and canyons (e.g., compare to Covault and Romans, 2009; Covault et al., 2016; Shanmugam, 2016). Some researchers have interpreted tunnel valleys to be fluvial even if glaciers have been close by (Keller et al., 2011).

Pleistocene tunnel valleys are somewhat more outstanding than more ancient “tunnel valleys,” up to 100 km long, 400 m deep and 5 km wide, but most common is c. 10 km, 100 m and 1.5 km, respectively, displaying a typical width/depth ratio around 10 (Vesely et al., 2021). While van der Vegt et al. (2012) mix descriptions of Ordovician “tunnel valleys” and Pleistocene tunnel valleys, cross-sections indicate that the Ordovician examples commonly are wider and not as deep. Furthermore, there are no intra-formal striated pavements in the Pleistocene, but these are common in the Ordovician tunnel valley sediments. Pleistocene tunnel valleys are better preserved but also display more of an appearance of a valley than pre-Pleistocene examples (Vesely et al., 2021, their Fig. 13).

The control of the distribution of Ordovician tunnel valleys may partly be from the existence of older crustal lineaments, and the valleys are bounded by faulted and/or folded zones (Ghienne et al., 2003; Le Heron et al., 2006), which may add a tectonic component to their origin. Keller et al. (2011) wrote: "The genesis of these tunnel (?) valleys is still a matter of debate." Le Heron et al. (2018a) wrote that there is an absence "of suitable modern analogues" to these tunnel valleys, even though they tried to solve the problem.

2.12.3. Raised channels, eskers and tunnel valleys

Except for the linear non-glacial landforms described in previous sections, there are more than 100 areas displaying inverted stream channels, i.e. wadis or other fluvial channels, which have been exhumed and stand out as long positive ridges (Zaki et al., 2021). These are present on almost all continents, from the Silurian until the Holocene, and these may be compared to Ordovician raised channels/eskers/tunnel valleys which are interpreted to be glaciogenic (Maizels, 1990a, 1990b; Zaki and Giegengack, 2016; Zaki et al. 2018, 2020, 2021). In Egypt, there are more than 7000 sinuous ridges, across ~40 000 km^2, up to 18 km in length, up to a few hundred meters in width and up to 33 m high, which are commonly interpreted to be inverted wadis (Zaki and Giegengack, 2016; Giegengack and Zaki, 2017; Zaki et al., 2018, 2020). In different areas, ridges may be up to approximately 500 km long, the heights may be more than 40 m and the widths up to 4 km (Zaki et al., 2021). Such raised channels could easily be mistaken for eskers or tunnel valleys, especially if they would not show up clearly in stratigraphic sections. In the Plio-Pleistocene sediments of Oman, there is a complicated network of many generations of raised channel systems, but also many deeply buried, some of which have been labeled with the term "pseudo-esker" (Maizels, 1990a, 1990b). These are up to 250 km long, in some places more than 2 km wide, but commonly <30 m in height, and they display similarities to the Ordovician "tunnel valleys" in shape, length and composition (compare Maizels, 1990a, 1990b, to e.g., Vesely et al., 2021).

In conclusion, there is a suggested similarity of pre-Pleistocene tunnel valleys and eskers to non-glacial channels, and a suggested difference to Pleistocene tunnel valleys and eskers.

2.13. Dropstones

2.13.1. Dropstones, similarities

Dropstones are often assumed as prime evidence for glaciation, with the consequence that cold climates have been interpreted for many areas. For example, Rodríguez-López et al. (2016) interpreted lonestones in Cretaceous sediments as dropstones, even though there is no other demanding evidence for glaciation. Similarly, Frakes and Krassay (1992) interpreted lonestones in Jurassic and Cretaceous fine grained sediments as probably glaciogenic dropstones, because there was a shortage of fossil driftwood in the strata. However, Donovan and Pickerill (1997, 2008) considered lonestones in the early Cenozoic of Jamaica as non-glaciogenic, as there was no evidence or possibility for glaciation at that place and time. And Doublet and Garcia (2004) interpreted dropstones from Mesozoic sediments in Spain as dropped from floating trees. LPIA dropstones in Argentina had dropped as rock fall from steep valley walls (Moxness et al., 2018).

Many different parameters are important for the appearance of clast penetration and sediment disturbance during impact. These parameters include water depth, properties of the bottom sediment, clast size and shape (Bronikowska et al., 2021), whether clasts are frozen to ice during sinking, simultaneous deposition of sediment by flowing water, and if the sediments are reworked by SGFs. Small dropstones, approximately a cm in size or smaller, may not produce much structures in bottom sediments (Bronikowska et al., 2021). Even if there are many unknowns, there are criteria which may help to determine if a lonestone has been dropped or has been transported by a SGF (see below).

Any violent disturbance of the environment, like glaciation, earthquakes, mass movements, tsunamis, and even larger storms, may induce scenarios that transport clasts which may display an appearance of dropstones (Tachibana, 2013; see also Shanmugam, 2012). Recent tsunamis have documented runups up to 524 meter above sea level, i.e. in 1958 in Alaska (Paris et al., 2018). Clasts can also be transported in water by biological rafting, as projectiles, and occasionally by floatation or strong whirlwinds (Liu and Gastaldo, 1992; Oberbeck et al., 1993a; Bennett et al., 1994, 1996; de Lange et al., 2008; Bronikowska et al., 2021). Deposition of all these clasts may display an appearance similar to glaciogenic dropstones, like compaction of sediment both during deposition and later because of dewatering and/or compression from superimposed sediments.

Iceberg dump mounds are accumulations of clasts dropped when icebergs overturn and release lots of material at once. These may be sorted, from the sinking of the sediments through the water column, may be conical or display different patterns of irregular outlines and different penetration of the underlying sediment (Thomas and Connell, 1985; Pisarska-Jamroży et al., 2018; Bronikowska et al., 2021). However, Aitken (1993) showed the mounds documented by Thomas and Connell (1985) to be small subaqueous fans and debris flows, even if they are in an area where there is deposition from icebergs. Another accumulation of sediments, labeled “till pellets,” can be found smeared out as if they have been molded by the overlying sediment (Miall, 1983; Visser, 1983a). Clast accumulations may be produced in any flowing media.

2.13.1.1. Transport by sediment gravity flows

Clasts transported with SGFs are often embedded in a clayey matrix (Bouma, 1964; Embley, 1982). Single clasts, up to 20 meter in diameter (Shanmugam, 2016, 2021b), or clusters of

clasts can be dragged along, slide on top of a sedimentary mass flow sequence, move upwards through the flow, or be winnowed out, and be deposited at different depths of a sedimentary sequence during single events (Postma et al., 1988; Scott, 1988b; Best, 1992; Pickering and Hiscott, 2015; Shanmugam, 2020, 2021b; Kennedy and Eyles, 2021). These clasts may display an appearance similar to clasts transported by icebergs, i.e. these are “left-overs” or lonestones, or “dumps” (Crowell, 1957, 1964; Schermerhorn, 1974a; Kim et al., 1995). Transport of lonestones by SGF deposits can be determined by fabric analyses (section 2.2.9).

In lahar deposits in Utah the clasts are often locally concentrated in clots high up in the sedimentary beds (Walton and Palmer, 1988), thus showing similarities with “iceberg roll dumps” (e.g., in the LPIA of Tasmania; Powell, 1990). Clasts with diameters of up to 15 cm had been transported more than 400 km, probably by water currents and/or SGFs. After deposition, the clasts became incorporated in SGFs. These clasts were earlier thought to have been transported with icebergs (Jansa and Carozzi, 1970).

2.13.1.2. Transport by vegetation, animals and floatation

Especially during a catastrophe (e.g., a tsunami) much material can be transported with up-rooted trees. In Carboniferous coal seams, boulders with weights up to 70 kg are present (Price, 1932; Woolfe, 1994). Boulders in Cretaceous and Carboniferous sediments have been transported up to 100 km or more, by floating with plants (Hawkes, 1943; Liu and Gastaldo, 1992). Boulders transported with contemporary tree roots have sizes up to 3 m (Bennett et al, 1996). Fossils of land-living plants are present from the Ordovician, even if their affinities are largely unknown (Servais et al., 2019).

Clasts dropped from kelp or vegetation may not display any differences to those dropped from icebergs (Doublet and Garcia, 2004). Probably hundreds of thousands of kelp rafts are

transporting attached clasts of “dropstones-to-be” today in the Southern Ocean alone (Waters and Craw, 2017), and ancient transport with kelp or other algae is documented (Bennett et al., 1994; Zalasiewicz and Taylor, 2001). Species of green and red algae may float on the water surface (Thiel and Gutow, 2005). Red algae are present in the Precambrian (1.6 billion years, Bengtson et al., 2017; 1.0 billion years, Gibson et al., 2018) and in Ordovician sediments (Fry, 1983), but these are commonly smaller species which could not transport larger clasts than maybe a few centimeters. Unspecified macroalgae (incomplete specimens >2 cm in length which are small parts of much larger algae) are present in close connection to “glacial” diamictites in the Neoproterozoic (Ye et al., 2015; Chen et al., 2015). Green algae are known from the Cambrian (Servais et al., 2019), but their origin may be placed in the Meso- or Neoproterozoic (Del Cortona et al., 2020). Kelp, which commonly refers to brown algae, are considered to have diverged some 100 million years ago (Silberfeld et al., 2010), and most larger forms maybe not until 25 million years ago (Rothman et al., 2017), even if some Precambrian to Jurassic fossils are classified as possible brown algae (Hollick, 1930; Fry, 1983; Zalasiewicz and Taylor, 2001; Silberfeld et al., 2010). Kelp transports much sediment onto beaches, including veneers of clasts, over distances of 5000 km, in sizes commonly up to 83 kg, and a record estimated weight of a large clast of 365 kg (Emery and Tschudy, 1941; Garden and Smith, 2011).

Microbial mats occasionally are lifted from the bottom surface and may transport clasts, sand clusters and clay fragments which are up to several cm long (Schieber, 1999; Thiel and Gutow, 2005). Pebbles up to 25 mm in length, can in rare instances float directly on the surface of the sea surface (Hume, 1963; Bennett et al., 1996). Gastroliths with weights up to 2.5 kg, and clusters of gastroliths up to 70 kg. had been recorded from sedimentary sequences (Bennett et al., 1996). However, the appearance of gastroliths, commonly displaying a “polished” rounded form, in most cases would be easy to sort out from dropstones.

2.13.3. Dropstones, differences

The amount of material which has been dropped by ice in Quaternary sedimentary deposits may be “astounding” over extensive areas and can even create “pathways”of dropstones (Korstgärd and Nielsen, 1989; Dionne, 1993; Pisarska-Jamroży et al., 2018), but pre-Pleistocene rafted material commonly is dispersed. Marine sedimentation from a large glacier would be more uniform over wider areas than deposition from SGFs (Clark and Hanson, 1983; Boulton, 1990).

Ancient dropstone-bearing strata often are deposited as blanketing layers on top of “tillites,” similar to turbidity deposits (compare, e.g., Talling et al., 2007; Shanmugam, 2016; Molén, 2017, 2021; Rampino, 2017). The sediments commonly are not present close to the outermost border of diamictites, or in bowls in the upper surface of the “tillite,” where marine, brackish and lake sediments usually are deposited (Deynoux, 1985b).

Thomas and Connell (1985) documented data and developed criteria for recognition of dropstones from a Pleistocene lake in Scotland, and these were further developed mainly by theoretical numerical process modeling by Bronikowska et al. (2021). The list below describes the most common features, and these are also those that are not commonly present in SGF deposits. The difference between the appearance of dropstones documented by Thomas and Connell (1985), in SGF deposits, and those in pre-Pleistocene strata, are mentioned in the comments.

a) Penetration of dropstones 5-20 cm in diameter is commonly about 1/3 of the clast size, but 2/3 if clasts display close to vertical orientation and are thin. Larger clasts penetrate more (Bronikowska et al., 2021). However, it is difficult to state anything conclusively concerning the magnitude of crushing and depressions in underlying laminae, because the firmness of the bottom sediments vary from hard to soft (Bronikowska et al., 2021).

Comment 1: Clasts transported by SGFs may not penetrate laminae. Laminae below clasts are almost always bent just by the compaction of the sediments, but sharp rocks commonly penetrate. Single penetrations of laminae are always to be expected for SGFs. Some reef blocks transported by mass flows are interpreted to have sunk down >1 m into underlying soft sediments (Rigby, 1958).

Comment 2: Dropstones in ancient diamictites do not usually cut through underlying laminae (Fig. 6), although a few authors report evidence of penetration (Binda and van Eden, 1972; Smith and Eriksson, 1979; Mustard and Donaldson, 1987a), and laminae that are not penetrated are not diagnostic of a dropstone origin (Thomas and Connell, 1985). Published photos and descriptions of ancient dropstones generally show that laminae have been bent around the clasts or slightly pressed down, not commonly cut or crushed (even if photos of such features are often chosen for publication, e.g., Molén, 2021), even though the clasts may be c. 0.6 m in diameter (Schenk, 1965; Visser and Kingsley, 1982; Gravenor et al., 1984; Kim et al., 1995; Craddock et al., 2019; Isbell et al., 2021; Table S3). The sediments thin out around clasts, both above and below, and the sediments are actually draping the clasts, which is what could be expected from SGFs (Dey et al., 2020; Molén, 2021). In some areas clast are "locally very abundant along bedding planes" (Kneller et al., 2004).

b) Variable clast size.

Comment 1: Clasts may be sorted in SGF deposits. In the Gowganda Formation dropstones are more common in coarse grained than in fine grained rhythmites (Mustard and Donaldson, 1987a).

Comment 2: Dropstones which have been transported by sea ice or vegetation will usually have a smaller size and better sorting and roundness than those which have been transported by glacier ice, the latter which may be up to 10 m in diameter (Gilbert, 1990). Diameters of Quaternary glaciogenic dropstones of diameters 0.5 m and larger are not uncommon (Dionne, 1993; Meyer et al., 2016; Pisarska-Jamroży et al., 2018; Bronikowska et al., 2021). The maximum size of "left-overs" in SGFs should in general be smaller than dropstones (Clark

and Hanson, 1983; Peakall et al., 2020), but as already documented (section 2.3.) the "erratics" in "tillites" are smaller than those in tills, and it is therefore necessary to compare relative sizes (Molén, 2021). While single supposed dropstones in pre-Pleistocene sediments may be up to 3 m in diameter (Rodríguez-López et al., 2016), and clasts many meters in size that are interpreted to be dropstones are present in massive debris flows or slides (Domack and Hoffman, 2011), pre-Pleistocene dropstones commonly are much smaller. As examples, dropstones in the Neoproterozoic outcrops are mostly pebble-sized (Schermerhorn, 1977) as opposed to common meter-sized dropstones of Precambrian affinity in Pleistocene and Holocene deposits (Dionne, 1993). In the Dwyka Group in South Africa dropstones are often only 2-5 cm, but may rarely be up to one meter across (Visser, 1982, 1983b), and in massive "glaciomarine" diamictites they may be a few meters (Haldorsen et al., 2001). Le Heron et al. (2017) mentioned "unequivocal" evidence for ice rafting, from the Neoproterozoic of Death Valley, but pictured dropstones were solely 2-3 cm in diameter and displaying only limited penetration, as would also be expected from lonestones. Maslov (2010) mentioned dropstones of sizes "up to 2 cm" in Paleoproterozoic sediments. It may be suspected that very small dropstones, with a diameter of only a few cm or smaller, will not penetrate much into sediments (Bronikowska et al. 2021), but in SGFs even the smallest clasts likely will disturb the laminations.

c) Most clasts are oversized.

Comment: In SGF deposits it is common that the clasts have a similar size or are smaller than the sediment beds within where they are buried. (Fig. 6, Table S3.)

d) No correlation between the size of clasts and thicknesses of beds.

Comment: SGF deposits may display correlation. (Fig. 6, Table S3.) In ancient "glaciogenic" deposits larger dropstones are often present in thicker layers, which suggest that they have been transported by SGFs (McCann and Kennedy, 1974, plate 2; Martin et al., 1985; Mustard and Donaldson, 1987a; Moncrieff and Hambrey, 1990, their Fig. 6C; Molén, 2021).

e) Fabrics – only measured on 50 clasts (Thomas and Connell, 1985). Clast orientation

seldom subparallel to stratification (4%), more often inclined (46%), but most are subvertical (50%).

Comment: Fabrics variable in SGF deposits, but planar fabrics and vertical clasts are not uncommon. (Section 2.2.9. Also, see planar fabrics for outsized clasts and “dropstones” in Lindsay et al., 1970; Kim et al., 1995.)

f) No current indicators.

Comment 1: In a laminated or rhythmic sediment section, any horizontal movement in the bottom sediments may result in disturbances around clasts. Evidence of movements may indicate that the deposition was not slow, i.e. not within an environment displaying more or less stagnant bottom water. Clasts which are transported within SGFs, whether the sediments will be deposited as laminations or not, may show both external and internal (within the sediment) structures indicating horizontal movement. (Fig. 6.)

Comment 2: There are often lee side structures connected with pre-Pleistocene “dropstones” (Lindsey, 1969; Ovenshine, 1970; Visser, 1983a; Aitken, 1991; Molén, 2017, 2021). In the Middle Permian of Australia brachiopod fossils are present on the lee sides of oversized clasts which are interpreted to be dropstones (Yang et al., 2018). In places the sediment has been pushed up in front of a dropstone, without any evidence of penetration of underlying beds, as if the clast has been moved along in a SGF (Mustard and Donaldson, 1987a, their Fig. 6G; Molén, 2017, 2021).

g) Sediment around clasts are commonly rucked (pushed up on both sides, commonly sharp folds), ruptured (lamination in sediment next to, below and/or above clast is broken and mixed) and/or onlapped (covering sediment next to clasts not draped around the clast, but stops at the clast, except for those laminae that cover the clast).

Comment: Draping is prevalent if clasts are transported by SGFs. Draping of clast may display laminae that commonly are covering the clasts on all sides, but the thickness of the sediments may change next to the clast. Some laminae may thicken next to the clasts, others may thin out. Some may only stop at the clast. Commonly there are not many sharp

sedimentary structures around clasts transported by SGFs. Laminae may become diffuse or split into more laminae, reflecting wake eddies (compare to Kim et al., 1995). (Fig. 6.)

Table S3 (Supplementary material) document dropstones which display features which are more compatible with transport by SGFs than to dropping from ice.

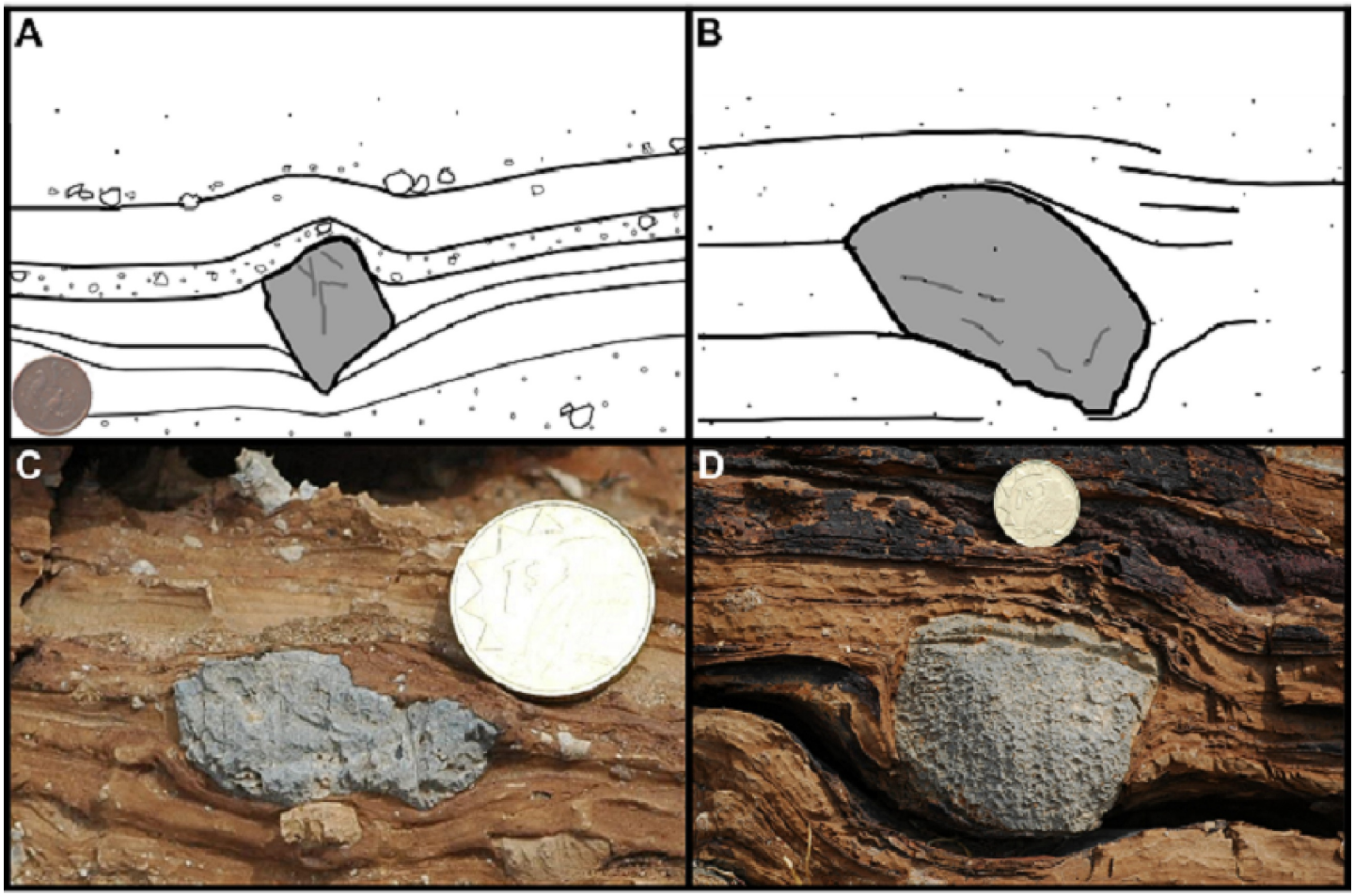

Fig. 6. Clasts which have been interpreted as dropstones from the Ghaub and Chuos Formations of Namibia. The irregularities and appearances displayed in the beds next to the clasts indicate currents and a SGF origin. If clasts as small as these would have been dropped from ice, they may not have disturbed the sediment much at all (Bronikowska et al., 2021). In general, the appearances displayed in these pictures are common in ancient “glaciogenic” sediments, but different from Quaternary dropstone bearing sections. A. The bed containing the clast becomes thicker next to the clast on both sides. There may be penetration of strata, but even if the clast is pointy it appears more that the sediment is slightly bent because of

compression during transport and therefore thins out beneath the clast. (Drawing after Hoffman www.geol.umd.edu/~jmerck/geol342/lectures/06.html). B. There is a small "impact" structure to right of the clast, but nothing on the left side. Laminae on the left are straight. To the right, the beds above the clast bend down over the clast. The appearance is one of diffuse wake eddies on the right side of the clast. Clast is c. 1.5 cm in length. (Drawing after Le Heron et al., 2021a.) C. The sediment bed becomes thicker next to the clast. The clast is regularly enclosed by sediment above and below. This is the most common appearance of pre-Pleistocene clasts interpreted to be dropstones. D. This clast is inside a thicker sediment bed. The bed thickens next to the clast, which is especially evident on the right side of the clast where the sediment surface enclosing the clast is at a lower level than on the left side. To the left, both the bedding and the underlying sediment are bent, as would be the case if the clast was transported in that direction enclosed in a SGF. It can be discussed if there is much evidence of penetration, or if the sediments mostly thin out beneath the clast. (Photographs by T. Bechstädt; Bechstädt et al., 2018.)

2.14. Laminated sediments

"Varved sediments" (laminated beds) which may be interpreted as deposited on a yearly basis can form instantaneously by SGFs, including hyperpycnal flows, and also from contour currents (the latter commonly move with speeds up to 3 m/s, and including cyclone driven bottom flows with velocities of up to 70 m/s), in many different environments (Kuenen, 1964; Pettijohn and Potter, 1964; Winterer, 1964; McKee et al., 1967; Lowe, 1982, 1988; Gravenor and Rocha-Campos, 1983; Domack, 1990; Dykstra, 2012; Zavala and Arcuri, 2016; Yawar and Schieber, 2017; Shanmugam, 2017a, 2021a; Tedesco et al., 2020; Isbell et al., 2021; Tian et al., 2021). There are criteria for distinguishing yearly varves from surge laminae, and also other rhythms, even though these criteria are not clear cut (Smith and Ashley, 1985), and there is a vigorous debate in this area (e.g., Andrews et al., 2018; Smith

and Bailey, 2018a, 2018b; Da Silva et al., 2019; Matys Grygar, 2019; Smith, 2019). Marine couplets, with affinities to annual lacustrine varves, often form in response to tidal water if there is an abundance of suspended sediment available, and may display double mud layers (Cowan and Powell, 1990; Smith et al., 1990; Shanmugam, 2016, 2017a, 2021a, 2021b). A recorded maximum of 1000 couplets have been deposited in three to four years time (Molnia, 1983b). In connection to the variation in differences in sedimentation in general, Shanmugam (2017a) concluded that “the grand ingrained principle of 'one deposit for one flow type' is nothing more than a misplaced optimism.”

In pre-Pleistocene “glacial” deposits many rhythmites with an appearance of yearly varves occur in what must have been marine settings (Schermerhorn, 1977). Annual varves can only form in fresh water, for example in a lake or perhaps sometimes on a shallow shelf where an abundance of meltwater is constantly draining from a large glacier. Experiments show that clay flocculates and will deposit as quickly as sand, if there is no stirring (Schieber et al., 2007, 2013; Sutherland et al., 2015), and thin silt/clay laminae which are often interpreted to be yearly varves are deposited simultaneously in both fresh and salt water (Yawar and Schieber, 2017). The only known marine rhythmites form in response to tidal water (Cowan and Powell, 1990), or originate by turbidity currents.

Pre-Pleistocene rhythmite sequences may exhibit features not shown by yearly varves. “Varves” in the Gowganda Formation may be very finely laminated as opposite to more thickly laminated Pleistocene yearly varves (Molén, 2021). They have been reinterpreted as non-annual (because of the rhythmite pattern) “distal” turbidites and may contain ripple marks (Jackson, 1965; Miall, 1983, 1985; Eyles et al., 1985; Smith and Bailey, 2018b). Rhythmites next to Precambrian “tillites” in the Appalachian mountains, and in the Gowganda Formation, have been put into question because the “winter layers” are thicker than the “summer layers” (Schwab, 1981; Molén, 2021), as this appearance is the opposite of

normal varve deposition, but may be possible in rare instances if produced during glaciation. In the LPIA Dwyka Group of South Africa this is a common appearance (Tavener-Smith and Mason, 1983). Rhythmites in the Dwyka Group have been reinterpreted to be deposited from turbidites or tidal activity (Isbell et al., 2008), and LPIA "varves" in Brazil are no longer considered to be annual (Kochhann et al., 2020)..

2.15. Glaciomarine (and lake) diamictites

There is an astounding number and a great diversity of submarine glacial features, linear, transverse and irregular, covering large areas, which have been produced by glaciers, from the Pleistocene until today (Dowdeswell et al., 2016a, 2016b). In glaciomarine sediments there would be grounding zones displaying pushed up transverse till and sea-bottom mud ridges, as well as different kinds of subglacial, englacial and supraglacial submarine fans where the upflow part of the deposits shows evidence of having been bordered by an ice-shelf or a glacier (Boulton, 1990; Powell, 1990; Zecchin et al., 2015). There is nothing remotely similar to this in the pre-Pleistocene record. There is either no record at all of similar features, the features are different than those in the Quaternary record, or there are only single examples where it would be expected to be large areas covered by similar features (Molén, 2021). And, there are no reports of observational evidence of removal of material by erosion of large areas of former subaqueous glaciogenic features, i.e. erosion of areas which would be more protected than terrestrial environments.

In pre-Pleistocene glaciomarine deposits, almost the only evidence given for glaciation is dropstones, especially if the clasts are found in rhythmites (Frakes et al., 1969; Binda and Eden, 1972; McCann and Kennedy, 1974; Anderson, 1983; Miall, 1983, 1985; Visser 1989a). But, if there are marine or lacustrine fossils close to or within sediments that are interpreted to be glaciogenic, interpretations should be regarded as tentative. As mentioned earlier c. 95%

of ancient "glaciogenic" deposits are interpreted to be marine (section 1.3.), and there are often marine fossils close to or even (autochthonously) within such diamictites (e.g., Allen, 1975; Bryan, 1983; González and Glasser, 2008; Caputo and Santos, 2020, Sterren et al., 2021; López-Gamundí et al., 2021). Marine fossils also are common in cyclone and tsunami deposits, which may trigger mass flows (Shanmugam, 2012).

Neoproterozoic "tillites" usually are not bordered by marine till and a wide zone of ice-rafted material (Schermerhorn, 1977). Diamictites in general are draped with shale or rhythmites with lonestones (e.g., Rampino, 2017; Molén, 2017, 2021; López-Gamundí et al., 2021). A submarine subglacial fan has been inferred from the Carboniferous of Tasmania, but with no diagnostic ice-contact features present (Powell, 1990). None of the other geological features have been clearly identified with diagnostic geologic features from any ancient deposit, but some features may be interpreted from commonly more restricted sedimentary assemblages to try to integrate the data into a glaciogenic framework (e.g., Aquino et al., 2016; Rosa et el., 2019; Dietrich and Hofmann, 2019).

2.16. Periglacial structures

Periglacial look-alike structures, with the appearance of e.g. ice-wedges, can form by processes other than freezing and thawing, for example, wetting and drying, thermal contraction, sedimentary compaction, gravitational loading, small scale tectonics, flexure over an uneven surface, and almost any volume change in sediments (Yehle, 1954; Flint, 1961; Schermerhorn, 1974a; Black, 1976; Walters, 1978; Eyles and Clark, 1985; Shanmugam, 2012; Robinson et al., 2017). In tropical waters, polygons originate by infilling of sediment from above, in fractures that form during cementation (SEPM, 2021). Sheeting joints in sandstones may display polygonal structures over large areas (Loope and Burberry, 2018).

Ice-wedges are normally filled with material from above and polygons frequently show stony margins (Frakes, 1979). This is not shown by pre-Pleistocene “permafrost” deposits. In Pleistocene to Holocene polygonal ice-wedge networks (or casts), polygon diameters may be between 1-46 m, wedge depth 0.25-50 m, and wedge width 0.1-10 m, while the same structures in the Neoproterozoic Port Askaig Formation were 0.35-1.5 m, 0.09-1.12 m and 0.05-0.3 m, respectively (Eyles and Clark, 1985). The latter was explained as non-glacial and interpreted to have been generated by gravitational downfolding, and similar structures are widely reported in shallow marine sequences (Fig. 7).

Clastic dykes have been documented in, for example, the Gowganda Formation in Canada (Young, 1981b) and the Dwyka Group in South Africa (Visser and Loock, 1982; Visser et al., 1987). “Ice wedges” from the Ordovician “glacial” in the Sahara likely are sandstone dykes radiating from sand volcanoes (Fairbridge, 1970; Bryan, 1983), and some sandstone dykes have been documented to cross each other with an appearance of polygons (Allen, 1975; Deynoux, 1985a). There are sandstone dykes also in, for example, the Neoproterozoic Port Askaig “tillites” in Scotland (Eyles and Clark, 1985) and the probable non-glacial diamictites in France (Eyles, 1990), and these have been interpreted as ice-wedges (Hambrey, 1983).

In the Ordovician of Sahara there are up to 1 km long domes which had been interpreted as pingos (Bryan, 1983). Further research showed that these structures are tectonically uplifted diapiric structures in soft sediments, from vertical loading or maybe from upwelling basalts (Fairbridge, 1971, 1979; Le Blanc Smith and Eriksson, 1979; Le Heron et al., 2005).

Other features which are present in periglacial sedimentary sequences are solifluction debris, loess, cover sands, ventifacted clasts, slope wash accumulations, frost shattered clasts, vertically aligned clasts, and size-sorting (Eyles and Clark, 1985), which are commonly not reported from the pre-Pleistocene.

On the whole it seems that “periglacial” structures are quite rare in pre-Pleistocene “tillites.” Instead, structures that mimic periglacial structures seem to be common, for example clastic or sandstone dykes formed by loading (Eyles and Clark, 1985). Dykes may be present below Quaternary tills but are not very common.

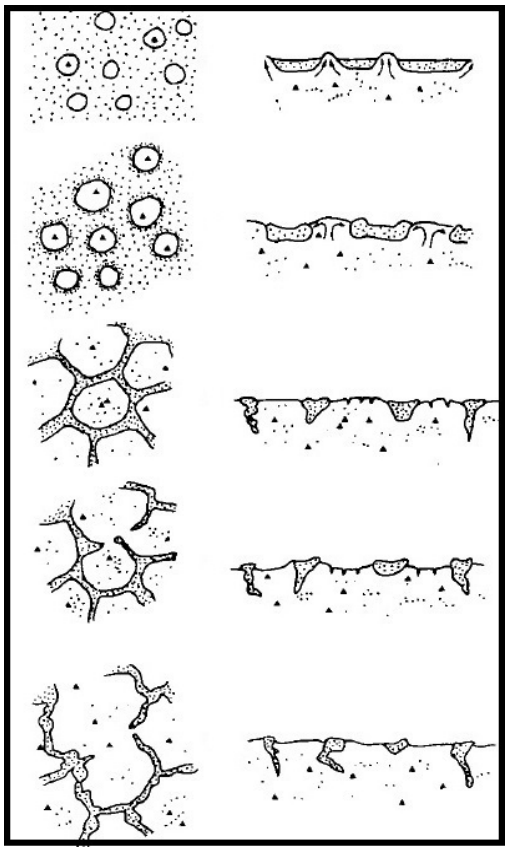

Fig. 7. The figure shows how loading and diapirism in sand have created polygonal patterns, superficially similar to permafrost polygons. Uppermost two pictures show diapirism and the lower three show the appearance after erosion. (Figure from: Eyles and Clark, B.M., 1985. Gravity induced soft sediment deformation in glaciomarine sequences of the Upper Proterozoic Port Askaig Formation, Scotland. Sedimentology 32, 789-814.)

2.17. Soft sediment deformation, tectonism

In both glaciogenic and mass flow environments there are soft sediment tectonic deformation,

both compressional and tensional (Sobiesiak et al., 2018). There are no simple specified criteria used to distinguish different environments from each other. Ancient deposits have commonly not been compared to data from Quaternary proved non-glaciogenic and glaciogenic sediments (Visser et al., 1984; Hart and Roberts, 1994; McCarroll and Rijsdijk, 2003), and the structures may be present in different sedimentary environments (Arnaud, 2012). Dreimanis (1993) listed eight glaciotectonic structures, and wrote that most of them may be found in mass flow deposits. He concluded that it would be best to use multiple stress-related criteria, including e.g., glacial abrasion marks over an area of several hundred meters, to track down the origin of the deposit. Only conjugate sets of steep-dipping fractures are stated to be more common in glaciotectonic deposits (Dreimanis, 1993).

A SGF origin may be more probable if there are (Visser et al., 1984; Dreimanis, 1993; Sobiesiak et al., 2018):

a) tensional and compressional stress regimes in one single horizon,

b) presence of dewatering structures,

c) restriction of deformation to specific lithologies (even leaving other beds above and below intact and without deformation),

d) intimate association with mass flow deposits,

e) random orientation of microfold axes,

f) sheared sediment lenses that usually are curved or bent in different ways,

g) overturned recumbent flows which usually do not have their anticlines sheared off, and/or are occasionally flattened at their base, and/or have a bulbous terminus often pointing in the downflow direction,

h) extension fractures which are filled by dykes that are localized on the distal side of the deposit and are accompanied by normal faults.

Some of the structures tabulated above are also present in tills and are interpreted as evidence

of glaciotectonic deformation, e.g., dewatering structures (Dreimanis, 1993).

Any mass flow which loses its velocity and comes to a stop will display both compressional and tensional regimes, except if it all stops as one large slab. If it is glaciotectonic there should commonly be more similar tectonism all through the sediments (e.g., Bennett et al., 2003), but occasionally more at the top parts of the deposits compared to the bottom.

Soft sediment deformation in diamictites in the LPIA of Brazil were interpreted to be glaciotectonically formed (Rosa et al., 2019), but there was no unequivocal evidence of glaciotectonics compared to tectonics formed by mass flows. Other soft sediment tectonics in the LPIA of Brazil is interpreted to be from mass flows, even if there are postulated glaciers nearby (Mottin et al., 2018), and some glaciotectonic features had been reinterpreted as non-glacial (Rodrigues et al., 2020).

2.18. SEM studies

SEM studies of surface microtextures on quartz sand grains is a quick method to easily distinguish glaciogenic sediments from other sediments (Mahaney, 2002; Molén, 2014, 2017). Glaciogenic quartz sand grains are characterized by fresh fractures which have been irregularly abraded all over the grain surface (Molén, 2014). The processes of fracturing and abrasion may take place at the same instant, as it is grinding rather than impacting that creates the fractures. It is possible to follow how a glaciogenic grain, which later will be transported glaciofluvially, will be abraded so that the typical glaciogenic surface microtextures will slowly first change to microtextures similar to those present in rivers (Molén, 2014; Kalińska et al., 2022), and after that will continue to change depending on the environment of deposition.

Single surface microtextures produced by glaciers, like different varieties of fractures, may form in any environment (Mahaney, 2002; Molén, 2014, 2017). This is basic physics, as there is no difference from the impact of similar forces from different environments. Therefore, there needs to be a systematic combination of surface microtextures if the origin of a sediment is to be revealed. Subglacial transport is necessary if surface microtextures typical for a glacial environment shall be acquired. Supraglacial till and flow tills (if they never have been transported subglacially), and to a large part englacial till, will not acquire any or only very few surface microtextures typical for a subglacial environment (Kalińska et al., 2022). But as soon as a glacier processes rock material subglacially, glaciogenic surface microtextures form quickly. Supraglacial till, englacial till, and supraglacial flow till, are usually a minor part of glaciogenic sediments, and these sediments are often loosely packed and surficial and therefore easily removed by later erosion. This is in contrast to basal till. Periglacial environments also do not imprint glaciogenic surface microtextures on quartz sand grains (Kalińska-Nartiša et al., 2017).

Surface microtextures often stand out more on sand grains >250 μm. Smaller grains retain older surface microtextures more easily which may therefore be preserved from the original environment, instead of the grain displaying more evidence of the latest environment or transport history (Molén, 2014).

A method of sorting surface microtextures based on the appearance of the complete grain surfaces, and not a multitude of small scale surface microtextures which may originate in different environments, has been shown to be simple and quick (Molén 2014). The data is easily visualized in a “2-History-Diagram” (Fig. 8). This diagram shows both the last geological history and the former. The former may be e.g., the origin before release from bedrock, or glaciation followed by fluvial or eolian transport. The method is described in detail in Molén (2014) and is applied in Molén (2017) and Molén and Smit (2022).

Soreghan et al. (2014) and Keiser et al. (2015), by referring to occurrences of single small-scale surface microtextures, misidentified grains that commonly originate from release from bedrock (compare to Mahaney, 2002; Molén, 2014), and interpreted these grains to be glaciogenic. This led them to suggest a glaciation at the Upper Paleozoic paleoequator. Immonen (2013) did not show any glacially abraded grains but only regular abrasion originating from movement by water, on e.g., fractures. Hore et al. (2020) and Alley et al. (2020) only showed unabraded fractures (some with regular rounding made from fluvial action) as evidence for glaciation in the Cretaceous of Australia. Le Heron et al. (2020) showed small fractures from Ordovician and LPIA sediments, which have no relevance to glaciation. Kalińska-Nartiša et al. (2017), Passchier et al. (2021) and Kut et al. (2021) correctly identified surface microtextures as not glaciogenic, in periglacial/permafrost climate. Reahl et al. (2021) could differentiate out non-glaciogenic grains.

Some typical glaciogenic grains, and a few multicyclical grains, are displayed in Fig. 9. No other environment except the subglacial environment displays the combination of fresh irregularly abraded fractures. Based on more than 50 years of research (but commonly described in a more complicated, not so straightforward way), if the combination of fresh irregularly abraded fractures is not present, then the sediment is not glaciogenic. This combination of surface microtextures is displayed even by processing from a very thin probable only c. 10 m thick glacier (Molén, 2014). Multicyclical, beach and river sand grains display fewer and smaller fractures, regular abrasion and more weathering, when compared to glaciogenic quartz grains (Mahaney, 2002; Molén, 2014, 2017). Grains in high energy environments, where there is no grinding similar to that occurring at the bottom of glaciers, like in a rockfall, a conglomerate or a SGF, may acquire many fractures but not much abrasion, at least not irregular abrasion (Mahaney, 2002; Molén and Smit, 2022).

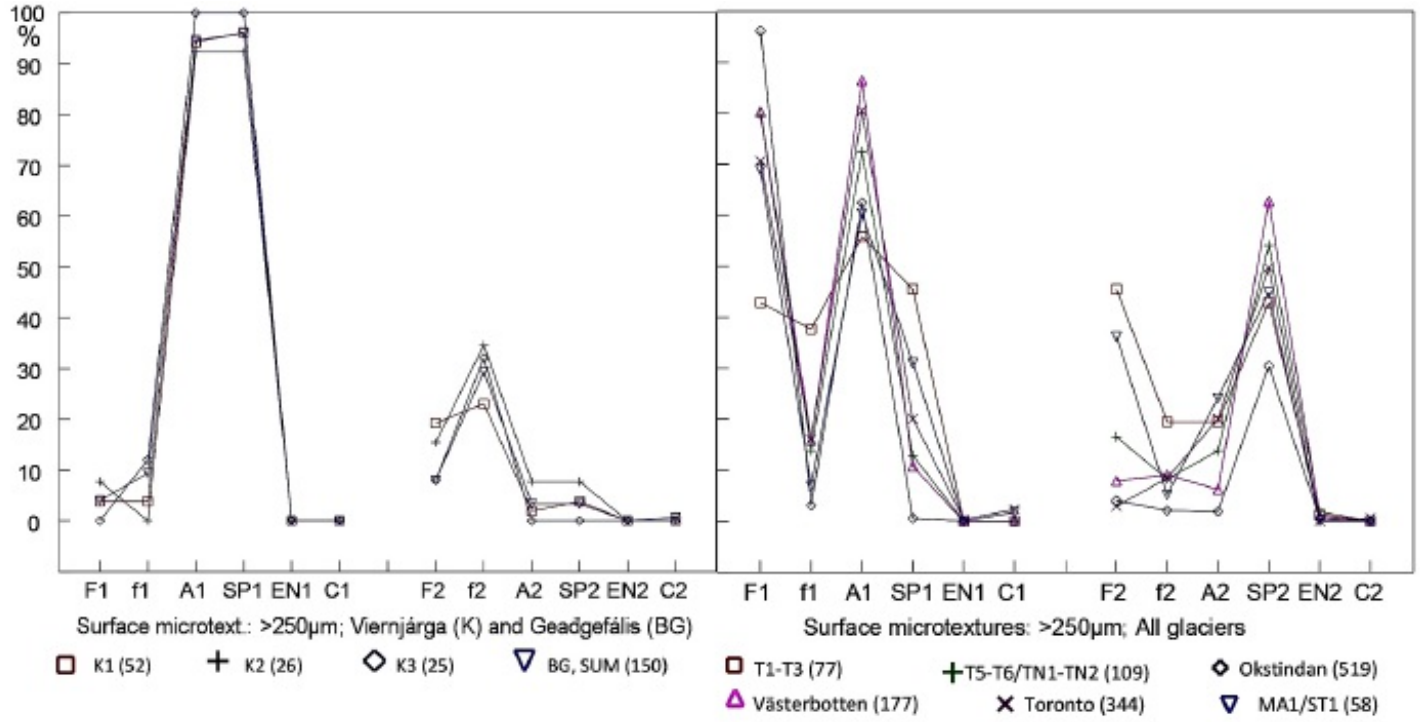

Fig. 8. A 2-History-Diagram displays a "geological signature" from the appearance of surface microtextures of quartz sand grains. The data is easily visualized, and the diagram is easy to construct. The left diagram show surface microtextures from multicyclical grains from a diamictite which commonly is interpreted to be glaciogenic (Neoproterozoic, northern Norway; Molén, 2017). Grains from this area display regular abrasion (similar all over the grain, whether the grain is round or angular in general shape) and weathering (A1 + SP1), and a few fractures, but no glacial surface microtextures (F1+A1) (Molén, 2017). The right diagram show data from Pleistocene and Neoglacial tills from Scandinavia and Ontario. T1-T3, T5-T6/TN1-TN2 and Okstindan are samples from small Neoglacial glaciers. Västerbotten (Sweden) and Toronto (Ontario) are samples from Pleistocene glaciers. MA1/ST1 are samples from Pleistocene tills in Ontario which were composed of >95% crushed limestone. The glaciogenic grains are easily identified by displaying fresh fractures which are irregularly abraded (F1+A1) (Molén, 2014).

F/f are large and small fractures, A is abrasion, EN are embayments/nodes where the grains were in contact with other bedrock material during cooling and crystallization, and C is chemically precipitated crystal surfaces. The number 1 displays the most recent surface

microtextures, from the most recent geological process, and number 2 are older overlapped surface microtextures. Percentages are numbers of grains displaying the documented surface microtexture compared to the total number of grains in the samples.

The connecting lines in the diagrams are drawn only to enhance visibility, as described in Molén (2014). These lines are important, as they visually indicate the general trend of the different surface microtextures, up or down, and therefore also display an easily distinguishable “geological signature” of the appearance of each sample. Number of studied quartz sand grains are within parentheses. (Figure from: Molén, M.O., 2017.)

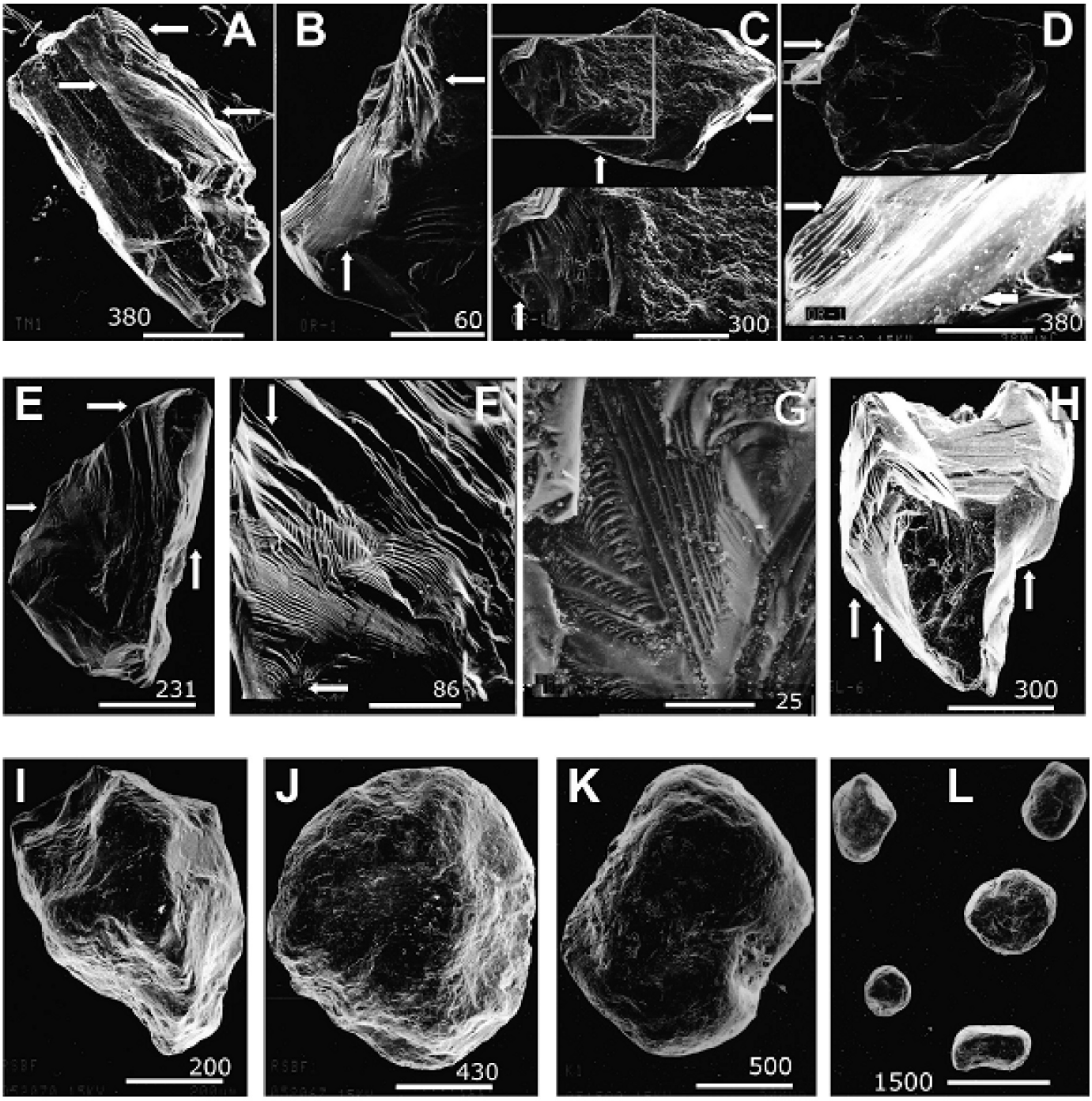

Fig. 9. SEM microphotographs of quartz sand grains from different environments. A is Neoglacial till and B-F are Pleistocene tills, Västerbotten county, Sweden. G-H are Pleistocene, Southern Ontario, Canada. I-L are multicyclical grains. Arrows point to fractures that have been irregularly abraded, i.e. typical for glaciogenic grains. A. Large fractures all over grain. On the upper surface all the fracture steps have been heavily abraded. B. Heavily fractured and abraded grain. The fracture steps on the light left surface have been abraded. C. Abrasion visible on fracture steps and in different parts of the grain surface. D. Large

fractures. Most abrasion shown in the insert, i.e. uneven abraded surface all over and fracture steps have been abraded. E. Multiple fractured grain. Many fractures are sharp, but irregular abrasion is present in many places all over the grain. F. Closeup of fracture faces displaying steps on grain E. Abrasion is best visible in lower left corner, but most other rounded surfaces are probably curved fractures. G. Closeup of spectacular fractures showing linear and curved steps. As this grain from a till is much magnified, only small areas displaying possible abrasion are visible. H. Multiple fractured grain. Many fractures are still sharp, but some have been heavily irregularly abraded. This is a short transported glaciofluvial quartz grain, and therefore the grain has not yet acquired regular abrasion typical for transport with running water. I-J. Grains displaying weathering and regular abrasion. Ordovician sandstone, Canada. K-L. Rounded grains displaying weathering and regular abrasion. These grains are from diamictites, formerly interpreted to be tillites, but the surface microtextures display the same appearance as multicyclical grains similar to e.g., the sandstone in Figs. 9 I-J. Neoproterozoic, Norway (Molén, 2017). (Scale bars are in μm.)

3. Discussion

A feature of dubious origin present in a "tillite" may be interpreted as evidence for a glaciogenic origin. This feature may later be used as evidence for a glacial origin for similar features in other deposits. Maybe it was a slip of the tongue when Deynoux and Trompette (1981a) wrote the following about some Upper Ordovician sandstones in Guinea that were correlated with the "glacial" sediments in the Sahara: "There is no evidence for the glacial origin of these sandstones." Similarly, Moncrieff and Hambrey (1990) acknowledged Schermerhorn´s (1974a) criticism of the glaciogenic interpretation of Neoproterozoic diamictites, but wrote that the glacial origin of many of the deposits has since then been confirmed, referring to Hambrey and Harland (1981). What they did not observe was the differences between what was reported in this extensive review volume of pre-Pleistocene

"glaciogenic" deposits and Pleistocene glaciogenic deposits, as reported here. Their own work (Moncrieff and Hambrey, 1990), concerning Neoproterozoic "glaciomarine" deposits in Greenland, showed that these outcrops did "... not have a suitable modern analogue." They also suggested that ancient glaciomarine deposits, including from the Neoproterozoic in Greenland, should be used to aid the interpretation of recent sediments instead of the opposite. More bluntly, Dey et al. (2020) wrote concerning the Neoproterozoic Blaini Formation in India "... that the idea of its glacial origin is more a belief than a scientific interpretation."

All this might end up as a philosophical problem. Actualism may be defined as the notion that physical natural laws do not change over time or space, or, uniformity of process (Gould 1987). Uniformitarianism (classical) is the notion that the rates and intensities of all processes have always been the same as today, or the same as during non-catastrophic conditions, and this concept is definitively falsified (Gould, 1987; Romano, 2015).

Instead of believing in uniformity of climatic changes (uniformitarianism), one should put stronger confidence in uniformity of physical natural laws and per se sedimentary processes (actualism). There is no natural law which states that the climate must have been cold and humid over large areas at many different occasions during earth history, just because there has been an ice-age quite recently. There is no evidence of uniformity of climatic change from the geological record even if it would be assumed that all "tillites" are glaciogenic or from theoretical considerations (the Milankovitch astronomical theory not withstanding, e.g., compare to Haldorsen et al., 2001). Bickert and Heinrich (2011) wrote " ... we are far away from understanding the dynamics and processes of the Earth´s climatic change." However, if the geological processes have changed during the ages (not only the rates or intensities), then also the natural laws must have changed.

The "exceptional" features which are frequently documented from ancient "glacial" periods and have been "pushed" into a glacial framework, indicate a need for a change of interpretations. The research which describe and explain processes from Quaternary glaciers and glaciations are invaluable, but they need to be accompanied by similar rigorous research of "tillites" and compare these to deposits resulting from SGFs and other non-glacial processes. Although some of the processes discussed in this paper have only been studied either in restricted areas or very rarely, we cannot reject explanations only on the basis of uniformitarianism. Many kinds of "catastrophes" have occurred, and the processes we have seen only on a local scale might on a number of occasions have been more widespread (Ager, 1981). But, there is no need for large catastrophes to explain the origin of diamictites, but only recent common processes and time.

It is essential to hold on to the basic concept that the recent is the key to the past, i.e. that the framework for scientific research should be actualism and not uniformitarianism. In the current paper the discussion has been concerning diamictites, glaciation and mass flows. In this context it is informative to quote researchers who have documented "missing" sediments:
a) By comparing ancient slides to Quaternary slides, Woodcock (1979) wrote "... where are the analogues of the larger continental margin slides in the ancient record?" (...) and "... submarine slides described from present day continental margins are on average several orders of magnitude larger in cross-sectional area than submarine slides described from ancient on-land sequences." There are marine sediments covering large areas of recent cratonic land surfaces, and there is no reason that there should have been large differences in the appearance of submarine slides during ancient transgressions.
b) Concerning the similarities of geological features which may originate by impacts followed by earthquakes and tsunamis and those in "tillites" (even if the interpretation of impacts was overstated initially) Oberbeck et al. (1993a) wrote: "How do ancient glacial deposits become preserved, while expected impact crater deposits equal to the thickest of the ancient tillites

(and with the same appearance as tillites) become removed without a trace?"

c) Shanmugam (2016) noted that "... the long-standing belief that submarine fans are composed of turbidites, in particular, of gravelly and sandy high-density turbidites, is a myth. This is because there are no empirical data ..." (from observations in the world´s oceans nor from experiments to validate this). "Mass-transport processes, which include slides, slumps, and debris flows (but no turbidity currents), are the most viable mechanisms for transporting gravels and sands into the deep sea." He also noted that the "geologic reality is that frequent short-term events that lasts for only a few minutes to hours or days (e.g., earthquakes, meteorite impacts, tsunamis, tropical cyclones, etc.)" are the more important processes of transporting and depositing sediments. Or, as Kneller et al. (2016) stated: "Mass failures thus include the largest sedimentation events on earth."

d) And why, as the final and most important question, should it be that: "The dominant 'glacial' facies in the rock record are subaqueous debris flow diamictites and turbidites recording the selective preservation of poorly-sorted glaciclastic sediment deposited in deep water basins by SGFs" (Eyles, 1993). Of course, the preservation potential is greatest in deeper basins, and therefore the question is if ancient glaciogenic material really has been preserved in any large abundance. It also appears that most "glaciations" can be correlated with tectonic movements (Eyles, 1993; Eyles and Januszczak, 2007; Kennedy and Eyles, 2021; Molén, 2021; Molén and Smit, 2022), which would trigger SGFs but not per se long term cold climate, even though long term climatic changes connected to magmatism and tectonism were suggested by Youbi et al. (2021).

Documented geological data indicate that many more diamictites than suspected may be mass flow deposits. SGF is the most abundant process of moving sediment today, both on land and in water, and would have been so even in ancient times (Moore et al., 1994; Moscardelli et al., 2006; Talling et al., 2015; Shanmugam, 2016, 2020; Ventra and Clarke, 2018).

One can conclude with the words of Johan N. J. Visser, formerly of the University of the Orange Free State in South Africa, that: "... ancient deposits do not always correspond with Cenozoic glaciation models" (Visser, 1989a), or, as stated by Grotzinger et al. (2011) "... geology is about what happened – not what should have happened."

4. Conclusion

Many geologic features which are assumed to originate only during a cold climate or by the action of ice, also form in many other environments and by non-glacial processes, especially by SGFs. Furthermore, many features which are present in deposits from the pre-Pleistocene "glacial" record are not present in the Pleistocene glacial record (and vice versa). These missing features commonly indicate an origin by different kinds of SGFs, combined with tectonic uplift or subsidence (e.g., Maxwell, 1959; Wilson, 1969; Eyles and Eyles, 1989; Eyles 1990, 1993; Kennedy and Eyles, 2021), rather than glacial or periglacial erosion and deposition. "Ancient ice-ages" may be mainly deposits from different kinds of SGFs, instead of glaciogenic deposits.

However, a glacial component can often not be excluded only on the basis of sedimentary and erosional structures. Glacial environments are often complex and it is therefore possible to argue for a glacial origin for many features present in an outcrop. But if all geological data from a formation are considered, even if nine out of ten features are consistent with glaciation but may also be formed by SGFs, a non-glaciogenic interpretation of many "tillites" may become a clear possibility.

Thus, many researchers have become aware that sediments from SGFs form a large number of recent and ancient sedimentary deposits. Furthermore, even if there may still be debates, many "glaciations" have been reinterpreted completely or in part as SGF deposits or other

non-glacial phenomena (e.g., Newell, 1957; van Houten, 1957; Dott, 1961; Schwarzbach, 1961; Winterer, 1964; Lindsay, 1966; Scott, 1966; Condie, 1967; Frakes et al., 1969; Volkheimer, 1969; Frakes, 1979; Schermerhorn, 1974a, 1974b, 1981; Cecioni, 1981; Vellutini and Vicat, 1983; Martin et al., 1985; Mahaney, 1987; Eyles and Eyles, 1989; Eyles, 1990, 1993; Bailey et al., 1990; Rampino, 1994, 2017; Eyles and Januszczak, 2007; Thompson, 2009; Carto and Eyles, 2012a, 2012b; Delpomdor et al., 2016; Isbell et al., 2016; Molén, 2017, 2021; Bechstädt et al., 2018; Moxness et al., 2018; Fedorchuk et al., 2019; Kennedy et al., 2019; Le Heron and Vandyk, 2019; Pauls et al., 2019; Dey et al., 2020; Kennedy and Eyles, 2019, 2021; Dufresne et al., 2021; Isbell et al., 2021; Vandyk et al., 2021; Molén and Smit, 2022). It appears that many diamictites which have been interpreted as “tillites” have been formed in a similar geological environment, but not in a similar climate.

The documentation of features from the current paper is summed up in the Appendix, a Diamict Origin Table. This table may be used as a working tool, and also as a reference in publications (Molén 2017, 2021). The documentation in the current paper has sorted out unequivocal criteria. Even if the current paper have reviewed most recent literature, because of a general lack of work in some research areas that have been discussed, a few of the similarities and differences between deposits with a different origin are provisional, requiring further documentation. Many of the features described need both better qualification and quantification before they can be used more conclusively. The evidence from surface microtextures may be the quickest way to interpret the origin of deposits, as the evidence from different surface microtextures from Pleistocene and Holocene deposits are not equivocal (Mahaney, 2002; Molén, 2014, 2017).

Acknowledgments

Scholarships from York University, Toronto, and the University of Umeå, provided support in writing parts of this paper. Thanks are due to a large number of geologists who have provided critical and enhancing comments from their specialities. The current paper benefited greatly from their assistance.

5. Appendix Diamict Origin Table

FEATURE	ORIGIN		
	Glaciog.	Mass flow.	Diamict Tect.
Areally continuous	2	1	
Areally dispersed	1	2	
Large areal extent	2	1	
Warm climate sediments	0-1	2	
Warm climate fossils	0-1	2	
Matrix supported/fine grained	2	1-2	
Clast/bed thickness correlation	0-1	2	
Sorting/grading	0-1	2	
Streaks of different sediments/diamictites	1	2	
Unconsol. transport. sediment	1	2	
Soft substrate	1-2	2	
Fabrics	2	2	
Strong	2	1	
Weak	1	2	
Bimodal	2	1	
Planar	1	2	
Variable in sections	1	2	
Erratics	2	2	
>1-3 m diameter	2	1-(2)	
Smaller in “tillite” than in mass flow	0	2	
Jigsaw fractures	-	1	
Striated clasts	1-2	1-2	
Subparallel striae	2	1	
Parallel striae	1	2	
Curved/random striae	1	2	
Crossing striae	2	1	
Soft angular not striated, hard rounded striated	1	2	
Faceted/polished clasts	1-2	1-(2)	
Pavement/striae/grooves	2	1	
Subparallel striae	2	1	
Parallel striae	1	2	
Crossing striae	2	1	
Polished striae	2	1	
Soft sediment pavement	1	2	
Sediment pressed down	-	2	

	Pressed up ridges	-	2
	Stacked	0-1	1-2
	Irregular horizontally and vertically	2	1-2
	Regular striations	0-1	1-2
	Continue over extensive areas	2	1
	Interlaminated sediment/traction carpet	-	1
	Ripples, laminae (etc.)	-	1
	Brecciation	1	1
	Overhanging walls (etc.)	0-1	1
	Rock polish chemical	(?)	1
2113	Iceberg keel scour marks and mimics	2	0-1
	Abundant where present	2	-
	Changing directions	2	0-1
	Superposed/stacked in same direction	-	1
	Parallel strations/grooves	1	2
	Undulous in cross-section	2	0-1
	Evidence of tides, wind and waves	2	0-1
	Grounding pits	2	(?)
	Glacier grounding-zone wedges	2	(1)
2114	Boulder pavements	2	1-2
2115	Roches moutonnés/plucking	2	(0-1)
	Uneven surface	0-1	1
2116	Fjords, overdeepened, regular, ridged outlet	2	(0-1)
2117	Eskers	2	(0-1)
	Sorting	2	1
	Large clasts on top	2	(?)
2118	Glaciofluvial restricted by ice, kames, etc.	2	-
2119	Dropstones/lonestones	2	2
	No fabric	2	1
	Weak fabric	1	2
	Varied size of clasts	2	1
	Small size	1	2
	Small size compared to other sediments	-	2
	Correlation: clast size and sediment thickness	-	2
	Larger clasts in thicker sediments	1	2
	Sorted	0-1	1-2
	Differently compressed laminae	1	2
	No/little penetration	1	2
	1/3 of clast penetrate	2	1
	Sediment thickness changes around clast	1	2
	Lee side structures/movement/wake eddies	1	2
	Rip-up clasts	0-1	1
2120	“Varves” (with dropstones) drape diamcitite	1	2
2121	Rythmites, thick "winter layer"	0-1	2
2122	Small tectonics, e.g., clastic dikes/water escape structures,	1	2
2123	especially within rhythmites		
2124	“Glaciomarine” deposits drape diamcitite	1	2
2125	Submarine glacial features	2	1
2126	“Periglacial” features not formed by frost	1	2
2127	Surface microtextures a) only fractured, or b) both	-	2
2128	weathered and regularly abraded		

Surface microtextures synchronously fractured and irregularly abraded	2	-

GEOLOGICAL FEATURES WHICH DISPLAY NO CRITERIA TO EASILY INTERPRET THE ORIGIN OF THESE FEATURES

Geochemistry	Too many exceptions and interpretations
Transverse/irregular landforms	Critera not fully documented
Mass flows	Difficult to see evidence of glaciation
Channels below “tillites”	Difficult to know the origin
Flutes	Critera not fully documented
Impact structures	Irrelevant, except if misinterpreted
Lineations	Too few criteria
Glacial valleys	Too much variation
Channels/tunnel valleys	Too few criteria
Large soft sediment tectonic structures	Too much variation

Diamict Origin Table of geologic features formed in environments of glaciation, mass flows and tectonics. Columns display how common a feature may be, and if it has a glaciogenic origin or a non-glacogenic origin (mass flows etc).

Tabulated features in the upper part of the table differ substantially between glaciogenic and non-glaciogenic deposits, and the more provisionally documented features are in the lower part. Even though the absolute differences are not known between different processes, relative values have been provided. Details of the origin of these structures are discussed in the text. Included in the SGF/tectonic column are also other non-glacial processes which have been discussed. Not all data discussed in the text are listed, but only those that more clearly help in interpreting the origin of a diamictite. Hence, provisional or insignificant (not fully) documented differences, and those that may be easily interpreted to have formed in different environments, are not tabulated but only discussed in the text.

In the column for glaciogenic origin, structures that form by non-glaciogenic processes in a glacial environment are not included, e.g., debris flows. However, if clasts in debrites are glacially striated, this may be evidence for glaciation. On the other hand, debrites, with no other evidence for a glacial environmen than striations that may form by debris flows, is not a very helpful evidence for interpreting presence of a glacial climate.

2 = more common, 1 = less common, 0 = very rare, - = no example known, parentheses = rare or commonly displaying a distinct appearance, ? = no well documented research known.

The complete, or parts of this table may be copied and used directly in publications (e.g. Molén, 2017, 2021). (Last column is left open for the area/outcrop studied.)

6. References

Aalto, K.R., 1971. Glacial marine sedimentation and stratigraphy of the Toby Conglomerate (Upper Proterozoic), southeastern British Columbia, northwestern Idaho and northeastern Washington. Canadian Journal of Earth Sciences 8, 753-787.

Abbott, D.H., Embley, R.W., 1982. Upslope flow of turbidity currents on abyssal hills in the eastern Nares abyssal plain. EOS Transactions, American Geophysical Union 63, 445.

Adie, R.J., 1975. Permo-Carboniferous glaciation of the Southern Hemisphere, in: Wright, A.E., Moseley, F. (Eds.), Ice Ages: Ancient and Modern. Seal House Press, Liverpool, pp. 287-300.

Ager, D.V., 1981. The Nature of the Stratigraphical Record, second ed. John Wiley and Sons, New York, 151 pp.

Aitken, J.D., 1991. Two Late Proterozoic glaciations, Mackenzie Mountains, northwestern Canada. Geology 19, 445-448.

Aitken, J.F., 1993. A re-appraisal of supposed iceberg “dump” and “grounding” structures from Pleistocene glaciolacustrine sediments, Aberdeenshire. Quaternary Newsletter 71, 1-10.

Ali, D.O., Spencer, A.M., Fairchild, I.J., Chew, K.J., Anderton, R., Levell, B.K., Hambrey, M.J., Dove, D., Le Heron, D.P., 2018. Indicators of relative completeness of the glacial record of the Port Askaig Formation, Garvellach Islands, Scotland. Precambrian Research 319, 65-78. https://doi.org/10.1016/j.precamres.2017.12.005.

2183 Aliotta, S., Perillo, G.M.E., 1987. A sand wave field in the entrance to Bahia Blanca estuary,
2184 Argentina. Marine Geology 76, 1-14.

2185 Allen, J.R.L., 1984. Sedimentary Structures: Their Character and Physical Basis. Elsevier,
2186 Amsterdam vol. 1, pp. 267-268, vol. 2, pp. 513-519.

2187 Allen, P., 1975. Ordovician glacials of the Central Sahara, in: Wright, A.E., Moseley, F.
2188 (Eds.), Ice Ages: Ancient and Modern. Seal House Press, Liverpool, pp. 275-286.

2189 Alley, N.F., Hore, S.B., Frakes, L.A., 2020. Glaciations at high-latitude Southern Australia
2190 during the Early Cretaceous. Australian Journal of Earth Sciences 67, 1045-1095.
2191 https://doi.org/10.1080/08120099.2019.1590457.

2192 Alonso-Muruaga, P.J., Limarino, C.O., Spalletti, L.A., Piñol, F.C., 2018. Depositional
2193 settings and evolution of a fjord system during the carboniferous glaciation in Northwest
2194 Argentina. Sedimentary Geology 369, 28-45. https://doi.org/10.1016/j.sedgeo.2018.03.002.

2195 Alves, T.M., 2015. Submarine slide blocks and associated soft-sediment deformation in
2196 deep-water basins: A review. Marine and Petroleum Geology 67, 262-285.
2197 https://doi.org/10.1016/j.marpetgeo.2015.05.010.

2198 Alves, T.M., Gamboa, D., 2020. Mass transport deposits as markers of local tectonism in
2199 extensional basins, in: Kei Ogata, K., Festa, A., Pini, G.A. (Eds.), Submarine Landslides:
2200 Subaqueous Mass Transport Deposits from Outcrops to Seismic Profiles. Geophysical
2201 Monograph 246, American Geophysical Union. John Wiley and Sons, Inc., Washington D.C.,
2202 pp. 71-90.

2203 Amblas, D., Gerber, T.P., Canals, M., Pratson, L.F., Urgeles, R., Lastras, G., Calafat, A.M.,
2204 2011. Transient erosion in the Valencia Trough turbidite systems, NW Mediterranean Basin.
2205 Geomorphology 130, 173-184. https://doi.org/10.1016/j.geomorph.2011.03.013.

2206 Anderson, A.M., McLachlan, I.R., 1976. The plant record in the Dwyka and Ecca series
2207 (Permian) of the south-western half of the Great Karroo Basin, South Africa. Palaeontologica
2208 Africana 19, 31-42.

2209 Anderson, J.B., 1983. Ancient glacial-marine deposits: their spatial and temporal distribution,
2210 in: Molnia, B.F. (Ed.), Glacial-Marine Sedimentation, Plenum Press, New York, pp. 3-92.

2211 Andrews, S.D., Cornwell, D.G., Trewin, N.H., Hartley, A.J., Archer, S.G., 2018. Reply to the
2212 discussion on `A 2.3 Million Year Lacustrine Record of Orbital Forcing from the Devonian of
2213 Northern Scotland`, Journal of the Geological Society, London 173, 474–488. Journal of the
2214 Geological Society 175, 563. https://doi-org.ezp.sub.su.se/10.1144/jgs2017-132.

2215 Andrews, G.D., McGrady, A.T., Brown, S.R., Maynard, S.M., 2019. First description of
2216 subglacial megalineations from the late Paleozoic ice age in southern Africa. PLoS ONE 14,
2217 e0210673. https://doi.org/10.1371/journal.pone.0210673.

2218 Aquino, C.D., Buso, V.V., Faccini, U.F., Milana, J.P., Paim, P.S.G., 2016. Facies and
2219 depositional architecture according to a jet efflux model of a late Paleozoic tidewater
2220 grounding-line system from the Itararé Group (Paraná Basin), southern Brazil. Journal of
2221 South American Earth Sciences 67, 180-200. https://doi.org/10.1016/j.jsames.2016.02.008.

2222 Armentrout, J.M., 1983. Glacial lithofacies of the Neogene Yakataga Formation Robinson
2223 Mountains, Southern Alaska Coast Range, Alaska, in: Molnia, B.F. (Ed.), Glacial-Marine
2224 Sedimentation. Plenum Press, New York, pp. 629-665.

2225 Arnaud, E., 2008. Deformation in the Neoproterozoic Smalfjord Formation, northern
2226 Norway: an indicator of glacial depositional conditions? Sedimentology 55, 335–356.

2227 Arnaud, E., 2012. The paleoclimatic significance of deformation structures in Neoproterozoic
2228 successions. Sedimentary Geology 243–244, 33–56.

2229 Arnaud, E., Eyles, C.H., 2006. Neoproterozoic environmental change recorded in the Port
2230 Askaig Formation, Scotland: Climatic vs tectonic controls. Sedimentary Geology 183,
2231 99-124. https://doi.org/10.1016/j.sedgeo.2005.09.014.

2232 Assine, M.L., de Santa Ana, H., Veroslavsky, G., Vesely, F.F., 2018. Exhumed subglacial
2233 landscape in Uruguay: Erosional landforms, depositional environments, and paleo-ice flow in
2234 the context of the late Paleozoic Gondwanan glaciation. Sedimentary Geology 369, 1-12.
2235 https://doi.org/10.1016/j.sedgeo.2018.03.011.

2236 Atkins, C.B., 2003. Characteristics of Striae and Clast Shape in Glacial and Non-Glacial
2237 Environments (Ph.D. thesis). Victoria University of Wellington.

2238 Atkins, C.B., 2004. Photographic atlas of striations from selected glacial and non-glacial
2239 environments. Antarctic Data Series 28. Victoria University of Wellington.

2240 Atkins, C.B., 2013. Geomorphological evidence of cold-based glacier activity in South
2241 Victoria Land, Antarctica. Geological Society, London, Special Publications 381, 299-318.
2242 https://doi.org/10.1144/SP381.18.

2243 Baas, J.H., Tracey, N.D., Peakall, J., 2021. Sole marks reveal deep-marine depositional
2244 process and environment: Implications for flow transformation and hybrid-event-bed models.
2245 Journal of Sedimentary Research 91, 986–1009. https://doi.org/10.2110/jsr.2020.104.

2246 Bahlburg, H., Dobrzinski, N., 2011. A review of the Chemical Index of Alteration (CIA) and
2247 its application to the study of Neoproterozoic glacial deposits and climate transitions, in:
2248 Arnaud, E., Halverson, G.P., Shields-Zhou, G. (Eds.), The Geological Record of
2249 Neoproterozoic Glaciations, Geological Society, London, Memoirs 36, pp. 81-92.
2250 https://doi.org/10.1144/M36.6.

2251 Bailey, R.A., Huber, K.N., Curry, R.R., 1990. The diamicton at Deadman Pass, Central Sierra
2252 Nevada, California: A residual lag and colluvial deposit, not a 3 Ma glacial till. GSA Bulletin
2253 102, 1165-1173.

2254 Baioumy, H., Anuar, M.N.A.B., Nordin, M.N.M., Arifin, M.H., Al-Kahtany, K., 2020.
2255 Source and origin of Late Paleozoic dropstones from Peninsular Malaysia: First record of
2256 Mississippian glaciogenic deposits of Gondwana in Southeast Asia. Geological Journal 55,
2257 6361-6375. https://doi.org/10.1002/gj.3809.

2258 Baker, V.R., Kochel, C., 1979. Martian channel morphology:Maja and Kasei Valles, Journal
2259 of Physical Research 84, 7961-7983.

2260 Baker, V.R., Milton, D.J., 1974. Erosion by catastrophic floods on Mars and Earth. Icarus 23,
2261 27-41.

2262 Banerjee, I., 1966. Turbidites in a glacial sequence: A study from the Talchir Formation,
2263 Raniganj Coalfield, India. Journal of Geology 74, 593-606.

2264 Barbolini, N., 2014. Palynostratigraphy of the South African Karoo Supergroup and
2265 Correlations with Coeval Gondwanan Successions (Ph.D. thesis). University of the
2266 Witwatersrand, Johannesburg.

2267 Barbolini, N., Rubidge, B., Bamford, M.K., 2018. A new approach to biostratigraphy in the
2268 Karoo retroarc foreland system: utilising restricted-range palynomorphs and their first
2269 appearance datums for correlation. Journal of African Earth Sciences 140, 114-133.
2270 https://doi.org/10.1016/j.jafrearsci.2017.11.031.

2271 Batchelor, C.L., Montelli, A., Ottesen, D., Evans, J., Dowdeswell, E.K., Christie, F.D.W.,
2272 Dowdeswell, J.A., 2020. New insights into the formation of submarine glacial landforms
2273 from high-resolution Autonomous Underwater Vehicle data. Geomorphology 370, 107396.
2274 https://doi.org/10.1016/j.geomorph.2020.107396.

2275 Bauch, D., Hölemann, J., Andersen, N., Dobrotina, E., Nikulina, A., Kassens, H., 2011. The
2276 Arctic shelf regions as a source of freshwater and brine-enriched waters as revealed from
2277 stable oxygen isotopes. Polarforschung 80, 127-140.
2278 https://doi.org/10.2312/polarforschung.80.3.127.

2279 Bauska, T.K., Baggenstos, D., Brook, E.J., Mix, A.C., Marcott, S.A., Petrenko, V.V.,
2280 Schaefer, H., Severinghaus, J.P., Lee, J.E., 2016. Carbon isotopes characterize rapid changes

in atmospheric carbon dioxide during the last deglaciation. PNAS 113, 3465-3470. https://doi.org/10.1073/pnas.1513868113.

Bechstädt, T., Jäger, H., Rittersbacher, A., Schweisfurth, B., Spence, G., Werner, G., Boni, M., 2018. The Cryogenian Ghaub Formation of Namibia – New insights into Neoproterozoic glaciations. Earth-Science Reviews 177, 678–714. https://doi.org/10.1016/j.earscirev.2017.11.028.

Bell, D., Hodgson, D.M., Pontén, A.S.M., Hansen, L.A.S., Flint, S.S., Kane, I.A., 2020. Stratigraphic hierarchy and three dimensional evolution of an exhumed submarine slope channel system. Sedimentology 67, 3259-3289. https://doi.org/10.1111/sed.12746.

Bengtson, S., Sallstedt, T., Belivanova, V., Whitehouse, M., 2017. Three-dimensional preservation of cellular and subcellular structures suggests 1.6 billion-year-old crown-group red algae. PLoS Biology 15, e2000735. https://doi.org/10.1371/journal.pbio.2000735.

Benn, D.I., Evans, D.J.A., 1996. The interpretation and classification of subglacially-deformed materials. Quaternary Science Reviews 15, 23-52. https://doi.org/10.1016/0277-3791(95)00082-8.

Bennett, M.R., Bullard, J.E., 1991. Correspondence: Iceberg tool marks: An example from Heinabergsjökull, southeast Iceland. Journal of Glaciology 37, 181-183.

Bennett, M.R., Doyle, P., Mather, A.E., Woodfin, J.L., 1994. Testing the climatic significance of dropstones: an example from southeast Spain. Geological Magazine 131, 845-848.

2301 Bennett, M.R., Doyle, P., Mather, A.E., 1996. Dropstones: their origin and significance.
2302 Palaeogeography, Palaeoclimatology, Palaeoecology 121, 331-339.

2303 Bennett, M.R., Waller, R.I., Midgley, N.G., Huddart, D., Gonzalez, S., Cook, S.J., Tomio, A.,
2304 2003. Subglacial deformation at sub-freezing temperatures? Evidence from
2305 Hagafellsjökull-Eystri, Iceland. Quaternary Science Reviews 22, 915–923.

2306 Bernardi, M., Petti, F.M., Benton, M.J., 2018. Tetrapod distribution and temperature rise
2307 during the Permian-Triassic mass extinction. Proceedings of the Royal Society B 285,
2308 20172331. https://doi.org/10.1098/rspb.2017.2331.
2309
2310 Bernhardt, A., Schwanghart, W., 2021. Where and why do submarine canyons remain
2311 connected to the shore during sea-level rise? Insights from global topographic analysis and
2312 Bayesian regression. Geophysical Research Letters 48, e2020GL092234.
2313 https://doi.org/10.1029/2020GL092234.

2314 Best, J.L., 1992. Sedimentology and event timing of a catastrophic volcaniclastic mass
2315 flow, Volcan Hudson, Southern Chile. Bulletin of Volcanology 54, 299-318.

2316 Bestmann, M., Rice, A.H.N., Langenhorst, F., Grasemann, B., Heidelbach, F., 2006.
2317 Subglacial bedrock welding associated with glacial earthquakes. Journal of the Geological
2318 Society 163, 417-420.

2319 Bickert, T., Heinrich, R., 2011. Climate records of deep-sea sediments: towards the Cenozoic
2320 ice house, in: Hüneke, H., Mulder, T. (Eds.), Developments in Sedimentology 63. Elsevier,
2321 Amsterdam, pp. 793-823.

2322 Bielenstein, H.U., Eisbacher, G.H., 1969. Tectonic interpretation of elastic-strain-recovery
2323 measurements at Elliot Lake, Ontario. Department of Energy, Mines and Resources Ottowa,
2324 Report R210, 64 pp.

2325 Bigarella, J.J., Salamuni, R., Fuck, R.A., 1967. Striated surfaces and related features,
2326 developed by the Gondwana ice sheets (State of Paraná, Brazil). Palaeogeography,
2327 Palaeoclimatology, Palaeoecology 3, 265-276.

2328 Biju-Duval, B., Deynoux, M., Rognon, P., 1981. Late Ordovician tillites of the Central
2329 Sahara, in: Hambrey, M.J., Harland, W.B. (Eds.), Earth´s Pre-Pleistocene Glacial Record.
2330 Cambridge University Press, Cambridge, pp. 99-107.

2331 Binda, P.L., Van Eden, J.G., 1972. Sedimentological Evidence on the Origin of the
2332 Precambrian Great Conglomerate (Kundelungu Tillite), Zambia. Palaeogeography,
2333 Palaeoclimatology, Palaeoecology 12, 151-168.

2334 Bjørlykke, K., 1967. The Eocambrian “Reusch Moraine” at Bigganjargga and the geology
2335 around Varangerfjord; Northern Norway. Norges Geologiske Undersøkelse 251, 18-44.

2336 Black, R.F., 1976. Periglacial features indicative of permafrost: Ice and soil wedges.
2337 Quaternary Research 6, 3-26.

2338 Blatt, H., 1992. Sedimentary Petrology, second ed. W.H. Freedman and Co, New York, pp.
2339 56-58.

2340 Blauw, M., 2012. Out of tune: the dangers of aligning proxy archives. Quaternary Science
2341 Reviews 36, 38-49.

2342 Blomenkemper, P., Kerp, H., Bomfleur, B., 2020. A treasure trove of peculiar Permian plant
2343 fossils. PalZ 94, 409–412. https://doi.org/10.1007/s12542-019-00489-4.

2344 Bond, G., 1981a. Late Paleozoic (Dwyka) glaciation in the Middle Zambezi Region, in:
2345 Hambrey, M.J., Harland, W.B. (Eds.), Earth´s Pre-Pleistocene Glacial Record. Cambridge
2346 University Press, Cambridge, pp. 55-57.

2347 Bond, G., 1981b. Late Paleozoic (Dwyka) glaciation in the Sabi-Limpopo Region,
2348 Zimbabwe, in: Hambrey, M.J., Harland, W.B. (Eds.), Earth´s Pre-Pleistocene Glacial Record.
2349 Cambridge University Press, Cambridge, pp. 58-60.

2350 Bose, P.K., Mukhopadhyay, G., Bhattacharyya, H.N., 1992. Glaciogenic coarse clastics in a
2351 Permo-Carboniferous bedrock through in India: A sedimentary model. Sedimentary Geology
2352 76, 79-97.

2353 Boulton, G.S., 1990. Sedimentary and sea level changes during glacial cycles and their
2354 control on glacimarine facies architecture, in: Dowdeswell, J.A., Scource, J.D. (Eds.),
2355 Glacimarine Environments: Processes and Sediments. Geological Society, London, Spec.
2356 Publ. 53, pp. 15-52.

2357 Boulton, G.S., Deynoux, M., 1981. Sedimentation in glacial environments and the
2358 identification of tills and tillites in ancient sedimentary sequences. Precambrian Research 15,
2359 397-422.

2360 Bouma, A.H., 1962. Sedimentology of some flysch deposits: A graphic approach to facies
2361 interpretation. Elsevier, Amsterdam, 168 pp..

2362 Bouma, A.H., 1964. Turbidites, in: Bouma, A.H., Brouwer, A. (Eds.), Turbidites. Elsevier,
2363 Amsterdam, pp. 251-256.

2364 Bourgeois, J., 2009. Geologic effects and records of tsunamis, in: Robinson. A.R., Bernard,
2365 E.N. (Eds.), The Sea, vol 15, Tsunamis. Harvard University Press, Cambridge, pp 53-91.

2366 Bowen, R.L., 1969. Late Paleozoic glaciations – the Parana Basin of South America, in:
2367 Amos, A.J. (Ed.), Gondwana Stratigraphy. IUGS Symposium in Buenos Aires 1967,
2368 UNESCO, pp. 589-597.

2369 Bronikowska, M., Pisarska-Jamroży, M., van Loon, A.J.T., 2021. Dropstone deposition:
2370 Results of numerical process modeling of deformation structures, and implications for the
2371 reconstruction of the water depth in shallow lacustrine and marine successions. Journal of
2372 Sedimentary Research 91, 507–519. https://doi.org/10.2110/jsr.2020.111.

2373 Broster, B.E., Seaman, A.A., 1991. Glacigenic rafting of weathered granite: Charlie Lake,
2374 New Brunswick. Canadian Journal of Earth Sciences 28, 649-654.
2375 https://doi.org/10.1139/e91-056.

2376 Bryan, M., 1983. Of shales and schists and ignimbrites, and other Rocky things (a report on
2377 the talks given at the 1983 Conference at Bradford University). OUGS Journal 4 (2), 31-53
2378 (Review of Prof. P. Allens lecture: Ice Ages in the Central Sahara, pp. 51-53.)

2379 Bryant, E.A, Young, R.W., 1996. Bedrock-sculpting by tsunami, south coast New South
2380 Wales, Australia. Journal of Geology 104, 565–582.

Bukhari, S., Eyles, N., Sookhan, S., Mulligan, R., Paulen, R., Krabbendam, M., Putkinen, N., 2021. Regional subglacial quarrying and abrasion below hard-bedded palaeo-ice streams crossing the Shield–Palaeozoic boundary of central Canada: the importance of substrate control. Boreas. https://doi.org/10.1111/bor.12522.

Burr, D.M., Grier, J.A., McEwen, A.S., Keszthelyi, L.P., 2002. Repeated aqueous flooding from the Cerberus Fossae: evidence for very recently extant, deep groundwater on Mars. Icarus 159, 53-73.

Bussert, R., 2010. Exhumed erosional landforms of the Late Palaeozoic glaciation in northern Ethiopia: Indicators of ice-flow direction, palaeolandscape and regional ice dynamics. Gondwana Research 18, 356-369. https://doi.org/10.1016/j.gr.2009.10.009.

Bussert, R., 2014. Depositional environments during the Late Palaeozoic ice age (LPIA) in northern Ethiopia, NE Africa. Journal of African Earth Sciences 99, 386-407. https://doi.org/10.1016/j.jafrearsci.2014.04.005.

Butler, R.W.H, McCaffrey, W.D., 2010. Structural evolution and sediment entrainment in mass-transport complexes: outcrop studies from Italy. Journal of the Geological Society 167, 617–631. https://doi.org/10.1144/0016-76492009-041.

Butler, R.W.H., Tavarnelli, E., 2006. The structure and kinematics of substrate entrainment into high-concentration sandy turbidites: a field example from the Gorgoglione ´flysch´ of southern Italy. Sedimentology 53, 655–670. https://doi.org/10.1111/j.1365-3091.2006.00789.x.

2401 Caetano-Filho, S., Sansjofre, P., Ader, M., Paula-Santos, G.M., Guacaneme, C., Babinski,
2402 M., Bedoya-Rueda, C., Kuchenbecker, M., Reis, H.L.S., Trindade, R.I.F., 2021. A large
2403 epeiric methanogenic Bambuí sea in the core of Gondwana supercontinent? Geoscience
2404 Frontiers 12, 203-218. https://doi.org/10.1016/j.gsf.2020.04.005.

2405 Cahen, L., Lepersonne, J., 1981. Proterozoic diamictites of Lower Zaire, in: Hambrey, M.J.,
2406 Harland, W.B. (Eds.), Earth´s Pre-Pleistocene Glacial Record. Cambridge University Press,
2407 Cambridge, pp.153-157.

2408 Canals, M., Puig, P., de Madron, X.D., Heussner, S., Palanques, A., Fabres, J., 2006.
2409 Flushing submarine canyons. Nature 444, 354-357. https://doi.org/10.1038/nature05271.

2410 Capra, L., Macias, J.L., 2002. The cohesive Naranjo debris-flow deposit (10 km^3): A dam
2411 breakout flow derived from the Pleistocene debris-avalanche deposit of Nevado de Colima
2412 Volcano (México). Journal of Volcanology and Geothermal Research 117, 213-235.

2413 Caputo, M.V., Crowell, J.C., 1985. Migration of glacial centers across Gondwana during
2414 Paleozoic Era. GSA Bulletin 96, 1020-1036.

2415 Caputo, M.V., Santos, R.O.B. dos, 2020. Stratigraphy and ages of four Early Silurian through
2416 Late Devonian, Early and Middle Mississippian glaciation events in the Parnaíba Basin and
2417 adjacent areas, NE Brazil. Earth-Science Reviews 207, 103002.
2418 https://doi.org/10.1016/j.earscirev.2019.103002.

2419 Cardona, S., Wood, L.J., Dugan, B., Jobe, Z., Strachan, L.J., 2020. Characterization of the
2420 Rapanui mass-transport deposit and the basal shear zone: Mount Messenger Formation,

2421 Taranaki Basin, New Zealand. Sedimentology 67, 2111-2148.
2422 https://doi.org.10.1111/sed.12697.

2423 Caron, V., .Mahieux, G., Ekomane, E., Moussango, P., Babinski, M., 2011. One, two or no
2424 record of Late Neoproterozoic glaciation in South-East Cameroon? Journal of African Earth
2425 Sciences 59, 111-124. https://doi.org/10.1016/j.jafrearsci.2010.09.004.

2426 Carter, R. M., 1975. A discussion and classification of subaqueous mass-transport with
2427 particular application to grain-flow, slurry-flow, and fluxoturbidites. Earth-Science Reviews
2428 11, 145-177.

2429 Carto, S.L., Eyles, N., 2012a. Identifying glacial influences on sedimentation in tectonically-
2430 active, mass flow dominated arc basins with reference to the Neoproterozoic Gaskiers
2431 glaciation (c. 580 Ma) of the Avalonian-Cadomian Orogenic Belt. Sedimentary Geology
2432 261–262, 1–14.

2433 Carto, S.L., Eyles, N., 2012b. Sedimentology of the Neoproterozoic (c. 580 Ma) Squantum
2434 "Tillite," Boston Basin, USA: Mass flow deposition in a deep-water arc basin lacking direct
2435 glacial influence. Sedimentary Geology 269, 1–14.

2436 Cecioni, G.O., 1957. Cretaceous Flysch and Molasse in Departamento Ultima Esperanza,
2437 Magallanes Province, Chile. Bulletin of the American Association of Petroleum Geologists
2438 41, 538-564.

2439 Cecioni, G.O., 1981. Cretaceous Lago Sofia Formation, Chilean Patagonia, in: Hambrey,
2440 M.J., Harland, W.B. (Eds.), Earth´s Pre-Pleistocene Glacial Record. Cambridge University
2441 Press, Cambridge, p. 834.

2442 Cerda, I.A., Carabajal, A.P., Salgado, L., Coria, R.A., Reguero, M.A., Tambussi, C.P, Moly,
2443 J.J., 2012. The first record of a sauropod dinosaur from Antarctica. Naturwissenschaften 99,
2444 83-87.

2445 Cernusak, L.A., Winter, K., Aranda, J., Turner, B.L., 2008. Conifers, angiosperm trees, and
2446 lianas: growth, whole-plant water and nitrogen use efficiency, and stable isotope composition
2447 ($\delta^{13}C$ and $\delta^{18}O$) of seedlings grown in a tropical environment. Plant Physiology 148, 642–659.
2448 www.plantphysiol.org/cgi/doi/10.1104/pp.108.123521.

2449 Cesta, J.M., 2015. Soft-sediment slickensides in the Stockton Formation, Stockton, New
2450 Jersey. Geological Society of America, Northeastern Section – 50th Annual Meeting (23-25
2451 March 2015), Paper 45-1.
2452 https://gsa.confex.com/gsa/2015NE/finalprogram/abstract_253490.htm.

2453 Charrier, R., 1986. The Gondwana glaciation in Chile: Description of alleged glacial deposits
2454 and paleogeographic conditions bearing on the extension of the ice cover in Southern South
2455 America. Palaeogeography, Palaeoclimatology, Palaeoecology 56, 151-175.
2456 https://doi.org/10.1016/0031-0182(86)90111-2.

2457 Chen, X., Kuang, H., Liu, Y., Wang, Y., Yang, Z., Vandyk, T.M., Le Heron, D.P., Wang, S.,
2458 Geng, Y., Bai, H., Peng, N., Xia, X., 2020. Subglacial bedforms and landscapes formed by an
2459 ice sheet of Ediacaran-Cambrian age in west Henan, North China. Precambrian Research 344,
2460 105727. https://doi.org/10.1016/j.precamres.2020.105727.

2461 Chen, X., Kuang, H., Liu, Y., Le Heron, D.P., Wang, Y., Peng, N., Wang, Z., Zhong, Q., Yu,
2462 H., Chen, J., 2021. Revisiting the Nantuo Formation in Shennongjia, South China: A new
2463 depositional model and multiple glacial cycles in the Cryogenian. Precambrian Research 356,

106132. https://doi.org/10.1016/j.precamres.2021.106132.

Clark, D., Stanbrook, D.A., 2001. Formation of large scale shear structures during deposition from high density turbidity currents, Grès d´Annot Formation, South East France, in: McCaffrey, W., Kneller, B.and Peakall, J. (Eds.), Particulate Gravity Currents. International Association of Sedimentologists, Special Publication 31, Blackwell Science Ltd., London, pp. 219-232.

Clark, D.L., Hanson, A., 1983. Central Arctic Ocean Sediment Texture: A Key to Ice Transport Mechanisms, in: Molnia, B.F. (Ed.), Glacial-Marine Sedimentation. Plenum Press, New York, pp. 301-330.

Clark, P.U., 1991. Striated clast pavements: Products of deforming subglacial sediment? Geology 19, 530-533.

Clarke, S., Hubble, T., Airey, D., Yu, P., Boyd, R., Keene, J., Exon, N., Gardner, J., Shipboard Party SS12/2008, 2012. Submarine landslides on the upper southeast Australian passive continental margin – preliminary findings, in:Yamada, Y., Kawamura. K., Ikehara, K., Ogawa, Y., Urgeles, R., Mosher, D., Chaytor, J., Strasser, M. (Eds.), Submarine Mass Movements and Their Consequences. Springer International Publ,. Switzerland, pp. 55-66. https://doi.org/10.1007/978-94-007-2162-3.

Coats, R.P., Preiss, W.V., 1987. Stratigraphy of the Umberatana Group, in: Drexel, J.F. (Ed.), Preiss, W.V. (compiler), The Adelaide geosyncline – Late Proterozoic Stratigraphy, Sedimentation, Palaeontology and Tectonics. Bulletin of the Geological Survey of South Australia 53, pp. 125-209.

Coles, R.J., 2014. The Cross-sectional Characteristics of Glacial Valleys and Their Spatial Variability (Ph.D. thesis). Geography Department, University of Sheffield, 335 pp..

Condie, K.C., 1967. Petrology of the Late Precambrian tillite(?) Association in Northern Utah. GSA Bulletin 78, 1317-1343.

Costa, J.E., 1984. Physical geomorphology of debris flows, in: Costa, J.E., Fleisher, P.J. (Eds.), Developments and Applications of Geomorphology. Springer-Verlag, Berlin, pp. 268-317.

Covault, J.A., Romans, B.W., 2009. Growth patterns of deep-sea fans revisited: Turbidite-system morphology in confined basins, examples from the California Borderland. Marine Geology 265, 51-66.

Covault, J.A., Sylvester, Z., Hubbard, S.M., Jobe, Z.R., Sech, R.P., 2016. The stratigraphic record of submarine-channel evolution. The Sedimentary Record 14, 4-11. https://doi.org/10:2110/sedred.2016.3.

Cowan, E.A., Powell, R.D., 1990. Suspended sediment transport and deposition of cyclically interlaminated sediment in a temperate glacial fjord, Alaska, U.S.A., in: Dowdeswell, J.A., Scource, J.D. (Eds.), Glacimarine Environments: Processes and Sediments. Geological Society, London, Spec. Publ. 53, pp. 75-89.

Craddock, J.P., Ojakangas, R.W., Malone, D.V., Konstantinou, A., Mory, A., Bauer, W., Thomas, R.J., Affinati, S.C., Pauls, K., Zimmerman, U., Botha, G., Rochas-Campos, A., dos Santos, P.R., Tohver, E., Riccomini, C., Martin, J., Redfern, J., Horstwood, M., Gehrels, G., 2019. Detrital zircon provenance of Permo-Carboniferous glacial diamictites across

Gondwana. Earth-Science Reviews 192, 285-316. https://doi.org/10.1016/j.earscirev.2019.01.014.

Creixell, C., Sepúlveda, F., Álvarez, J., Vásquez, P., Velásquez, R., 2021. The Carboniferous onset of subduction at SW Gondwana revisited: Sedimentation and deformation processes along the late Paleozoic forearc of north Chile (21°–33° S). Journal of South American Earth Sciences 107, 103149. https://doi.org/10.1016/j.jsames.2020.103149.

Crosby, B.T., Whipple, K.X., Gasparini, N.M., Wobus, C.W. 2007. Formation of fluvial hanging valleys: Theory and simulation, Journal of Geophysical Research 112, F03S10. https://doi.org/10.1029/2006JF000566.

Crowell, J.C., 1957. Origin of pebbly mudstones. Bulletin of the Geological Society of America 68, 993-1010.

Cuneo, R.N., Isbell, J., Taylor, E.D., Taylor, T.M., 1993. The Glossopteris flora from Antarctica: taphonomy and paleoecology. Comptes Rendus XII ICC-P 2, 13-40.

Da, J., Zhang, Y.G., Li, G., Meng, X., Ji, J., 2019. Low CO2 levels of the entire Pleistocene epoch. Nature Communications 10, 4342. https://doi.org/10.1038/s41467-019-12357-5.

Da Silva, A.C., Dekkers, M.J., De Vleeschouwer, D., Hladil, J., Chadimova, L., Slavík, L., Hilgen, F.J., 2019. Millennial-scale climate changes manifest Milankovitch combination tones and Hallstatt solar cycles in the Devonian greenhouse world: Reply. Geology 47, e489-e490. https://doi.org/10.1130/G46732Y.1.

Daily, B., Gostin, V.A., Nelson, C.A., 1973. Tectonic origin for an assumed glacial pavement of Late Proterozoic age, South Australia. Journal of the Geological Society of Australia 20, 75-78. https://doi.org/10.1080/14400957308527896.

Dakin, N., Pickering, K.T., Mohrig, D., Bayliss, N.J., 2013. Channel-like features created by erosive submarine debris flows: field evidence from the Middle Eocene Ainsa Basin, Spanish Pyrenees. Marine and Petroleum Geology 41, 62-71.

Dal Cin, R., 1968. “Pebble clusters”: Their origin and utilization in the study of paleocurrents. Sedimentary Geology 2, 233-241. https://doi.org/10.1016/0037-0738(68)90001-8.

Dasgupta, P., 2003. Sediment gravity flow – the conceptual problems. Earth-Science Reviews 62, 265-281.

De Blasio, F.V., Engvik, L.E., Elverhøi, A., 2006. Sliding of outrunner blocks from submarine landslides. Geophysical Research Letters 33, L06614. https://doi.org/10.1029/2005GL025165.

de Lange, W.P., de Lange, P.J., Moon, V.G., 2006. Boulder transport by waterspouts: An example from Aorangi Island, New Zealand. Marine Geology 230,115–125. https://doi.org/10.1016/j.margeo.2006.04.006.

de Wit, M.C.J., 2016a. Dwyka eskers along the northern margin of the main Karoo Basin, in: Linol, B., de Wit, M.J. (Eds.), Origin and Evolution of the Cape Mountains and Karoo Basin, Regional Geology Reviews. Springer International Publishing, Switzerland, pp. 87-99. https://doi.org/10.1007/978-3-319-40859-0_9.

de Wit, M.C.J., 2016b. Early Permian diamond-bearing proximal eskers in the Lichtenburg/Ventersdorp area of the North West Province, South Africa. South African Journal of Geology 119, 585-606. https://doi.org/10.2113/gssajg.119.4.585.

Decombeix, A.-L., Durieux, T., Harper, C.J., Serbet, R., Taylor, E.L., 2021. A Permian nurse log and evidence for facilitation in high latitude Glossopteris forests. Lethaia 54, 96–105. https://doi.org/10.1111/let.12386.

Del Cortona, A., Jackson, C.J., Bucchini, F., Van Bel, M., D'hondt, S., Škaloud, P., Delwiche, C.F., Knoll, A.H., Raven, J.A., Verbruggen, H., Vandepoele, K., De Clerck, O., Leliaert, F., 2020, Neoproterozoic origin and multiple transitions to macroscopic growth in green seaweeds: PNAS 117, 2551–2559. https://doi.org/10.1073/pnas.1910060117.

Delpomdor, F., Eyles, N., Tack, L., Préat, A., 2016. Pre- and post-Marinoan carbonate facies of the Democratic Republic of the Congo: Glacially- or tectonically-influenced deep-water sediments? Palaeogeography, Palaeoclimatology, Palaeoecology 457, 144–157. https://doi.org/10.1016/j.palaeo.2016.06.014.

Denis, M., Guiraud, M., Konaté, M., 2010. Subglacial deformation and water-pressure cycles as a key for understanding ice stream dynamics: evidence from the Late Ordovician

succession of the Djado Basin (Niger). International Journal of Earth Sciences 99, 1399–1425. https://doi.org/10.1007/s00531-009-0455-z.

Derbyshire, E., 1979. Glaciers and environment, in: John, B.S. (Ed.), The Winters of the World. Davies and Charles, Newton Abbot, pp. 58-106.

DeVore, M.L., Pigg, K.B., 2020. The Paleocene-Eocene thermal maximum: plants as paleothermometers, rain gauges, and monitors, in: Martinetto, E., Tschopp, E., Gastaldo, R. (Eds.), Nature through Time. Springer Textbooks in Earth Sciences, Geography and Environment. Springer, Cham, pp. 109-128. https://doi.org/10.1007/978-3-030-35058-1_4.

Dey, S., Dasgupta, P., Das, K., Matin, A., 2020. Neoproterozoic Blaini Formation of Lesser Himalaya, India: fiction and fact. GSA Bulletin 132, 2267-2281. https://doi.org/10.1130/B35483.1.

Deynoux, M., 1983. Late Precambrian and Upper Ordovician glaciations in the Taoudeni Basin, West Africa, in: Deynoux, M. (Ed.), Till Mauretania 83. Centre National de la Recherche Scientifique, Paris, pp. 44-86.

Deynoux, M., 1985a. Les Glaciations du Sahara. La Recherche 16, 986-997.

Deynoux, M., 1985b. Terrestrial or waterlain glacial diamictites? Three case studies from the Late Precambrian and Late Ordovician glacial drifts in West Africa. Palaeogeography, Palaeoclimatology, Palaeoecology 51, 97-141. https://doi.org/10.1016/0031-0182(85)90082-3.

2581 Deynoux, M., Ghienne, J.-F., 2004. Late Ordovician glacial pavements revisited: a
2582 reappraisal of the origin of striated surfaces. Terra Nova 16, 95-101.
2583 https://doi.org/10.1111/j.1365-3121.2004.00536.x.

2584 Deynoux, M., Ghienne, J.-F., 2005. Reply. Late Ordovician glacial pavements revisited: a
2585 reappraisal of the origin of striated surfaces. Terra Nova 17, 488-491.

2586 Deynoux, M., Trompette, R., 1976. Discussion: Late Precambrian mixtites: glacial and/or
2587 nonglacial? Dealing especially with the mixtites of West Africa. American Journal of Science
2588 276, 1302-1315.

2589 Deynoux, M., Trompette, R., 1981a. Late Ordovician Tillites of the Taoudeni Basin, West
2590 Africa, in: Hambrey, M.J., Harland, W.B. (Eds.), Earth´s Pre-Pleistocene Glacial Record.
2591 Cambridge University Press, Cambridge, pp. 89-96.

2592 Deynoux, M., Trompette, R., 1981b. Late Precambrian tillites of the Taoudeni Basin, West
2593 Africa, in: Hambrey, M.J., Harland, W.B. (Eds.), Earth´s Pre-Pleistocene Glacial Record.
2594 Cambridge University Press, Cambridge, pp. 123-131.

2595 Dietrich, P., Hofmann, A., 2019. Ice-margin fluctuation sequences and grounding zone
2596 wedges: The record of the Late Palaeozoic ice age in the eastern Karoo Basin (Dwyka Group,
2597 South Africa). Depositional Record 5, 247–271. https ://doi.org/10.1002/dep2.74.

2598 Dietrich, P., Franchi, F., Setlhabi, L., Prevec, R., Bamford, M., 2019. The nonglacial
2599 diamictite of Toutswemogala Hill (Lower Karoo Supergroup, Central Botswana):

Implications on the extent of the Late Paleozoic ice age in the Kalahari-Karoo Basin. Journal of Sedimentary Research 89, 875–889. https://doi.org/10.2110/jsr.2019.48.

Dietrich, P., Griffis, N.P., Le Heron, D.P., Montañez, I.P., Kettler, C., Robin, C., Guillocheau, F., 2021. Fjord network in Namibia: A snapshot into the dynamics of the late Paleozoic glaciation. Geology 49. https://doi.org/10.1130/G49067.1.

Dill, R.F., 1964. Sedimentation and erosion in Scripps Submarine Canyon head, in: Miller, R.L. (Ed.), Papers in Marine Geology. Macmillan, New York, pp. 23-41.

Dill, R.F., 1966. Sand Flows and Sand Falls, in: Fairbridge, R.W. (Ed.), The Encyclopedia of Oceanography. Reinhold Publ., New York, pp. 763-765.

Dionne, J.-C., 1992. Ring structures made by shore ice in muddy tidal flat, St. Lawrence estuary, Canada. Sedimentary Geology 76, 285-292.

Dionne, J.-C., 1993. Sediment load of shore ice and ice rafting potential, upper St. Lawrence Estuary, Québec, Canada. Journal of Coastal Research 9, 628-646.

Domack, E.W., 1990. Laminated terrigenous sediments from the Antarctic Peninsula: the role of subglacial and marine processes, in: Dowdeswell, J.A., Scource, J.D. (Eds.), Glacimarine Environments: Processes and Sediments. Geological Society, London, Special Publications 53, pp. 91-103.

2617 Domack, E.W., Hoffman, P.F., 2011. An ice grounding-line wedge from the Ghaub glaciation
2618 (635 Ma) on the distal foreslope of the Otavi carbonate platform, Namibia, and its bearing on
2619 the snowball Earth hypothesis. GSA Bulletin 123, 1448-1477.
2620 https://doi.org/10.1130/B30217.1.

2621 Donovan, S.K., Pickerill, R.K., 1997. Dropstones: their origin and significance: a comment.
2622 Palaeogeography, Palaeoclimatology, Palaeoecology 131, 175-178.

2623 Donovan, S.K., Pickerill, R.K., 2008. The Paleogene Richmond Formation of Jamaica: Not
2624 an impact-related succession. Scripta Geologica 136, 107-111.

2625 Doré, F., 1981. Late Precambrian tilloids of Normandy (Armorican Massif), in: Hambrey,
2626 M.J., Harland, W.B. (Eds.), Earth´s Pre-Pleistocene Glacial Record. Cambridge University
2627 Press, Cambridge, pp. 643-646.

2628 Dott, R.H., 1961. Squantum “tillite,” Massachusetts – evidence of glaciation or subaqueous
2629 mass movements? GSA Bulletin 72, 1289-1305.

2630 Dott, R.H., 1963. Dynamics of subaqueous gravity depositional processes. Bulletin of the
2631 American Association of Petroleum Geologists 47, 104-128.

2632 Dott, R.H., Batten, R.L., 1976. Evolution of the Earth, second ed. McGraw-Hill, New York,
2633 p. 285.

2634 Dou, L., Best, J., Bao, Z., Hou, J., Zhang, L., Liua, Y., 2021. The sedimentary architecture of
2635 hyperpycnites produced by transient turbulent flows in a shallow lacustrine environment.
2636 Sedimentary Geology 411, 105804. https://doi.org/10.1016/j.sedgeo.2020.105804.

2637 Doublet, S., Garcia, J.P., 2004. The significance of dropstones in a tropical lacustrine setting,
2638 eastern Cameros Basin (Late Jurassic-Early Cretaceous, Spain). Sedimentary Geology 163,
2639 293-309.

2640 Dow, D.B., Beyth, M., Hailu, T., 1971. Palaeozoic glacial rocks recently discovered in
2641 northern Ethiopia. Geological Magazine 108, 53-60.

2642 Dowdeswell, J.A., Hogan, K.A., 2016. Huge iceberg ploughmarks and associated corrugation
2643 ridges on the northern Svalbard shelf, in: Dowdeswell, J.A., Canals, M., Jakobsson, M.,
2644 Todd, B.J., Dowdeswell, E.K., Hogan, K.A. (Eds.), Atlas of Submarine Glacial Landforms:
2645 Modern, Quaternary and Ancient. Geological Society, London, Memoirs 46, pp. 269-270.
2646 https://doi.org/10.1144/M46.4.

2647 Dowdeswell, J.A., Ottesen, D., 2013. Buried iceberg ploughmarks in the early Quaternary
2648 sediments of the central North Sea: A two-million year record of glacial influence from 3D
2649 seismic data. Marine Geology 344, 1-9. https://doi.org/10.1016/j.margeo.2013.06.019.

2650 Dowdeswell, J.A., Canals, M., Jakobsson, M., Todd, B.J., Dowdeswell, E.K., Hogan, K.A.,
2651 2016a. The variety and distribution of submarine glacial landforms and implications for
2652 ice-sheet reconstruction, in: Dowdeswell, J.A., Canals, M., Jakobsson, M., Todd, B.J.,
2653 Dowdeswell, E.K., Hogan, K.A. (Eds.), Atlas of Submarine Glacial landforms: Modern,

Quaternary and Ancient. Geological Society, London, Memoirs, 46, pp. 519-552. https://doi.org/10.1144/M46.183.

Dowdeswell, J.A., Canals, M., Jakobsson, M., Todd, B.J., Dowdeswell, E.K., Hogan, K.A. (Eds.), 2016b. Atlas of Submarine Glacial landforms: Modern, Quaternary and Ancient. Geological Society, London, Memoirs 46, 618 pp. https://doi.org/10.1144/M46.

Draganits, E., Schlaf, J., Grasemann, B., Argles, T., 2008. Giant submarine landslide grooves in the Neoproterozoic/Lower Cambrian Phe Formation, northwest Himalaya: Mechanisms of formation and palaeogeographic implications. Sedimentary Geology 205, 126–141. https://doi.org/10.1016/j.sedgeo.2008.02.004.

Dreimanis, A., 1993. Small to medium-sized glacitectonic structures in till and in its substratum and their comparison with mass movement structures. Quaternary International, 18, 69-79.

du Toit, A.L., 1926. The Geology of South Africa. Oliver and Boyd, Edinburgh, pp. 205-215.

Dufresne, A., Davies, T.R., 2009. Longitudinal ridges in mass movement deposits. Geomorphology 105, 171-181.

Dufresne, A., Geertsema, M., Shugar, D.H., Koppes, M., Higman, B., Haeussler, P.J., Stark, C., Venditti, J.G., Bonno, D., Larsen,C., Gulick, S.P.S., McCall, N., Walton, M., Loso, M.G., Willis, M.J., 2018. Sedimentology and geomorphology of a large tsunamigenic landslide,

Taan Fiord, Alaska. Sedimentary Geology 364, 302-318. https://doi.org/10.1016/j.sedgeo.2017.10.004.

Dufresne, A., Zernack, A., Bernard, K., Thouret, J.-C., Roverato, M., 2021. Sedimentology of volcanic debris avalanche deposits, in: Roverato, M., Dufresne, A., Procter, J. (Eds.), Volcanic Debris Avalanches. Advances in Volcanology. Springer, Cham, pp. 175-210. https://doi.org/10.1007/978-3-030-57411-6_8.

Dykstra, M., 2012. Deep-water tidal sedimentology, in: Davies, R.A., Jr., Dalrymple, R.W. (Eds.), Principles of Tidal Sedimentology. Springer, Dordrecht, pp. 371-395. https://doi.org/10.1007/978-94-007-0123-6_14.

Dykstra, M., Garyfalou, K. Kertznus, V., Kneller, B., Milana, J.P., Molinaro, M., Szuman, M., Thompson, P., 2011. Mass-transport deposits: Combining outcrop studies and seismic forward modeling to understand lithofacies distributions, deformation, and their seismic stratigraphic expression, in: Shipp, R.C., Weimer, P., Posamentier, H.W. (Eds.), Mass-Transport Deposits in Deepwater Settings. SEPM Special Publication 96, pp. 293–310.

Ebert, D.A., 1996. Origin and significance of mud-filled incised valleys (Upper Cretaceous) in southern Alberta, Canada. Sedimentology 43, 459-477.

Eggenhuisen, J.T., McCaffrey, W.D., Haughton, P.D.W., Butler, R.W.H., 2011. Shallow erosion beneath turbidity currents and its impact on the architectural development of turbidite sheet systems. Sedimentology 58, 936–959, https://doi.org/10.1111/j.1365-3091.2010.01190.x.

2692 Eisbacher, G.H., 1981. The Late Precambrian Mount Lloyd George diamictites, northern
2693 British Columbia, in: Hambrey, M.J., Harland, W.B. (Eds.), Earth´s Pre-Pleistocene Glacial
2694 Record. Cambridge University Press, Cambridge, pp. 728-729.

2695 Elfström, Å., 1987. Large boulder deposits and catastrophic floods. Geografiska Annaler
2696 69A, 101-121.

2697 El-Makhrouf, A.A. 1988. Tectonic interpretation of Jabal Eghei area and its regional
2698 application to Tibesti ol ogenic belt, south central Libya (S.P.L.A.J.). Journal of African Earth
2699 Sciences 7, 945-967.

2700 Embleton, C., King, C.A.M., 1968. Glacial and Periglacial Geomorphology. Edward Arnold,
2701 London, p. 304.

2702 Embley, R.W., 1976. New Evidence for occurrence of debris flow deposits in the deep sea.
2703 Geology 4, 371-374.

2704 Embley, R.W., 1980. The role of mass transport in the distribution and character of deep-
2705 ocean sediments with special reference to the North Atlantic. Marine Geology 38, 23-50.

2706 Embley, R.W., 1982. Anatomy of some Atlantic margin sediment slides and some comments
2707 on ages and mechanisms, in: Saxov, S., Nieuwenhuis, J.K. (Eds.), Marine Slides and Other
2708 Mass Movements. Plenum Press, New York, pp. 189-213.

2709 Embley, R.W., Morley, J.J., 1980. Quaternary sedimentation and paleoenvironmental studies
2710 off Namibia (South-West Africa). Marine Geology 36, 183-204.

2711 Emery, K.O., Tschudy, R.H., 1941. Transportation of rock by kelp. Bulletin of the Geological
2712 Society of America 52, 855-862.

2713 Enos, P., 1969. Anatomy of flysch. Journal of Sedimentary Research 39, 680-723.

2714 Eriksson, P.G., 1991. A note on coarse-grained gravity-flow deposits within Proterozoic
2715 Lacustrine sedimentary rocks, Transvaal Sequence, South Africa. Journal of African Earth
2716 Sciences 12, 549-553.

2717 Erginal, A.E., Ertek, T.A., 2002. Geomorphology of Hereke-Körfez area and its relation to
2718 the submarine morphology of the centre basin of the Gulf of Izmit. Turkish Journal of Marine
2719 Sciences 8, 67-89.

2720 Evans, D.J.A., Roberts, D.H., Evans, S.C., 2016. Multiple subglacial till deposition: A
2721 modern exemplar for Quaternary palaeoglaciology. Quaternary Science Reviews 145,
2722 183-203. https://doi.org/10.1016/j.quascirev.2016.05.029.

2723 Evans, D.J.A., Phillips, E.R., Hiemstra, J.F., Auton, C.A., 2006. Subglacial till: Formation,
2724 sedimentary characteristics and classification. Earth-Science Reviews 78, 115-176.
2725 https://doi.org/10.1016/j.earscirev.2006.04.001.

2726 Evenson, E.B., Dreimanis, A., Newsome, J.W., 1977. Subaquatic flow tills: a new
2727 interpretation for the genesis of some laminated deposits. Boreas, 6 115-133.
2728 https://doi.org/10.1111/j.1502-3885.1977.tb00341.x.

2729 Eyles, C.H., Eyles, N., 1989. The Upper Cenozoic White River “tillites” of Southern Alaska:
2730 subaerial slope and fan-delta deposits in a strike-slip setting. GSA Bulletin 101, 1091-1102.

2731 Eyles, C.H., Eyles, N., 2000. Subaqueous mass flow origin for Lower Permian diamictites
2732 and associated facies of the Grant Group, Barbwire Terrace, Canning Basin, Western
2733 Australia. Sedimentology 47, 343-356.

2734 Eyles, C.H., Lagoe, M.-B., 1998. Slump-generated megachannels in the Pliocene-Pleistocene
2735 glaciomarine Yakataga Formation, Gulf of Alaska. GSA Bulletin 110, 395-408.

2736 Eyles, C.H., Eyles, N., Miall A.D., 1985. Models of glaciomarine sediment and their
2737 application to the interpretation of ancient glacial sequences. Palaeogeography,
2738 Palaeoclimatology, Palaeoecology 51, 15-84.

2739 Eyles, N., 1990. Marine debris flows: Late Precambrian “tillites” of the Avalonian-Cadomian
2740 orogenic belt. Palaeogeography, Palaeoclimatology, Palaeoecology 79, 73-98.

2741 Eyles, N., 1993. Earth´s glacial record and its tectonic setting. Earth-Science Reviews 35,
2742 1-248.

2743 Eyles, N., Boyce, J.I., 1998. Kinematic indicators in fault gouge: tectonic analog for
2744 soft-bedded ice sheets. Sedimentary Geology 116, 1-12.

2745 Eyles, N., Clark, B.M., 1985. Gravity induced soft sediment deformation in glaciomarine
2746 sequences of the Upper Proterozoic Port Askaig Formation, Scotland. Sedimentology 32,
2747 789-814. https://doi.org/10.1111/j.1365-3091.1985.tb00734.x.

2748 Eyles, N., Januszczak, N., 2007. Syntectonic subaqueous mass flows of the Neoproterozoic
2749 Otavi Group, Namibia: where is the evidence of global glaciation? Basin Research 19, 179-
2750 198.

2751 Eyles, N., Dearman, W.R., Douglas, T.D., 1983. The Distribution of glacial landsystems in
2752 Britain and North America, in: Eyles, N. (Ed.), Glacial Geology. Pergamon Press, pp.
2753 213-228. https://doi.org/10.1016/B978-0-08-030263-8.50015-4.

2754 Eyles, N., Moreno, L.A., Sookhan, S., 2018. Ice streams of the Late Wisconsin Cordilleran
2755 Ice Sheet in western North America. Quaternary Science Reviews 179, 87-122.
2756 https://doi.org/10.1016/j.quascirev.2017.10.027.

2757 Ezpeleta, M., Rustán, J.J., Balseiro, D., Dávila, F.M., Dahlquist, J.A., Vaccari, N.E., Sterren,
2758 A.F., Prestianni, C., Cisterna, G.A., Basei, M., 2020. Glaciomarine sequence stratigraphy in
2759 the Mississippian Río Blanco Basin, Argentina, southwestern Gondwana. Basin analysis and
2760 palaeoclimatic implications for the Late Paleozoic Ice Age during the Tournaisian. Journal of
2761 the Geological Society 177, 1107-1128. https://doi-org.ezp.sub.su.se/10.1144/jgs2019-214.

2762 Fairbridge, R.W., 1970. South Pole reaches the Sahara. Science 168, 878-881.

2763 Fairbridge, R.W., 1971. Upper Ordovician glaciation in Northwest Africa? Reply. GSA
2764 Bulletin 82, 269-274.

2765 Fairbridge, R.W., 1979. Traces from the desert: Ordovician, in: John, Brian S. (Ed.), The
2766 Winters of the World. Davies and Charles, Newton Abbot, pp. 131-153.

2767 Fairbridge, R.W., Finkl, C.W. Jr., 1980. Cratonic erosional unconformities and peneplains.
2768 Journal of Geology 88, 69-86.

2769 Fairchild, I.J., Fleming, E.J., Bao, H., Benn, D.I., Boomer, I., Dublyansky, Y.V., Halverson,
2770 G.P., Hambrey,M., Hendy, C., Mcmillan, E.A., Spötl, C., Stevenson, C.T.E., Wynn, P.M.,
2771 2016. Continental carbonate facies of a Neoproterozoic panglaciation, north-east Svalbard.
2772 Sedimentology 63, 443-497. https://doi.org/10.1111/sed.12252.

2773 Falvey, H.T., 1990. Cavitation in Chutes and Spillways. A Water Resources Technical
2774 Publication Engineering Monograph 42. United States Department of the Interior Bureau of
2775 Reclamation, Denver, 163 pp.

2776 Fedorchuk, N.D., Isbell, J.L., Griffis, N.P., Montañez, I.P., Vesely, F.F., Iannuzzi, R., Mundil,
2777 R., Yin, Q-Z., Pauls, K.N., Rosa; E.L.M., 2019. Origin of paleovalleys on the Rio Grande do
2778 Sul Shield (Brazil): Implications for the extent of late Paleozoic glaciation in west-central
2779 Gondwana. Palaeogeography, Palaeoclimatology, Palaeoecology 531, Part B, 108738.
2780 https://doi.org/10.1016/j.palaeo.2018.04.013.

2781 Fedorchuk, N.D., Griffis, N.P., Isbell, J.L., Goso, C., Rosa, E.L.M., Montañez, I.P., Yin, Q.-
2782 Z., Huyskens, M.H., Sanborn, M.E., Mundil, R., Vesely, F.F., Iannuzzi, R., 2021. Provenance
2783 of late Paleozoic glacial/post-glacial deposits in the eastern Chaco-Paraná Basin, Uruguay and
2784 southernmost Paraná Basin, Brazil. Journal of South American Earth Sciences 106, 102989.
2785 https://doi.org/10.1016/j.jsames.2020.102989.

2786 Festa, A., Ogata, K., Pini, G.A., Dilek, Y., Alonso, J.L., 2016. Origin and significance of
2787 olistostromes in the evolution of orogenic belts: a global synthesis. Gondwana Research
2788 39, 180–203. https://doi.org/10.1016/j.gr.2016.08.002.

2789 Festa, A., Pini, G.I., Ogata, K., Dilek, Y., 2019. Diagnostic features and field-criteria in
2790 recognition of tectonic, sedimentary and diapiric mélanges in orogenic belts and exhumed
2791 subduction-accretion complexes. Gondwana Research 74, 7-30.
2792 https://doi.org/10.1016/j.gr.2019.01.003.

2793 Finkl, C.W. Jr., Fairbridge, R.W., 1979. Paleogeographic evolution of a rifted cratonic
2794 margin: S.W. Australia. Palaeogeography, Palaeoclimatology, Palaeoecology 26, 221-252.

2795 Fiorillo, A.R., Kobayashi, Y., McCarthy, P.J., Tanaka, T., Tykoski, R.S., Lee, Y.-N.,
2796 Takasaki, R., Yoshida, J., 2019. Dinosaur ichnology and sedimentology of the Chignik
2797 Formation (Upper Cretaceous), Aniakchak National Monument, southwestern Alaska;
2798 Further insights on habitat preferences of high-latitude hadrosaurs. PLoS ONE 14, e0223471.
2799 https://doi.org/10.1371/journal.pone.0223471.

2800 Fleisher, P.J., Lachniet, M.S., Muller, E.H., Bailey, P.K., 2006. Subglacial deformation of
2801 trees within overridden foreland strata, Bering Glacier, Alaska. Geomorphology 75, 201-211.
2802 https://doi.org/10.1016/j.geomorph.2005.01.013.

2803 Flint, R.F., 1961. Geological evidence of cold climate, in: Nairn, A.E.M. (Ed.), Descriptive
2804 Palaeoclimatology. Interscience Publ., New York, pp. 140-155.

2805 Flint, R.F., 1971. Glacial and Quaternary Geology. John Wiley and Sons, New York, 892 pp..

2806 Flint, R.F., 1975. Features other than diamicts as evidence of ancient glaciations, in: Wright,
2807 A.E., Moseley, F. (Eds.), Ice Ages: Ancient and Modern. Seal House Press, Liverpool, pp.
2808 121-136.

2809 Fonnesu, M., Patacci, M., Haughton, P.D.W., Felletti, F., McCaffrey, W.D., 2016. Hybrid
2810 event beds generated by local substrate delamination on a confined-basin floor. Journal of
2811 Sedimentary Research 86, 929–943. https://doi.org/10.2110/jsr.2016.58.

2812 Frakes, L.A., 1979. Climates through Geologic Time. Elsevier, Amsterdam, 304 pp.

2813 Frakes, L.A., Crowell, J.C., 1969. Late Paleozoic glaciation: I, South America. GSA Bulletin
2814 80, 1007-1042.

2815 Frakes, L.A., Crowell, J.C., 1970. Late Paleozoic glaciation: II, Africa exclusive of the Karoo
2816 Basin. GSA Bulletin 81, 2261-2286.

Frakes, L.A., Krassay, A.A., 1992. Discovery of probable ice-rafting in the Late Mesozoic of the Northern Territory and Queensland. Australian Journal of Earth Sciences 39, 115-119. https://doi.org/10.1080/08120099208728006.

Frakes, L.A., Amos, A.A., Crowell, J.C., 1969. Origin and stratigraphy of Late Paleozoic diamictites in Argentina and Bolivia, in: Amos, A.J. (Ed.), Gondwana Stratigraphy. IUGS Symposium in Buenos Aires 1967, UNESCO, pp. 821-843.

Francis, J.E., 1990. Polar fossil forests. Geology Today 6, May-June, 92-95.

Frimmel, H.E., 2010. On the reliability of stable carbon isotopes for Neoproterozoic chemostratigraphic correlation. Precambrian Research 182, 239-253. https://doi.org/10.1016/j.precamres.2010.01.003.

Frimmel, H.E., 2018. The Gariep Belt, in: Siegesmund, S., Basei, M., Oyhantçabal, P., Oriolo, S. (Eds.), Geology of Southwest Gondwana. Regional Geology Reviews. Springer, Cham. https://doi.org/10.1007/978-3-319-68920-3_13.

Fry, W.L., 1983. An algal flora from the Upper Ordovician of the Lake Winnipeg Region, Manitoba, Canada. Review of Palaeobotany and Palynology 39, 313-341.

Gales, J.A., Leat, P.T., Larter, R.D., Kuhn, G., Hillenbrand, C.-D., Graham, A.G.C., Mitchell, N.C., Tate, A.J., Buys, G.B., Jokat W., 2014. Large-scale submarine landslides, channel and gully systems on the southern Weddell Sea margin, Antarctica. Marine Geology 348, 73–87. https://doi.org/10.1016/j.margeo.2013.12.002.

2836 Garden, C.J., Smith, A.M., 2011. The role of kelp in sediment transport: Observations from
2837 southeast New Zealand. Marine Geology 281, 35-42.

2838 Garzanti, E., Resentini, A., 2016. Provenance control on chemical indices of weathering
2839 (Taiwan river sands). Sedimentary Geology 336, 81-95.
2840 https://doi.org/10.1016/j.sedgeo.2015.06.013.

2841 Gastaldo, F.A., Bamford, M., Calder, J., DiMichele, W.A., Iannuzzi, R., Jasper, A., Kerp, H.,
2842 McLoughlin, S., Opluštil, S., Pfefferkorn, H.W., Rößler, R., Wang, J., 2020a. The non-analog
2843 vegetation of the Late Paleozoic icehouse–hothouse and their coal-forming forested
2844 environments, in: Martinetto, E., Tschopp, E., Gastaldo, R. (Eds.), Nature through Time.
2845 Springer Textbooks in Earth Sciences, Geography and Environment. Springer, Cham, pp.
2846 291-316. https://doi.org/10.1007/978-3-030-35058-1_12.

2847 Gastaldo, F.A., Bamford, M., Calder, J., DiMichele, W.A., Iannuzzi, R., Jasper, A., Kerp, H.,
2848 McLoughlin, S., Opluštil, S., Pfefferkorn, H.W., Rößler, R., Wang, J., 2020b. The coal farms
2849 of the Late Paleozoic, in: Martinetto, E., Tschopp, E., Gastaldo, R. (Eds.), Nature through
2850 Time. Springer Textbooks in Earth Sciences, Geography and Environment. Springer, Cham,
2851 pp. 317-343. https://doi.org/10.1007/978-3-030-35058-1_13.

2852 Gateway to the Paleobiology Database. http://fossilworks.org/ (accessed 29 January 2020).

2853 Gaucher, C., Sial, A.N., Frei, R., 2015. Chemostratigraphy of Neoproterozoic banded iron
2854 formation (BIF): types, age and origin, in: Ramkumar, M. (Ed.), Chemostratigraphy:

2855 Concepts, Techniques, and Applications. Elsevier, Amsterdam, pp. 433-449.
2856 https://doi.org/10.1016/B978-0-12-419968-2.00017-0.

2857 Gee, M.J.R., Gawthorpe, R.L., Friedmann, J.S., 2005. Giant striations at the base of a
2858 submarine landslide. Marine Geology 214, 287–294.

2859 Gee, M.J.R., Uy, H.S., Warren, J., Morley, C.K., Lambiase, J.J., 2007. The Brunei slide: A
2860 giant submarine landslide on the North West Borneo Margin revealed by 3D seismic data.
2861 Marine Geology 246, 9–23. https://doi.org/10.1016/j.margeo.2007.07.009.

2862 Georgiopoulou, A., Masson, D.G, Wynn, R.B., Krastel, S., 2010. Sahara Slide: Age,
2863 initiation, and processes of a giant submarine slide. Geochemistry, Geophysics, Geosystems
2864 11, Q07014. https://doi.org/10.1029/2010GC003066.

2865 Germs, G.J.B., Gaucher, C., 2012. Nature and extent of a late Ediacaran (c. 547 Ma)
2866 glacigenic erosion surface in southern Africa. South African Journal of Geology 115, 91–102.

2867 Gibson, T.M., Shih, P.M., Cumming, V,M., Fischer, W.W., Crockford, P.W., Hodgskiss,
2868 M.S.W., Wörndle, S., Creaser, R.A., Rainbird, R.H., Skulski, T.M., Halverson, G.P., 2018.
2869 Precise age of Bangiomorpha pubescens dates the origin of eukaryotic photosynthesis.
2870 Geology 46, 135–138. https://doi.org/10.1130/G39829.1.

2871 Ghienne, J.-F., 2003. Late Ordovician sedimentary environments, glacial cycles, and
2872 post-glacial transgression in the Taoudeni Basin, West Africa. Palaeogeography,
2873 Palaeoclimatology, Palaeoecology 189, 117-145.

2874 Ghienne, J.-F., Deynoux, M., Manatschal, G, Rubino, J.L., 2003. Palaeovalleys and fault-
2875 controlled depocentres in the Late-Ordovician glacial record of the Murzuq Basin (central
2876 Libya). Comptes Rendus Geoscience 335, 1091-1100.

2877 Ghienne, J.-F., Le Heron, D.P., Moreau, J., Denis, M., Deynoux, M., 2007. The Late
2878 Ordovician glacial sedimentary system of the North Gondwana platform, in: Hambrey, M.J.,
2879 Christoffersen, P., Glasser, N.F., Hubbard, B. (Eds) Glacial Sedimentary Processes and
2880 Products. International Association of Sedimentologists Special Publication 39, Blackwell
2881 Publishing, Victoria, pp. 295-319.

2882 Ghuma, M.A., Rogers, J.J.W., 1978. Geology geochemistry, and tectonic setting of the
2883 Ben Ghnema batholith, Tibesti massif, southern Libya. GSA Bulletin 89, 1351-1358.

2884 Giddings, J.A., Wallace, M.W., Haines, P.W., Mornane, K., 2010. Submarine origin for the
2885 Neoproterozoic Wonoka canyons, South Australia. Sedimentary Geolology 223, 35–50.

2886 Giegengack, R.F., Zaki, A.S., 2017. Inverted topographic features, now submerged beneath
2887 the water of Lake Nasser, document a morphostratigraphic sequence of high-amplitude late-
2888 Pleistocene climate oscillation in Egyptian Nubia. Journal of African Earth Sciences 136,
2889 176-187. https://doi.org/10.1016/j.jafrearsci.2017.06.027.

2890 Gilbert, R., 1990. Rafting in glacimarine environments, in: Dowdeswell, J.A., Scource, J.D.
2891 (Eds.), Glacimarine Environments: Processes and Sediments. Geological Society, London,
2892 Spec. Publ. 53, pp. 105-120.

Glicken, H., 1996. Rockslide-debris avalanche of May 18, 1980, Mount St. Helens Volcano, Washington. US Geological Survey, Open-File Report 96-677.

Glock, W.D., Studhalter, R.A., Agerter, S.R., 1960. Classification and multiplicity of growth layers in the branches of trees at the extreme lower forest border. Smithsonian Miscellaneous Collections 140, Smithsonian Institution, Washington, 294 pp.

Gómez-Peral, L.E., Sial, A.N., Arrouy, M.J., Richiano, S., Ferreira, V.P., Kaufman, A.J., Poiré, D.G., 2017. Paleo-climatic and paleo-environmental evolution of the Neoproterozoic basal sedimentary cover on the Río de La Plata Craton, Argentina: Insights from the $\delta^{13}C$ chemostratigraphy. Sedimentary Geology 353, 139-157.

González, C.R., Glasser, N.F., 2008. Carboniferous glacial erosional and depositional features in Argentina. Geologica et Palaeontologica 48, 39-54.

Gore, D.B., Taylor M.P. 2003. Discussion and Reply: Grooves and striations on the Stanthorpe Adamellite: Evidence for a possible late Middle – Late Triassic age glaciation. Australian Journal of Earth Sciences 50, 467-470.

Götz, A.E., Ruckwied, K., Wheeler, A., 2018. Marine flooding surfaces recorded in Permian black shales and coal deposits of the Main Karoo Basin (South Africa): implications for basin dynamics and cross-basin correlation. International Journal of Coal Geology 190, 178–190. https://doi.org/10.1016/j.coal.2017.10.014.

2911 Gould, S.J., 1987. Time´s Arrow, Time´s Cycle. Harvard University Press, Cambridge, 222
2912 pp.

2913 Gravenor, C.P., 1979. The nature of the Late Paleozoic glaciation in Gondwana as determined
2914 from an analysis of garnets and other heavy minerals. Canadian Journal of Earth Sciences 16,
2915 1137-1153.

2916 Gravenor, C.P., 1986. Magnetic and pebble fabrics in subaquatic debris-flow deposits.
2917 Journal of Geology 94, 683-698.

2918 Gravenor, C.P., Rocha-Campos, A.C., 1983. Patterns of Late Paleozoic glacial sedimentation
2919 on the southeast side of the Paraná Basin, Brazil. Palaeogeography, Palaeoclimatology,
2920 Palaeoecology 43, 1-39.

2921 Gravenor, C.P., Von Brunn, V., 1987. Aspects of Late Paleozoic glacial sedimentation in
2922 parts of the Paraná Basin, Brazil, and the Karoo Basin, South Africa, with special reference to
2923 the origin of massive diamictite, in: McKenzie, G.D. (Ed.), Gondwana Six: Stratigraphy,
2924 Sedimentology and Paleontology. Geophysical Monograph 41, pp. 103-111.

2925 Gravenor, C.P., Von Brunn, V., Dreimanis, A., 1984. Nature and classification of waterlain
2926 glaciogenic sediments, exemplified by Pleistocene, Late Paleozoic and Late Precambrian
2927 deposits. Earth-Science Reviews 20, 105-166.

2928 Griffis, N.P., Montañez, I.P., Fedorchuk, N., Isbell, J., Mundil, R., Vesely, F., Weinshultz, L.,
2929 Iannuzzi, R., Gulbransen, E., Taboada, A., Pagani, A., Sanborn, M.E., Huyskens, M.,

2930 Wimpenny, J., Linol, B., Yin, Q.-Z., 2019. Isotopes to ice: Constraining provenance of glacial
2931 deposits and ice centers in west-central Gondwana. Palaeogeography, Palaeoclimatology,
2932 Palaeoecology 531, 108745. https://doi.org/10.1016/j.palaeo.2018.04.020.

2933 Grotzinger, J.P., Fike, D.A., Fischer, W.W., 2011. Enigmatic origin of the largest-known
2934 carbon isotope excursion in Earth´s history. Nature Geoscience 4, 285-292.
2935 https://doi.org/10.1038/NGEO1138.

2936 Gulbranson, E.L., Ryberg, P.E., Decombeix, A.-L., Taylor, E.L., Taylor, T.N., Isbell, J.L.,
2937 2014. Leaf habit of Late Permian Glossopteris trees from high-palaeolatitude forests. Journal
2938 of the Geological Society 171, 493-507.

2939 Gupta, S., 2007. Making the paper. Nature 448, xv.

2940 Gupta, S., Collier, J.S., Palmer-Felgate1, A., Graeme Potter, G., 2007. Catastrophic flooding
2941 origin of shelf valley systems in the English Channel. Nature 448, 342-346.

2942 Gupta, S., Collier, J.S., Garcia-Moreno, D., Oggioni, F., Trentesaux, A., Vanneste, K., De
2943 Batist, M., Camelbeek, T., Potter, G., Van Vliet-Lanoe, B., Arthur, J.C.R., 2017. Two-stage
2944 opening of Dover Strait and the origin of island Britain. Nature Communications 8, 1-12.

2945 Gürbüz, A., 2010. Geometric characteristics of pull-apart basins. Lithosphere 2, 199-206.
2946 https://doi.org/10.1130/L36.1.

2947 Haflidason, H., Sejrup, H.P., Nygård, A., Mienert, J., Bryn, P., Lien, R., Forsberg, C.F., Berg,
2948 K., Masson, D., 2004. The Storegga Slide: architecture, geometry and slide development.
2949 Marine Geology 213, 201–234. https://doi.org/10.1016/j.margeo.2004.10.007.

2950 Haldorsen, S., 1983. The characteristics and genesis of Norwegian tills, in: Ehlers, J. (Ed.),
2951 Glacial Deposits in North-west Europe. A. A. Balkema, Rotterdam, pp. 11-17.

2952 Haldorsen, S., Von Brunn, V., Maud, R., Truter, E.D., 2001. A Weichselian deglaciation
2953 model applied to the early Permian glaciation in the northeast Karoo Basin, South Africa.
2954 Journal of Quaternary Science 16, 583-593. https://doi.org/10.1002/jqs.637.

2955 Hall, K.J., 1989. Clast shape, in: Barett, P.J. (Ed.), Antarctic Cenozoic History from the
2956 CIROS-1 Drillhole, McMurdo Sound. DSIR Bulletin 245, pp. 63-66.

2957 Hall, K.J., Visser, J.N.J., 1984. Observations on the relationship between clast size, shape,
2958 and lithology from the Permo-Carboniferous glaciogenic Dwyka Formation in the western
2959 part of Karoo Basin. Transactions of the Geological Society of South Africa 87, 225-232.

2960 Hambrey, M.J., 1983. Correlation of Late Proterozoic tillites in the North Atlantic region and
2961 Europe. Geological Magazine 120, 209-232.

2962 Hambrey, M.J., Harland, W.B. (Eds.), 1981. Earth´s Pre-Pleistocene Glacial Record.
2963 Cambridge University Press, Cambridge. (Reissued edition in 2011.)

Hambrey, M.J., Harland, W.B., 1981. Criteria for the identification of glacigenic deposits, in: Hambrey, M.J., Harland, W.B. (Eds.), Earth´s Pre-Pleistocene Glacial Record. Cambridge University Press, Cambridge, 14-20.

Hampton, M.A., 1972. The role of subaqueous debris flow in generating turbidity currents. Journal of Sedimentary Petrology 42, 775-793.

Hancox, P.J., Götz, A.E., 2014. South Africa´s coalfields – A 2014 perspective. International Journal of Coal Geology 132, 170–254. https://doi.org/10.1016/j.coal.2014.06.019.

Hansen, L.A.S., Hodgson, D.M., Pontén, A., Bell, D., Flint, S., 2019. Quantification of basin-floor fan pinchouts: examples from the Karoo Basin, South Africa. Frontiers in Earth Science 7, article 12. https://doi.org/10.3389/feart.2019.00012.

Hansom, J.D., 1983. Ice-formed intertidal boulder pavements in the Sub-Antarctic. Journal of Sedimentary Petrology 53, 135-145.

Hara, Y., Thorn, C.E., 1982. Preliminary quantitative study of alpine subnival boulder pavements, Colorado, Front Range, U.S.A. Arctic and Alpine Research 14, 361-367.

Harker, R.I., 1993. Fracture patterns in clasts of diamictites (? tillites). Journal of the Geological Society 150, 251-254. https://doi.org/10.1144/gsjgs.150.2.0251.

Harker, R.I., Giegengack, R., 1989. Brecciation of clasts in diamictites of the Gowganda Formation, Ontario, Canada. Geology 17, 123-126.

2982 Harland, W.B., Herod, K.N., 1975. Glaciations through time, in: Wright, A.E., Moseley, F.
2983 (Eds.), Ice Ages: Ancient and Modern. Seal House Press, Liverpool, pp. 189-216.

2984 Harrington, H.J., 1971. Glacial-like “striated floor” originated by debris-laden torrential water
2985 flows. AAPG Bulletin 55, 1344-1347.

2986 Harris, P.T., Barrie, J.V., Conway, K.W., Greene, H.G., 2014. Hanging canyons of Haida
2987 Gwaii, British Columbia, Canada: Fault-control on submarine canyon geomorphology along
2988 active continental margins. Deep Sea Research Part II: Topical Studies in Oceanography 104,
2989 83-92. http://dx.doi.org/10.1016/j.dsr2.2013.06.017.

2990 Hart, J.K., Roberts, D.H., 1994. Criteria to distinguish between subglacial glaciotectonic and
2991 glaciomarine sedimentation, I. Deformation styles and sedimentology. Sedimentary Geology
2992 91, 191-213. https://doi.org/10.1016/0037-0738(94)90129-5.

2993 Hartley, A., Kurjanski, B., Pugsley, J., Armstrong, J., 2020, Ice-rafting in lakes in the early
2994 Neoproterozoic: dropstones in the Diabaig Formation, Torridon Group, NW Scotland.
2995 Scottish Journal of Geology 56, 47–53. https://doi.org/10.1144/sjg2019-017.

2996 Hawkes, L., 1943. The erratics of the Cambridge Greensand – their nature provenance and
2997 mode of transport. Quaterly Journal of the Geological Society of London 99, 93-104.

2998 He, Y., Xie, X., Kneller, B.C., Wang, Z., Li, X., 2013. Architecture and controlling factors of
2999 canyon fills on the shelf margin in the Qiongdongnan Basin, northern South China Sea.

Marine and Petroleum Geology 41, 264-276.
https://doi.org/10.1016/j.marpetgeo.2012.03.002.

Heezen, B.C., Hollister, C.D., 1971. The Face of the Deep. Oxford University Press, New York, pp. 293-304.

Hicock, S.R., 1991. On subglacial stone pavements in till. Journal of Geology 99, 607-619.

Hicock, S.R., Dreimanis, A., 1992a. Sunnybrook drift in the Toronto area, Canada: Reinvestigation and reinterpretation, in: Clark, P.U., Lea, P.D. (Eds.), The Last Interglacial Transition in North America. Geological Society of America Special Paper 270, Boulder, Colorado, pp. 139-161. https://doi.org/10.1130/SPE270-p139.

Hicock, S.R., Dreimanis, A., 1992b. Deformation till in the Great Lakes region: implications for rapid flow along the south-central margin of the Laurentide Ice Sheet. Canadian Journal of Earth Sciences 29, 1565-1579.

Hill, P., Aksu, A.E., Piper, D.J.W., 1982. The deposition of thin bedded subaqueous debris flow deposits, in: Saxov, S., Nieuwenhuis, J.K. (Eds.), Marine Slides and Other Mass Movements. Plenum Press, New York, pp. 273-287.

Hodgson, D.M., Brooks, H.L., Ortiz-Karpf, A., Spychala, Y., Lee, D.R., Jackson, C.A.-L., 2018. Entrainment and abrasion of megaclasts during submarine landsliding and their impact on flow behaviour, in: Lintern, D.G., Mosher, D.C., Moscardelli, L.G., Bobrowsky, P.T., Campbell, C., Chaytor, J.D., Clague, J.J., Georgiopoulou, A., Lajeunesse, P., Normandeau,

A., Piper, D.J.W., Scherwath, M., Stacey, C., Turmel, D. (Eds.), Subaqueous Mass Movements and Their Consequences: Assessing Geohazards, Environmental Implications and Economic Significance of Subaqueous Landslides. Geological Society, London, Special Publications 477, 223-240. https://doi.org/10.1144/SP477.26.

Hoffman, P.F., 2011. A history of Neoproterozoic glacial geology, 1871–1997, in: Arnaud, E., Halverson, G.P., Shields-Zhou, G. (Eds.), The Geological Record of Neoproterozoic Glaciations. Geological Society, London, Memoirs 36, pp. 17-37. https://doi.org/10.1144/M36.2

Hoffman, P.F., Kaufman, A.J., Halverson, G.P., 1998. Comings and goings of global glaciations on a Neoproterozoic tropical platform in Namibia. Geological Society of America Today 8, 1-9.

Hoffman, P.F., Halverson, G.P., 2008. Otavi Group of the Northern Platform and the Northern Margin Zone, in: Miller, R.McG. (Ed.), The Geology of Namibia. Neoproterozoic to Lower Paleozoic, vol. 2. Geological Survey of Namibia, Windhoek, pp. 13.69-13.136.

Hoffman, P.F., Calver, C.R., Halverson, G.P., 2009. Cottons breccia of King Island, Tasmania: Glacial or non-glacial, Cryogenian or Ediacaran? Precambrian Research 172, 311-322. https://doi.org/10.1016/j.precamres.2009.06.003.

Hoffman, P.F., Halverson, G.P., Schrag, D.P., Higgins, J.A., Domack, E.W., Macdonald, F.A., Pruss, S.B., Blättler, C.L., Crockford, P.W., Hodgin, E.B., Bellefroid, E.J., Johnson, B.W., Hodgskiss, M.S.W., Lamothe, K.G., LoBianco, S.J.C., Busch, J.F., Howes, B.J.,

Greenman, J.W., Nelson, L.L., 2021. Snowballs in Africa: Sectioning a long-lived Neoproterozoic carbonate platform and its bathyal foreslope (NW Namibia). Earth-Science Reviews 219, 103616. https://doi.org/10.1016/j.earscirev.2021.103616.

Hollick, A., 1930. The Upper Cretaceous Floras of Alaska, U.S. Geological Survey Professional Paper 159, 214 pp (including plates).

Holme, C., Gkinis, V., Lanzky, M., Morris, V., Olesen, M., Thayer, A., Vaughn, B.H., Vinther, B.M., 2019. Varying regional δ^{18}O-temperature relationship in high-resolution stable water isotopes from east Greenland. Climate of the Past 15, 893–912. https://doi.org/10.5194/cp-15-893-2019.

Hoppe, G., 1981. Glacial traces on the Island of Hopen, Svalbard: A correction. Geografiska annaler 63A, 67-68.

Horan, K., 2015. Falkland Islands (Islas Malvinas) in the Permo-Carboniferous. Springer Earth System Sciences, Springer, Cham, pp. 45-70. https://doi.org/10.1007/978-3-319-08708-5_4.

Hore, S.B., Hill, S.M., Alley, N.F., 2020. Early Cretaceous glacial environment and paleosurface evolution within the Mount Painter Inlier, northern Flinders Ranges, South Australia. Australian Journal of Earth Sciences 67, 1117-1160. https://doi.org/10.1080/08120099.2020.1730963.

3057 Hu, W., McSaveney, M.J., 2018. A polished and striated pavement formed by a rock
3058 avalanche in under 90 s mimics a glacially striated pavement. Geomorphology 320, 154-161.

3059 Huber, H., Koeberl, C., Mcdonald, I., Reimold, W.U., 2001. Geochemistry and petrology of
3060 Witwatersrand and Dwyka diamictites from South Africa: search for an extraterrestrial
3061 component. Geochimica et Cosmochimica Acta 65, 2007-2016.

3062 Hume, J.D., 1963. Floating sand and pebbles near Barrow, Alaska. Geological Society of
3063 America, Memoir 73, Abstracts for 1962, New York, p. 176.

3064 Hume, J.D., Schalk, M., 1964. The effects of ice-push in Arctic beaches. American Journal of
3065 Science 262, 267-273.

3066 Ilstad, T., De Blasio, F.V., Elverhøi, A., Harbitz, C.B., Engvik, L., Longvad, O., Marr, J.G.,
3067 2004. On the frontal dynamics and morphology of submarine debris flows. Marine Geology
3068 213, 481–497.

3069 Imbo, Y., De Batist, M., Canals, M., Prieto, M.J., Baraza, J., 2003. The Gebra Slide: a
3070 submarine slide on the Trinity Peninsula Margin, Antarctica. Marine Geology 193, 235–252.

3071 Immonen, N., 2013. Surface microtextures of ice-rafted quartz grains revealing glacial ice
3072 in the Cenozoic Arctic. Palaeogeography, Palaeoclimatology, Palaeoecology 374, 293-302.

3073 Isbell, J.L., 2010. Environmental and paleogeographic implications of glaciotectonic
3074 deformation of glaciomarine deposits within Permian strata of the Metschel Tillite, southern

Victoria Land, Antarctica, in: López-Gamundí, O.R., Buatois, L.A. (Eds.), Late Paleozoic Glacial Events and Postglacial Transgressions in Gondwana. Geological Society of America Special Paper 468, pp. 81–100. https://doi.org/10.1130/2010.2468(03).

Isbell, J.L., Miller, M.F., Babcock, L.E., Hasiotis, S.T., 2001. Ice-marginal environment and ecosystem prior to initial advance of the late Palaeozoic ice sheet in the Mount Butters area of the central Transantarctic Mountains, Antarctica. Sedimentology 48, 953-970.

Isbell, J.L., Cole, D.I., Catuneanu, O., 2008. Carboniferous-Permian glaciation in the main Karoo Basin, South Africa: Stratigraphy, depositional controls, and glacial dynamics, in: Fielding, C.R., Frank, T.D., Isbell, J.L. (Eds.), Resolving the Late Paleozoic Ice Age in Time and Space. Geological Society of America Special Paper 441, pp. 71–82. https://doi.org/10.1130/2008.2441(05).

Isbell, J.L., Henry, L.C., Gulbranson, E., Limarino, C.O., Fraiser, M.L., Koch, Z.J., Ciccioli, P.L., Dineen, A.A., 2012. Glacial paradoxes during the late Paleozoic ice age: Evaluating the equilibrium line altitude as a control on glaciation. Gondwana Research 22, 1–19.

Isbell, J.L., Henry, L.C., Reid, C.M, Fraiser, M.L., 2013. Sedimentology and palaeoecology of lonestone-bearing mixed clastic rocks and cold-water carbonates of the Lower Permian basal beds at Fossil Cliffs, Maria Island, Tasmania (Australia): Insight into the initial decline of the late Palaeozoic ice age, in: Gasiewicz, A., Słowakiewicz, M. (Eds.), Palaeozoic Climate Cycles: Their Evolutionary and Sedimentological Impact. Geological Society, London, Special Publications 376, pp. 307–341. https://doi.org/10.1144/SP376.2.

Isbell, J.L., Biakov, A.S., Vedernikov, I.L., Davydov, V.I., Gulbranson, E.L., Fedorchuk, N.D., 2016. Permian diamictites in northeastern Asia: Their significance concerning the bipolarity of the late Paleozoic ice age. Earth-Science Reviews 154, 279–300. https://doi.org/10.1016/j.earscirev.2016.01.007.

Isbell, J.L., Vesely, F.F., Rosa, E.L.M., Pauls, K.N., Fedorchuk, N.D., Ives, L.R.W., McNall, N.B., Litwin, S.A., Borucki, M.K., Malone, J.E., Kusick, A.R., 2021. Evaluation of physical and chemical proxies used to interpret past glaciations with a focus on the late Paleozoic Ice Age. Earth-Science Reviews 221, 103756. https://doi.org/10.1016/j.earscirev.2021.103756.

Isotta, C.A.L., Rocha-Campos, A.C., Yoshida, R., 1969. Striated pavement of the Upper Pre-Cambrian glaciation in Brazil. Nature 222, 466-468.

Iverson, N.R., 1991. Morphology of glacial striae: Implications for abrasion of glacier beds and fault surfaces. GSA Bulletin 103, 1308-1316.

Ives, L.R.W., Isbell, J.L., 2021. A lithofacies analysis of a South Polar glaciation in the Early Permian: Pagoda Formation, Shackleton Glacier region, Antarctica. Journal of Sedimentary Research 91, 611–635. https://doi.org/10.2110/jsr.2021.004.

Jackson, T.A., 1965. Power-spectrum analysis of two “varved” argillites in the Huronian Cobalt Series (Precambrian) of Canada. Journal of Sedimentary Petrology 35, 877-886.

Jansa, L.F., Carozzi, A.V., 1970. Exotic pebbles in La Salle limestone (Upper Pennsylvanian), La Salle, Illinois. Journal of Sedimentary Petrology 40, 688-694.

John, B.S., 1979. The great ice age: Permo-Carboniferous, in: John, B.S. (Ed.), The Winters of the World. Davies and Charles, Newton Abbot, pp.154-172.

Johnson, M.R., Van Vuuren, C.J., Visser, J.N.J., Cole, D.I., Wickens, H.D.V., Christie, A.D.M., Roberts, D.L., 1997. The foreland Karoo Basin, South Africa, in: Selley, R.C. (Ed.), African Basins, Sedimentary Basins of the World 3. Elsevier, Amsterdam, pp. 269-317.

Kalińska-Nartiša, E., Woronko, B., Ning, W., 2017. Microtextural inheritance on quartz sand grains from Pleistocene periglacial environments of the Mazovian Lowland, Central Poland. Permafrost and Periglacial Processes 28, 741-756. https://doi.org/10.1002/ppp.1943.

Kalińska, E., Lamsters, K., Karušs, J., Krievāns, M., Rečs, A., Ješkins, J., 2022. Does glacial environment produce glacial mineral grains? Pro- and supra-glacial Icelandic sediments in microtextural study. Quaternary International 617, 101-111.. https://doi.org/10.1016/j.quaint.2021.03.029.

Karlsrud, K., Edgers, L., 1982. Some aspects of slope stability, in: Saxov, S., Nieuwenhuis, J. K. (Eds.), Marine Slides and Other Mass Movements. Plenum Press, New York, pp. 61-81.

Keiser, L.J., Soreghan, G.S., Kowalewski, M., 2015. Use of quartz microtextural analysis to assess possible proglacial deposition for the Pennsylvanian-Permian Cutler Formation (Colorado, U.S.A.). Journal of Sedimentary Research 85, 1310-1322.

Keller, M., Hinderer, M., Al-Ajmi, H., Rausch, R., 2011. Palaeozoic glacial depositional environments of SW Saudi Arabia: process and product. Geological Society, London, Special Publications 354, 129-152. https://doi.org/10.1144/SP354.8 .

Kennedy, K., Eyles, N., 2019. Subaqueous debrites of the Grand Conglomérat Formation, Democratic Republic of Congo: A model for anomalously thick Neoproterozoic: “Glacial” diamictites. Journal of Sedimentary Research 89, 935–955. https://doi.org/10.2110/jsr.2019.51.

Kennedy, K., Eyles, N., 2021. Syn-rift mass flow generated ´tectonofacies´ and ´tectonosequences´ of the Kingston Peak Formation, Death Valley, California, and their bearing on supposed Neoproterozoic panglacial climates. Sedimentology 68, 352-381. https://doi.org/10.1111/sed.12781.

Kennedy, K., Eyles, N., Broughton, D., 2019. Basinal setting and origin of thick (1.8 km) mass-flow dominated Grand Conglomérat diamictites, Kamoa, Democratic Republic of Congo: Resolving climate and tectonic controls during Neoproterozoic glaciations. Sedimentology 66, 556–589. https://doi.org/10.1111/sed.12494.

Kent, D.V., Muttoni, G., 2020. Pangea B and the Late Paleozoic ice age. Palaeogeography, Palaeoclimatology, Palaeoecology 553, 109753. https://doi.org/10.1016/j.palaeo.2020.109753.

Kerr, R.A., 1993. Fossils tell of mild winters in an ancient hothouse. Science 261, 682.

Kerr, R.A., 2008. More climate wackiness in the Cretaceous supergreenhouse? Science 319, 145.

Kilfeather, A.A., Ó Cofaigh, C., Dowdeswell, J.A., van der Meer, J.J.M.,, Evans, D.J.A., 2010. Micromorphological characteristics of glacimarine sediments: implications for distinguishing genetic processes of massive diamicts. Geo-Marine Letters 30, 77–97 . https://doi.org/10.1007/s00367-009-0160-8.

Kim, S.B., Chough, S.K., Chun, S.S., 1995. Bouldery deposits in the lowermost part of the Cretaceous Kyokpori Formation, SW Korea: cohesionless debris flows and debris falls on a steep-gradient delta slope. Sedimentary Geology 98, 97-119. https://doi.org/10.1016/0037-0738(95)00029-8.

Klein, T., Ramon, U., 2019. Stomatal sensitivity to CO_2 diverges between angiosperm and gymnosperm tree species. Functional Ecology 33, 1411-1424. https://doi.org/10.1111/1365-2435.13379.

Kneller, B.C., Edwards, D., McCaffrey, W.D., Moore, R., 1991. Oblique reflection of turbidity currents. Geology 14, 250-252.

Kneller, B., Milana, J.P., Buckee, C., al Ja´aidi. O., 2004. A depositional record of deglaciation in a paleofjord (Late Carboniferous [Pennsylvanian] of San Juan Province, Argentina): The role of catastrophic sedimentation. GSA Bulletin 116, 348–367. https://doi.org/10.1130/B25242.1.

Kneller, B., Dykstra, M., Fairweather, L., Milana, J.P., 2016. Mass-transport and slope accommodation: Implications for turbidite sandstone reservoirs. AAPG Bulletin 100, 213-235. https://doi.org/10.1306/09011514210.

Kochhann, M.V.L., Cagliari, J., Kochhann, K.G.D., Franco, D.R., 2020. Orbital and millennial-scale cycles paced climate variability during the Late Paleozoic Ice Age in the southwestern Gondwana. Geochemistry, Geophysics, Geosystems 21, e2019GC008676. https://doi.org/10.1029/2019GC008676.

Kohn, M.W., 2010. Carbon isotope compositions of terrestrial C3 plants as indicators of (paleo)ecology and (paleo)climate. PNAS 107, 19691-19695. https://doi.org/10.1073/pnas.1004933107.

Komar, P.D., 1970. The competence of turbidity current flow. GSA Bulletin 81, 1555-1562.

Korstgärd, J.A., Nielsen, O.B., 1989. Provenance of dropstones in Baffin Bay and Labrador Sea, Leg 105, in: Srivastava, S.P., Arthur, M.L, Clement, B., Aksu, A., Baldauf, J., Bohrmann, G., Busch, W., Cederberg, T., Cremer, M., Dadey, K., De Vernal, A., Firth, J., Hall, F., Head, M., Hiscott, R., Jarrard, R., Kaminski, M., Lazarus, D., Monjanel, A.L., Nielsen, O.B., Stein, R., Thiebault, F., Zachos, J., Zimmerman, H. (Eds.), Proceedings of the Ocean Drilling Program, Scientific Results 105. Texas A&M University, College Station, pp. 65-69. https://doi.org/10.2973/odp.proc.sr.105.200.1989.

Krüger, J., 1984. Clasts with stoss-lee form in lodgement tills: a discussion. Journal of Glaciology 30:241-243.

Kuenen, P.H., 1964. Deep sea sands and ancient turbidites, in: Bouma, A.H., Brouwer, A. (Eds.), Turbidites. Elsevier Publ., Amsterdam, pp. 3-33.

Kuhn, T.S., 1970. Science does not develop by accumulation (excerpts from The Structure of Scientific Revolutions), in: Neurath, O. (Ed.), International Encyclopedia of Unified Science 2. The University of Chicago Press, Chicago, pp. 219-228.

Kulling, O., 1951. Spår av Varangeristiden i Norrbotten. SGU C503, Stockholm, 44 pp.

Kumar, P.C., Omosanya, K.O., Eruteya, O.E., Sain, K., 2021. Geomorphological characterization of basal flow markers during recurrent mass movement: A case study from the Taranaki Basin, offshore New Zealand. Basin Research, 00:1–25. https://doi.org/10.1111/bre.12560.

Kurtz, D.D., Anderson, J.B., 1979. Recognition and sedimentologic description of recent debris flow deposits from the Ross and Weddel Seas, Antarctica. Journal of Sedimentary Petrology 49, 1159-1170.

Kut, A.A.,Woronko, B., Spektor, V.V., Klimova, I.V., 2021. Grain-surface microtextures in deposits affected by periglacial conditions (Abalakh High-Accumulation Plain, Central Yakutia, Russia). Micron 146, 103067. https://doi.org/10.1016/j.micron.2021.103067.

Kyser, K.T., 1986. Stable isotope variations in the mantle, in: Valley, J.W., Taylor, H.P., O´Neil, J.R. (Eds.), Stable Isotopes in High Temperature Geologic Processes. Reviews in

Mineralogy and Geochemistry 16, De Gruyter, Washington, pp. 141–164. https://doi.org/10.1515/9781501508936.

LaMarche, V.C. Jr., 1969. Environment in relation to age of Bristlecone pines. Ecology 50, 53-59. https://doi.org/10.2307/1934662.

Lamb, M.P., 2008. Formation of Amphitheater-Headed Canyons (Ph.D. thesis). University of California, Berkeley, 311 pp.

Lamb, M.P., Mackey, B.H., Farley, K.A., 2014. Amphitheater-headed canyons formed by megaflooding at Malad Gorge, Idaho. PNAS 111, 57-62. https://doi.org/10.1073/pnas.1312251111.

Lang, J., Le Heron, D.P., Van den Berg, J.H., Winsemann, J., 2020. Bedforms and sedimentary structures related to supercritical flows in glacigenic settings. Sedimentology 68, 1539-1579. https://doi.org/10.1111/sed.12776.

Larsen, V., Steel, R.J., 1978. The sedimentary history of a debris-flow dominated, Devonian alluvial fan–a study of textural inversion. Sedimentology 25, 37-59.

Lascelles, D.F., Lowe, R.J., 2021. Tsunami deposits on a Paleoproterozoic unconformity? The 2.2 Ga Yerrida marine transgression on the northern margin of the Yilgarn Craton,Western Australia. Journal of Marine Science and Engineering 9, 213. https://doi.org/10.3390/jmse9020213.

Lawson, D.E., 1979. A comparison of the pebble orientations in ice and deposits of the Matanuska Glacier, Alaska. Journal of Geology 87, 629-645.

Le Blanc Smith, G., Eriksson, K.A., 1979. A fluvioglacial and glaciolacutsrine deltaic depositional model for Permo-Carboniferous coals of the northeastern Karoo Basin, South Africa. Palaeogeography, Palaeoclimatology, Palaeoecology 27, 67-84.

Le Heron, D.P., 2010. Interpretation of Late Ordovician glaciogenic reservoirs from 3-D seismic data: an example from the Murzuq Basin, Libya. Geological Magazine 147, 28-41.

Le Heron, D.P., 2018. An exhumed Paleozoic glacial landscape in Chad. Geology 46, 91-94. https://doi.org/10.1130/G39510.1.

Le Heron, D.P., Vandyk, T., 2019. A slippery slope for Cryogenian diamcitites? Depositional Record 5, 306-321. https://doi.org/10.1002/dep2.67.

Le Heron, D., Sutcliffe, O., Bourgig, K., Craig, J., Visentin, C., Whittington, R., 2004. Sedimentary architecture of Upper Ordovician tunnel valleys, Gargaf Arch, Libya: Implications for the genesis of a hydrocarbon reservoir. GeoArabia 9, 137-160.

Le Heron, D.P, Sutcliffe, O.E., Whittington, R.J., Craig, J., 2005. The origins of glacially related soft-sediment deformation structures in Upper Ordovician glaciogenic rocks: implication for ice-sheet dynamics. Palaeogeography, Palaeoclimatology, Palaeoecology 218, 75-103.

3243 Le Heron, D.P., Craig, J., Sutcliffe, O., Whittington, R., 2006. Late Ordovician glaciogenic
3244 reservoir heterogeneity: an example from the Murzuq Basin, Libya. Marine and Petroleum
3245 Geology 23, 655-677.

3246 Le Heron, D.P., Armstrong, H.A., Wilson, C., Howard, J.P., Gindre, L., 2010. Glaciation and
3247 deglaciation of the Libyan Desert: The Late Ordovician record. Sedimentary Geology 223,
3248 100-125. https://doi.org/10.1016/j.sedgeo.2009.11.002.

3249 Le Heron, D.P., Busfield, M.E., Collins, A.S., 2014. Bolla Bollana boulder beds: A
3250 Neoproterozoic trough mouth fan in South Australia? Sedimentology 61, 978–995.
3251 https://doi.org/10.1111/sed.12082.

3252 Le Heron, D.P., Tofaif, S, Vandyk, T., Ali, D.O., 2017. A diamictite dichotomy: Glacial
3253 conveyor belts and olistostromes in the Neoproterozoic of Death Valley, California, USA.
3254 Geology 45, 31-34.

3255 Le Heron, D.P., Tofaif, S., Melvin, J., 2018a. The Early Palaeozoic glacial deposits of
3256 Gondwana: overview, chronology, and controversies, in: Menzies, J., van der Meer, J.J.M.
3257 (Eds.), Past Glacial Environments, second ed. Elsevier, Amsterdam, pp. 47-73.
3258 https://doi.org/10.1016/B978-0-08-100524-8.00002-6.

3259 Le Heron, D.P., Vandyk, T.M., Wu, G., Li, M., 2018b. New perspectives on the Luoquan
3260 Glaciation (Ediacaran Cambrian) of North China. The Depositional Record 4, 274-292.
3261 https://doi.org/10.1002/dep2.46.

Le Heron, D.P., Vandyk, T.M., Kuang, H., Liu, Y., Chen, X., Wang, Y., Yang, Z., Scharfenberg, L., Davies, B., Shields, G., 2019a. Bird's-eye view of an Ediacaran subglacial landscape. Geology 47, 705–709. https://doi.org/10.1130/G46285.1.

Le Heron, D.P., Dietrich, P., Busfield, M.E., Kettler, C., Bermanschläger, S., Grasemann, B., 2019b. Scratching the surface: footprint of a late Carboniferous ice sheet. Geology 47, 1034-1038. https://doi.org/10.1130/G46590.1.

Le Heron, D.P., Heninger, M., Baal, C., Bestmann, M., 2020. Sediment deformation and production beneath soft-bedded Palaeozoic ice sheets. Sedimentary Geology 408, 105761. https://doi.org/10.1016/j.sedgeo.2020.105761.

Le Heron, D.P., Busfield, M.E., Kettler, C., 2021a, Ice-rafted dropstones in "postglacial" Cryogenian cap carbonates: Geology 49, 263–267. https://doi.org/10.1130/G48208.1.

Le Heron, D.P., Kettler, C., Griffis, N.P., Dietrich, P., Montañez, I.P., Osleger, D.A., Hofmann, A, Douillet, G., Mundil, R., 2021b. The Late Palaeozoic Ice Age unconformity in southern Namibia viewed as a patchwork mosaic. Depositional Record 00:1-17. https://doi.org/10.1002/dep2.163.

Leask, H.J., Wilson, L., Mitchell, K.L., 2007. Formation of Mangala Valles outflow channel, Mars: Morphological development and water discharge and duration estimates. Journal of Geophysical Research 112, E08003. https://doi.org/10.1029/2006JE002851.

Legros, F., Cantagrel, J.-M., Devouard, B., 2000. Pseudotachylyte (Frictionite) at the base of the Arequipa Volcanic landslide deposit (Peru): Implications for emplacement mechanisms. Journal of Geology 108, 601–611.

Leonard, J.E., Cameron, B., Pilkey, O.H., Friedman, G.M., 1981. Evaluation of cold-water carbonates as a possible paleoclimatic indicator. Sedimentary Geology 28, 1-28.

Liégeois, J.-P., 2006. The Hoggar swell and volcanism, Tuareg shield, Central Sahara: Intraplate reactivation of Precambrian structures as a result of Alpine convergence. http://www.mantleplumes.org/WebpagePDFs/Hoggar.pdf (accessed 20 March 2021).

Limarino, C.O., López-Gamundí, O.R., 2021. Late Paleozoic basins of South America: Insights and progress in the last decade. Journal of South American Earth Sciences 107, 103150. https://doi.org/10.1016/j.jsames.2020.103150.

Linch, L.D., Dowdeswell, J.A., 2016. Micromorphology of diamicton affected by iceberg-keel scouring, Scoresby Sund, East Greenland. Quaternary Science Reviews 152, 169–196. https://doi.org/10.1016/j.quascirev.2016.09.013.

Lindsay, J.F., 1966. Carboniferous subaqueous mass-movement in the Manning-Macleay Basin, Kempsey, New South Wales. Journal of Sedimentary Petrology 36, 719-732.

Lindsay, J.F., 1968. The development of clast fabric in mudflows. Journal of Sedimentary Petrology 38, 1242-1253.

Lindsay, J.F., 1970a. Depositional environment of Paleozoic glacial rocks in the Central Transantarctic Mountains. GSA Bulletin 81, 1149-1171.

Lindsay, J.F., 1970b. Clast fabrics of till and its development. Journal of Sedimentary Petrology 40, 629-641.

Lindsay, J.F., Summerson, C.H., Barrett, P.J., 1970. A long-axis clast fabric comparison of Squantum "Tillite," Massachusetts and the Gowganda Formation, Ontario. Journal of Sedimentary Petrology 40, 475-479.

Lindsey, D.A., 1969. Glacial sedimentology of the Precambrian Gowganda Formation, Ontario, Canada. GSA Bulletin 80, 1685-1701 and plate section.

Liu, E., Wang, H., Pan, S., Qin, C., Jiang, P., Chen, S., Yan, D., Lü, X., Jing, Z.. 2021. Architecture and depositional processes of sublacustrine fan systems in structurally active settings: An example from Weixinan Depression, northern South China Sea. Marine and Petroleum Geology 134, 105380. https://doi.org/10.1016/j.marpetgeo.2021.105380.

Liu, Y., Gastaldo, R.A., 1992. Characteristics and provenance of log-transported gravels in a Carboniferous channel deposit. Journal of Sedimentary Petrology 62, 1072-1083.

Loope, D.B., Burberry, C.M., 2018. Sheeting joints and polygonal patterns in the Navajo Sandstone, southern Utah: Controlled by rock fabric, tectonic joints, buckling, and gullying. Geosphere 14, 1818–1836. https://doi.org/10.1130/GES01614.1.

López-Gamundí, O.R., 2010. Transgressions related to the demise of the Late Paleozoic Ice Age: Their sequence stratigraphic context, in: López-Gamundí, O.R., Buatois, L.A. (Eds.), Late Paleozoic Glacial Events and Postglacial Transgressions in Gondwana. Geological Society of America Special Paper 468, pp. 1-35. https://doi.org/10.1130/2010.2468(01).

López-Gamundí, O., Sterren, A.F., Cisterna, G.A., 2016. Inter- and intratill boulder pavements in the Carboniferous Hoyada Verde Formation of West Argentina: An insight on glacial advance/retreat fluctuations in Southwestern Gondwana. Palaeogeography, Palaeoclimatology, Palaeoecology 447, 29-41. https://doi.org/10.1016/j.palaeo.2016.01.038.

López-Gamundí, G., Limarino, C.O., Isbell, J.L., Pauls, K., Césari, S.N., Alonso-Muruaga, P.J., 2021. The late Paleozoic Ice Age along the southwestern margin of Gondwana: Facies models, age constraints, correlation and sequence stratigraphic framework. Journal of South American Earth Sciences 107, 103056. https://doi.org/10.1016/j.jsames.2020.103056.

Lowe, D.R., 1979. Sediment gravity flows: Their Classification and some Problems of Application to Natural Flows and Deposits. SEPM Special Publication 27, 75-82.

Lowe, D.R., 1982. Sediment gravity flows: II. Depositional models with special reference to the deposits of high-density turbidity currents. Journal of Sedimentary Petrology 52, 279-297.

Lowe, D.R., 1988. Suspended-load fallout rate as an independent variable in the analysis of current structures. Sedimentology 35, 765-776.

3335 Lucchitta, B.K., 2001. Antarctic ice streams and outflow channels on Mars. Geophysical
3336 Research Letters 28, 403-406.

3337 Lundqvist, J., 1979. Morphogenetic classification of glaciofluvial deposits, SGU 767C,
3338 Uppsala, 72 pp.

3339 Macdonald, F.A., 2020. Deep-time paleoclimate proxies, AGU Advances 1,
3340 e2020AV000244. https://doi.org/10.1029/2020AV000244.

3341 Macdonald, H.A., Wynn, R.B., Huvenne, V.A.I., Peakall, J., Masson, D.G., Weaver, P.P.E,
3342 McPhail, S.D., 2011. New insights into the morphology, fill, and remarkable longevity (>0.2
3343 m.y.) of modern deep-water erosional scours along the northeast Atlantic margin. Geosphere
3344 7, 845-867. https://doi.org/10.1130/GES00611.1.

3345 Maghfouri, S., Hosseinzadeh. M.R., Lentz, D.R., Choulet, F., 2020. Geological and
3346 geochemical constraints on the Farahabad vent-proximal sub-seafloor replacement SEDEX-
3347 type deposit, Southern Yazd basin, Iran. Journal of Geochemical Exploration 209, 106436.

3348 Mahaney, W.C., 1987. Pleistocene glaciation on Le Mont Aigoual, Massif Central Français:
3349 Fact or fiction? Zeitschrift für Geomorphologie 31, 371-377.

3350 Mahaney, W.C., 1990. Ice on the Equator: Quaternary Geology of Mount Kenya, East Africa.
3351 Wm Caxton Ltd., Ellison Bay, 386 pp.

Mahaney, W.C., 2002. Atlas of Sand Grain Surface Textures and Applications. Oxford University Press, New York, 237 pp.

Maizels, J., 1990a. Raised channel systems as indicators of palaeohydrologic change: a case study from Oman. Palaeogeography, Palaeoclimatology, Palaeoecology 76, 241-277.

Maizels, J., 1990b. Long-term palaeochannel evolution during episodic growth of an exhumed Plio-Pleistocene alluvial fan, Oman, in: Rachocki, A.H., Michael, C. (Eds.), Alluvial Fans: A Field Approach. John Wiley and Sons Ltd., Chichester, pp. 271-304.

Major, J.J., 1998. Pebble orientation on large, experimental debris-flow deposits. Sedimentary Geology 117, 151-164. https://doi.org/10.1016/S0037-0738(98)00014-1.

Major, J.J., Pierson, T.C., Scott, K.M., 2005. Debris flows at Mount St. Helens, Washington, USA, in: Jakob, M., Hungr, O. (Eds.), Debris-Flow Hazards and Related Phenomena. Praxis/Springer, Berlin/Heidelberg, pp. 685-731.

Malahoff, A., Embley, R.W., Fornari, D.J., 1979. Geological observations from alvin of the continental margin from Baltimore Canyon to Norfolk Canyon. EOS Transactions, American Geophysical Union 60, 287.

Mangerud, J., Hughes, A.L.C., Sæle, T.H., Svendsen, J.I., 2019. Ice-flow patterns and precise timing of ice sheet retreat across a dissected fjord landscape in western Norway. Quaternary Science Reviews 214, 139-163. https://doi.org/10.1016/j.quascirev.2019.04.032.

Margold, M., Stokes, C.R., Clark, C.D., 2015. Ice streams in the Laurentide Ice Sheet: Identification, characteristics and comparison to modern ice sheets. Earth-Science Reviews 143, 117-146. https://doi.org/10.1016/j.earscirev.2015.01.011.

Markgren, M., Lassila, M., 1980. Problems of moraine morphology: Rogen moraine and Blattnick moraine. Boreas 9, 271-274. https://doi.org/10.1111/j.1502-3885.1980.tb00704.x.

Marshall, J.D., Brooks, J.R., Lajtha, K., 2007. Sources of variation in the stable isotopic composition of plants, in: Michener, R., Lajtha, K. (Eds.), Stable Isotopes in Ecology and Environmental Science, second ed. Blackwell Publishing Ltd., Malden, Oxford, Victoria, pp. 22-60. https://doi.org/10.1002/9780470691854.ch2.

Martin, H., 1981a. The Late Paleozoic Dwyka Group of the South Kalahari Basin in Namibia and Botswana, and the subglacial valleys of the Kaokoveld in Namibia, in: Hambrey, M.J., Harland, W.B. (Eds.), Earth´s Pre-Pleistocene Glacial Record. Cambridge University Press, Cambridge, pp. 61-66.

Martin, H., 1981b. The late Palaeozoic Gondwana glaciation. Geologische Rundschau 70, 480-496.

Martin, H., Porada, H., Walliser, O.H., 1985. Mixtite deposits of the Damara sequence, Namibia, Problems of interpretation. Palaeogeography, Palaeoclimatology, Palaeoecology 51, 159-196.

Maslov, A.V., 2010. Glaciogenic and related sedimentary rocks: Main lithochemical

features. Communication 1. Late Archean and Proterozoic. Lithology and Mineral Resources 45, 377–397. https://doi.org/10.1134/S0024490210040061.

Matys Grygar, T., 2019. Millennial-scale climate changes manifest Milankovitch combination tones and Hallstatt solar cycles in the Devonian greenhouse world: Comment. Geology 47, e487. https://doi.org/10.1130/G46452C.1.

Maxwell, J.C., 1959. Turbidite, tectonic and gravity transport, Northern Appenine Mountains, Italy. Bulletin of the American Association of Petroleum Geologists 43, 2701-2719.

Mays, C., Vajda, V., Frank, T.D., Fielding, C.R., Nicoll, R.S., Tevyaw, A.P., McLoughlin, S., 2020. Refined Permian–Triassic floristic timeline reveals early collapse and delayed recovery of south polar terrestrial ecosystems. GSA Bulletin 132, 1489–1513. https://doi.org/10.1130/B35355.1.

McCann, A.M., Kennedy, M.J., 1974. A probable glacio-marine deposit of Late Ordovician – Early Silurian age from the north central Newfoundland Appalachian Belt. Geological Magazine 111, 549-563.

McCarroll, D., Rijsdijk, K.F., 2003. Deformation styles as a key for interpreting glacial depositional environments. Journal of Quaternary Science 18, 473-489.

McClure, H.A., 1980. Permian-Carboniferous glaciation in the Arabian Peninsula. GSA Bulletin 91, 707-712.

3407 McKee, E.D., Crosby, E.J., Berryhill, H.L. Jr., 1967. Flood deposits, Bijou Creek, Colorado,
3408 June 1965. Journal of Sedimentary Petrology 37, 829-851.

3409 McLoughlin, S., 2011. Glossopteris – insights into the architecture and relationships of an
3410 iconic Permian Gondwanan plant. Journal of the Botanical Society of Bengal 65, 1-14.

3411 Menard, H.W., 1955. Deep-sea channels, topography, and sedimentation. AAPG Bulletin 39,
3412 236-255.

3413 Meyer, K.S., Young, C.M., Sweetman, A.K., Taylor, J., Soltwedel, T., Bergmann, M., 2016.
3414 Rocky islands in a sea of mud: biotic and abiotic factors structuring deep-sea dropstone
3415 communities. Marine Ecology Progress Series 556, 45-57.
3416 https://doi.org/10.3354/meps11822.

3417 Meyerhoff, A.A., Boucot, A.J., Meyerhoff Hull, D., Dickins, J.M., 1996. Phanerozoic faunal
3418 and floral realms of the Earth: the intercalary relations of the Malvinokaffric and Gondwana
3419 faunal realms with the Tethyan faunal realm. Geological Society of America, Memoir 189,
3420 Boulder, 69 pp. https://doi.org/10.1130/MEM189.

3421 Miall, A.D., 1983. Glaciomarine Sedimentation in the Gowganda Formation (Huronian),
3422 Northern Ontario. Journal of Sedimentary Petrology 53, 477-491.

3423 Miall, A.D., 1985. Sedimentation on an early Proterozoic continental margin under glacial
3424 influence: the Gowganda Formation (Huronian), Elliot Lake area, Ontario, Canada.
3425 Sedimentology 32, 763-788.

Middleton, G.V., Hampton, M.A., 1976. Subaqueous sediment transport and deposition by sediment gravity flows, in: Stanley, D.J., Swift, D.J.P. (Eds.), Marine Sediment Transport and Environmental Management. John Wiley, New York, pp. 197-218.

Middleton, G.V., Neal, W.J., 1989. Experiments on the thickness of beds deposited by turbidity currents. Journal of Sedimentary Petrology 59, 297-307.

Mikhailova, K., Rogov, M.A., Ershova, V.B., Vasileva, K.Y., Pokrovsky, B.G., Baraboshkin, E.Y., 2021. New data on stratigraphy and distributions of glendonites from the Carolinefjellet Formation (Middle Aptian – Lower Albian, Cretaceous), Western Spitsbergen. Stratigraphy and Geological Correlation 29, 21–35.

Miller, M.F., Knepprath, N.E., Cantrill, D.J., Francis, J.E., Isbell, J.L., 2016. Highly productive polar forests from the Permian of Antarctica. Palaeogeography, Palaeoclimatology, Palaeoecology 441, 292-304. https://doi.org/10.1016/j.palaeo.2015.06.016.

Mitchell, N.C., 2006. Morphologies of knickpoints in submarine canyons. GSA Bulletin 18, 589–605. https://doi.org/10.1130/B25772.1.

Molén, M.O., 2014. A simple method to classify diamicts by scanning electron microscope from surface microtextures. Sedimentology 61, 2020-2041. https://doi.org/10.1111/sed.12127.

Molén, M.O., 2017. The origin of Upper Precambrian diamictites; Northern Norway: A case study applicable to diamictites in general, Geologos 23, 163-181. https://doi.org/10.1515/logos-2017-0019.

Molén, M.O., 2021. Field evidence suggests that the Palaeoproterozoic Gowganda Formation in Canada is non-glacial in origin. Geologos 27, 73-91. https://doi.org/10.2478/logos-2021-0009.

Molén, M.O., Smit, J.J., 2022. Reconsidering the glaciogenic origin of Gondwana diamictites, Dwyka Group, South Africa. ***

Molnia, B.F. (Ed.), 1983a. Glacial-Marine Sedimentation. Plenum Press, New York, preface.

Molnia, B.F., 1983b. Subarctic Glacial-Marine Sedimentation: A Model, in: Molnia, B.F. (Ed.), Glacial-Marine Sedimentation. Plenum Press, New York, pp. 95-144.

Moncrieff, A.C.M., Hambrey, M.J., 1988. Late Precambrian glacially-related grooved and striated surfaces in the tillite group of central east Greenland. Palaeogeography, Palaeoclimatology, Palaeoecology 65, 183-200.

Moncrieff, A.C.M., Hambrey, M.J., 1990. Marginal-marine glacial sedimentation in the Late Precambrian succession of east Greenland, in: Dowdeswell, J.A., Scource, J.D. (Eds.), Glacimarine Environments: Processes and Sediments. Geological Society, London, Spec. Publ. 53, pp. 387-410.

3462 Montañez, I.P., Poulsen, C.J., 2013. The Late Paleozoic Ice Age: An evolving paradigm.
3463 Annual Review of Earth and Planetary Sciences 41, 629-656.
3464 https://doi.org/10.1146/annurev.earth.031208.100118.

3465 Montgomery, D.R., 2002. Valley formation by fluvial and glacial erosion. Geology 30, 1047-
3466 1050. https://doi-org.ezp.sub.su.se/10.1130/0091-7613(2002)030<1047:VFBFAG>2.0.CO;2.

3467 Moore, J.G., Clague, D.A., Holcomb, R.T., Lipman, P.W., Normark, W.R., Torresa, M.E.,
3468 1989. Prodigious submarine landslides on the Hawaiian Ridge. Journal of Geophysical
3469 Research 94 (B12), 17465-17484. https://doi.org/10.1029/JB094iB12p17465.

3470 Moore, J.G., Normark, W.R., Holcomb, R.T, 1994. Giant Hawaiian underwater landslides.
3471 Science 264, pp. 46-47.

3472 Moore, J.G., Bryan, W.B., Beeson, M.E., Normark, W.R., 1995. Giant blocks in the South
3473 Kona landslide, Hawaii. Geology 23, 125-128.

3474 Moosdorf, N., Cohen, S., von Hagke, C., 2018. A global erodibility index to represent
3475 sediment production potential of different rock types. Applied Geography 101, 36-44.
3476 https://doi.org/10.1016/j.apgeog.2018.10.010.

3477 Mori, H., Druckenmiller, P.S., Erickson, G.M., 2016. A new Arctic hadrosaurid from the
3478 Prince Creek Formation (lower Maastrichtian) of northern Alaska. Acta Palaeontologica
3479 Polonica 61, 15-32. https://doi.org/10.4202/app.00152.2015.

Mörner, N.-A., 2008. Paleoseismicity and Uplift of Sweden. 33 IGC excursion No 11, 109 pp.

Morris, S.C., 1985. Polar forests of the past. Nature 318, 739.

Moscardelli, L., Wood, L., 2016. Morphometry of mass-transport deposits as a predictive tool. GSA Bulletin 128, 47-80. https://doi.org/10.1130/B31221.1.

Moscardelli, L., Wood, L., Mann, P., 2006. Mass-transport complexes and associated processes in the offshore area of Trinidad and Venezuela. AAPG Bulletin 90, 1059–1088. https://doi.org/10.1306/02210605052.

Mottin, T.E., Vesely, F.F., Rodrigues, M.C.N.L., Kipper, F., Souza, P.A., 2018. The paths and timing of late Paleozoic ice revisited: New stratigraphic and paleo-ice flow interpretations from a glacial succession in the upper Itararé Group (Paraná Basin, Brazil). Palaeogeography, Palaeoclimatology, Palaeoecology 490, 488-504. https://doi.org/10.1016/j.palaeo.2017.11.031.

Mountjoy, E.W., Cook, H.E., Pray, L.C., McDaniel, P.N., 1972. Allochthonous carbonate debris flow – worldwide indicators of reef complexes, banks or shelf margins, in: McLaren, D.J., Middleton, G.V. (Eds.), Stratigraphy and Sedimentology. 24th International Geological Congress, Section 6, Montreal, pp. 172-189.

Mountjoy, J.J., Howarth, J.D., Orpin, A.R., Barnes, P.M., Bowden, D.A., Rowden, A.A., Schimel, A.C.G., Holden, C., Horgan, H.J., Nodder, S.D., Patton, J.R., Lamarche, G.,

Gerstenberger, M., Micallef, A., Pallentin, A., Kane, T., 2018. Earthquakes drive large-scale submarine canyon development and sediment supply to deep-ocean basins. Science Advances 4, eaar3748.

Moxness, L.D., Isbell, J.A., Pauls, K.N., Limarino, C.O., Schencman, J., 2018. Sedimentology of the mid-Carboniferous fill of the Olta paleovalley, eastern Paganzo Basin, Argentina: Implications for glaciation and controls on diachronous deglaciation in western Gondwana during the late Paleozoic Ice Age. Journal of South American Earth Sciences 84, 127-148. https://doi.org/10.1016/j.jsames.2018.03.015.

Mustard, P.S., Donaldson, J.A., 1987a. Early Proterozoic ice-proximal glaciomarine deposition: The Lower Gowganda Formation at Cobalt, Ontario, Canada. GSA Bulletin 98, 373-387.

Mustard, P.S., Donaldson, J.A., 1987b. Substrate quarrying and subglacial till deposition by Early Proterozoic ice sheet: evidence from the Gowganda Formation at Cobalt, Ontario, Canada. Precambrian Research 34, 347-368.

Naugolnykh, S.V., Uranbileg, L., 2018. A new discovery of Glossopteris in southeastern Mongolia as an argument for distant migration of Gondwanan plants. Journal of Asian Earth Sciences 154, 142-148. https://doi.org/10.1016/j.jseaes.2017.11.039.

Newell, N.D., 1957. Supposed Permian tillites in northern Mexico are submarine slide deposits. Bulletin of the Geological Society of America 68, 1569-1576.

Newton, A., Huuse, M., Brocklehurst, S., 2016. Buried iceberg scours reveal reduced North Atlantic Current during the stage 12 deglacial. Nature Communications 7, 10927. https://doi.org/10.1038/ncomms10927.

Nissen, S.E., Haskell, N.L., Steiner, C.T., Coterill, K.L., 1999. Debris flow outrunner blocks, glide tracks, and pressure ridges identified on the Nigerian continental slope using 3-D seismic coherency. Leading Edge 18, 595–599.

Normandeau, A., Lajeunesse, P., St-Onge, G., 2015. Submarine canyons and channels in the Lower St. Lawrence Estuary (Eastern Canada): Morphology, classification and recent sediment dynamics. Geomorphology 241, 1-18. https://doi.org/10.1016/j.geomorph.2015.03.023.

Nugraha, H.D., Jackson A.-L., Johnson, H.D., Hodgson, D.A., 2020. Lateral variability in strain along the toewall of a mass transport deposit: a case study from the Makassar Strait, offshore Indonesia. Journal of the Geological Society 177, 1261-1279. https://doi.org/10.1144/jgs2020-071.

Nwoko, J., Kane, I., Huuse, M., 2020a. Megaclasts within mass-transport deposits: their origin, characteristics and effect on substrates and succeeding flows. Geological Society, London, Special Publications 500, 515-530. https://doi.org/10.1144/SP500-2019-146.

Nwoko, J., Kane, I., Huuse, M., 2020b. Mass transport deposit (MTD) relief as a control on post-MTD sedimentation: Insights from the Taranaki Basin, offshore New Zealand. Marine and Petroleum Geology 120, 104489. https://doi.org/10.1016/j.marpetgeo.2020.104489.

3538 Oberbeck, V.R, Marshall, J.B., Aggarwal, H., 1993a. Impacts, tillites and the breakup of
3539 Gondwanaland. Journal of Geology 101, 1-19.

3540 Oberbeck, V.R, Marshall, J.B., Aggarwal, H., 1993b. Impacts, tillites and the breakup of
3541 Gondwanaland: A reply. Journal of Geology 101, 679-683.

3542 Oberbeck, V.R., Hörz, F., Bunch, T., 1994. Impacts, tillites, and the breakup of
3543 Gondwanaland: A second reply. Journal of Geology 102, 485-489.

3544 Ogata, K., Festa, A., Pini, G.A., Pogačnik, Ž., Lucente, C.C., 2019. Substrate deformation and
3545 incorporation in sedimentary mélanges (olistostromes): Examples from the northern
3546 Apennines (Italy) and northwestern Dinarides (Slovenia). Gondwana Research 74, 101-125.

3547 Ortiz-Karpf, A., Hodgson, D.M., Jackson, C.A.-L., McCaffrey, W.D., 2017. Influence of
3548 seabed morphology and substrate composition on mass-transport flow processes and
3549 pathways: insights from the Magdalena Fan, offshore Colombia. Journal of Sedimentary
3550 Research 87, 189-209. https://doi.org/10.2110/jsr.2017.10.

3551 Ovenshine, A.T., 1970. Observations of iceberg rafting in Glacier Bay, Alaska, and the
3552 identification of ancient ice-rafted deposits. GSA Bulletin 81, 891-894.

3553 Paris, R., Ramalho, R.S., Madeira, J., Ávila, S., May, S.M., Rixhon, G., Engel, M., Brückner.
3554 H., Herzog, M., Schukraft, G., Perez-Torrado, F.J., Rodriguez-Gonzalez, A., Carracedo, J.C.,
3555 Giachetti, T., 2018. Mega-tsunami conglomerates and flank collapses of ocean island
3556 volcanoes. Marine Geology 395, 168-187. https://doi.org/10.1016/j.margeo.2017.10.004.

Passchier, S., Hansen, M.A., Rosenberg, J., 2021. Quartz grain microtextures illuminate Pliocene periglacial sand fluxes on the Antarctic continental margin. Depositional Record 7, 564-581. https://doi.org/10.1002/dep2.157.

Pauls, K.N., Isbell, J.L., McHenry, L., Limarino, C.O., Moxness, L.D., Schencman, L.J., 2019. A paleoclimatic reconstruction of the Carboniferous-Permian paleovalley fill in the eastern Paganzo Basin: Insights into glacial extent and deglaciation of southwestern Gondwana. Journal of South American Earth Sciences 95, 102236. https://doi.org/10.1016/j.jsames.2019.102236.

Pauls, K.N., Isbell, J.L., Limarino, C.O., Alonso-Murauga, P.J., Moxness, L.D., 2021. Constraining late paleozoic ice extent in the Paganzo basin of western Argentina: Provenance of the lower Paganzo group strata. Journal of South American Earth Sciences 105, 102899. https://doi.org/10.1016/j.jsames.2020.102899.

Pazos, P.J., Bettucci, L.S., Loureiro, J., 2008. The Neoproterozoic glacial record in the Río de la Plata Craton: a critical reappraisal, in: Pankhurst, R.J., Trouw, R.A.J., De Brito Neves, B.B., de Wit, M.J. (Eds.), West Gondwana:Pre-Cenozoic Correlations Across the South Atlantic Region. Geological Society, London, Special Publications 294, pp. 343–364. https://doi.org/10.1144/SP294.18.

Peakall, J., Best, J., Baas, J.H., Hodgson, D.M., Clare, M.A., Talling, P.J., Dorrell, R.M., Lee, D.R., 2020. An integrated process-based model of flutes and tool marks in deep-water environments: Implications for palaeohydraulics, the Bouma sequence and hybrid event beds. Sedimentology 67, 1601–1666. https://doi.org/10.1111/sed.12727.

3578 Pehlivan, V., 2019. Slope Channels on an Active Margin; A 3D Study of the Variability,
3579 Occurrence, and Proportions of Slope Channel Geomorphology in the Taranaki Basin, New
3580 Zealand (M.Sc. thesis). Colorado School of Mines, Golden.

3581 Permenter, J.L., Oppenheimer, C., 2007. Volcanoes of the Tibesti massif (Chad, northern
3582 Africa). Bulletin of Volcanology 69, 609–626. https://doi.org/10.1007/s00445-006-0098-x.

3583 Petit, J.P., Laville, E., 1987. Morphology and microstructures of hydroplastic slickensides in
3584 sandstone, in: Jones, M.E., Preston, R.M. (Eds.), Deformation of Sediments and Sedimentary
3585 Rocks. Geological Society, London, Special Publications 29, pp. 107-121.

3586 Pettijohn, F.J., Potter, P.E., 1964. Atlas and Glossary of Primary Sedimentary Structures.
3587 Springer-Verlag, New York, 424 pp.

3588 Peyrot, D., Playford, G., Mantle, D.J., Backhouse, J., Milne, L.A., Carpenter, R.J., Foster, C.,
3589 Mory, A.J., McLoughlin, S., Vitacca, J., Scibiorski, J., Mack, C.L., Bevan, J., 2019. The
3590 greening of Western Australian landscapes: the Phanerozoic plant record. Journal of the
3591 Royal Society of Western Australia 102, 52-82.

3592 Pickering, K.T., Corregidor, J., 2005. Mass-transport complexes (MTCs) and tectonic control
3593 on basin-floor submarine fans, Middle Eocene, south Spanish Pyrenees. Journal of
3594 Sedimentary Research 75, 761–783. https://doi.org/10.2110/jsr.2005.062.

3595 Pickering, K.T., Hiscott, R.N., 2015. Deep Marine Systems: Processes, Deposits,
3596 Environments, Tectonics and Sedimentation. John Wiley and Sons, Oxford, 672 pp.

3597 Pickering, K.T., Underwood, M.B., Taira, A., 1992. Open-ocean to trench turbidity-current
3598 flow in the Nankai Trough: flow collapse and reflection. Geology 20, 1099-1102.

3599 Pierson, T.C., Janda, R.J., Thouret, J.-C., Borrero, A.C., 1990. Perturbation and melting of
3600 snow and ice by the 13 November 1985 eruption of Nevado del Ruiz, Colombia, and
3601 consequent mobilization, flow and deposition of lahars. Journal of Volcanology and
3602 Geothermal Research 41, 17-66.

3603 Piotrowski, J.A., Mickelson, D.M., Tulaczyk, S. Krzyszkowski, D., Junge, F.W., 2001. Were
3604 deforming subglacial beds beneath past ice sheets really widespread? Quaternary International
3605 86, 139–150.

3606 Piotrowski, J.A., Mickelson, D.M., Tulaczyk, S. Krzyszkowski, D., Junge, F.W., 2002. Reply
3607 to the comments by G.S. Boulton, K.E. Dobbie, S. Zatsepin on: Deforming soft beds under
3608 ice sheets: how extensive were they? Quaternary International 97-98, 173-177.

3609 Piotrowski, J.A., Larsen, N.K., Junge, F.W., 2004. Reflections on soft subglacial beds as a
3610 mosaic of deforming and stable spots. Quaternary Science Reviews 23, 993–1000.

3611 Piper, D.J.W., Cochonat, P., Morrison, M.L., 1999. The sequence of events around the
3612 epicentre of the 1929 Grand Banks earthquake: initiation of debris flows and
3613 turbidity current inferred from sidescan sonar. Sedimentology 46, 79–97.

Pisarska-Jamroży, M., van Loon, A.J.T., Bronikowska, M., 2018. Dumpstones as records of overturning ice rafts in a Weichselian proglacial lake (Rügen Island, NE Germany). Geological Quaterly 62, 917-924. http://dx.doi.org/10.7306/gq.1448.

Plafker, G., Richter, D.H., Hudson, T., 1977. Reinterpretation of the origin of inferred Tertiary tillite in the northern Wrangell Mountains, Alaska. U.S. Geological Survey Circular 751-B, B52-B54.

Plescia, J.B., 2003. Cerberus Fossae, Elysium, Mars: a source for lava and water. Icarus 164, 79–95.

Plumstead, E.P., 1964. Palaeobotany of Antarctica, in: Adie, Raymond J. (Ed.), Antarctic Geology. North-Holland Publ. Co., Amsterdam, pp. 643-652.

Porter, A.S., Yiotis, C., Montañez, I.P., McElwain, J.C., 2017. Evolutionary differences in $\Delta^{13}C$ detected between spore and seed bearing plants following exposure to a range of atmospheric O_2:CO_2 ratios; implications for paleoatmosphere reconstruction. Geochimica et Cosmochimica Acta 213, 517–533. https://doi.org/10.1016/j.gca.2017.07.007.

Posamentier, H.W., Kolla, V., 2003. Seismic geomorphology and stratigraphy of depositional elements in deep-water settings. Journal of Sedimentary Research 73, 367-388.

Postma, G., Nemec, W., Kleinspehn K.L., 1988. Large floating clasts in turbidites: a mechanism for their emplacement. Sedimentary Geology 58, 47-61.

Powell, R.D., 1990. Glacimarine processes at grounding-line fans and their growth to ice-contact deltas, in: Dowdeswell, J.A., Scource, J.D. (Eds.), Glacimarine Environments: Processes and Sediments. Geological Society, London, Special Publications 53, pp. 53-73.

Prasicek, G., Otto, J.-C., Montgomery, D.R., Schrott, L., 2014. Multi-scale curvature for automated identification of glaciated mountain landscapes. Geomorphology 209, 53–65. https://doi.org/10.1016/j.geomorph.2013.11.026.

Price, P.H., 1932. Erratic boulders in Sewell Coal of West Virginia. Journal of Geology 40, 62-73.

Prior, D.B., Coleman, J.M., Bornhold, B.D., 1982. Results of known seafloor instability event. Geo-Marine Letters 2, 117-122.

Procter, J.N., Zernack, A.V., Cronin, S.J., 2021. Computer simulation of a volcanic debris avalanche from Mt. Taranaki, New Zealand, in: Roverato, M., Dufresne, A., Procter, J. (Eds.), Volcanic Debris Avalanches. Advances in Volcanology. Springer, Cham, pp. 281-310. https://doi.org/10.1007/978-3-030-57411-6_11.

Prothero, D.R., Dott, R.H. Jr., 2003. Evolution of the Earth, seventh ed. McGraw-Hill, New York.

Puga Bernabéu, Á., Webster, J.M., Beaman, R.J., Thran, A., López Cabrera, J., Hinestrosa, G., Daniell, J., 2020. Submarine landslides along the mixed siliciclastic carbonate margin of the great barrier reef (offshore Australia), in: Ogata, K., Festa, A., Pini, G.A. (Eds.),

Submarine Landslides: Subaqueous Mass Transport Deposits from Outcrops to Seismic Profiles. Geophysical Monograph 246, American Geophysical Union. John Wiley and Sons, Inc., pp. 313-337. https://doi.org/10.1002/9781119500513.ch19.

Rainbard, R.H., 1993. The sedimentary record of mantle plume uplift preceding eruption of the Neoproterozoic Natkusiak flood basalt. Journal of Geology 101, 305-318.

Rampino, M.R., 1994. Tillites, diamictites, and ballistic ejecta of large impacts. Journal of Geology 102, 439-456.

Rampino, M.R., 2017. Are some tillites impact-related debris-flow deposits? Journal of Geology 125, 155-164. https://doi.org/10.1086/690212.

Reahl, J.N., Cantine, M.D., Wilcots, J., Mackey, T.J., Bergmann, K.D., 2021. Meta-analysis of Cryogenian through modern quartz microtextures reveals sediment transport histories. Journal of Sedimentary Research, accepted. https://doi.org/10.1002/essoar.10504352.1.

Rees-Owen, R.L., Gill, F.L., Newton, R.N., Ivanović, R.F., Francis, J.E., Riding, J.B., Vane, C.H., Lopes dos Santos, R.A., 2018. The last forests on Antarctica: Reconstructing flora and temperature from the Neogene Sirius Group, Transantarctic Mountains. Organic Geochemistry 118, 4-14. https://doi.org/10.1016/j.orggeochem.2018.01.001.

Rehmer, J., 1981. The Squantum Tilloid Member of the Roxbury Conglomerate of Boston, Massachusetts, in: Hambrey, M.J., Harland, W.B. (Eds.), Earth´s Pre-Pleistocene Glacial Record. Cambridge University Press, Cambridge, pp. 756-759.

Retallack, G.J., Broz, A.P., Lai, L.S.-H., Gardner, K., 2021. Neoproterozoic marine chemostratigraphy, or eustatic sea level change? Palaeogeography, Palaeoclimatology, Palaeoecology 562, 110155. https://doi.org/10.1016/j.palaeo.2020.110155.

Ricci Lucchi, F., 1995. Sedimentographica: Photographic Atlas Of Sedimentary Structures, second ed. New York, Columbia University Press, digital version. http://www.columbia.edu/dlc/cup/ricci/index.html.

Rice, A.H.N., Hofmann, C.C., 2000. Evidence for a glacial origin of Neoproterozoic III striations at Oaibaĉčannjar´ga, Finnmark, northern Norway. Geological Magazine 137, 355–366.

Rigby, J.K., 1958. Mass movements in Permian rocks of Trans-Pecos Texas. Journal of Sedimentary Petrology 28, 298-315.

Robinson, J.E., Bacon, C.R., Major, J.J., Wright, H.M., Vallance, J.M., 2017. Surface morphology of caldera-forming eruption deposits revealed by lidar mapping of Crater Lake National Park, Oregon – Implications for deposition and surface modification. Journal of Volcanology and Geothermal Research 342, 61-78.

Rocha-Campos, A.C., Santos, P.R. dos, 1981. The Itararé Subgroup, Aquidauana Group and San Gregório Formation, Paraná Basin, Southeastern South America, in: Hambrey, M.J., Harland, W.B. (Eds.), Earth´s Pre-Pleistocene Glacial Record. Cambridge University Press, Cambridge, pp. 842-852.

Rodrigues, M.C.N.d.L., Trzaskos, B., Alsop, G.I., Vesely, F.F., 2020. Making a homogenite: An outcrop perspective into the evolution of deformation within mass-transport deposits. Marine and Petroleum Geology 112, 104033. https://doi.org/10.1016/j.marpetgeo.2019.104033.

Rodriguez, J.A.P., Sasaki, S., Kuzmin, R.O., Dohm, J.M., Tanaka, K.L., Miyamoto, H., Kurita, K., Komatsu, G., Fairéni, A.G., Ferris, J.C., 2005. Outflow channel sources, reactivation, and chaos formation, Xanthe Terra, Mars. Icarus 175, 36–57.

Rodríguez-López, J.P., Liesa, C.L., Pardo, G., Meléndе, N., Soria, A.R., Skilling, I., 2016. Glacial dropstones in the western Tethys during the late Aptian–early Albian cold snap: Palaeoclimate and palaeogeographic implications for the mid-Cretaceous. Palaeogeography, Palaeoclimatology, Palaeoecology 452, 11–27. https://doi.org/10.1016/j.palaeo.2016.04.004.

Rodríguez-López, J.P., Van Vliet-Lanoë, B., López-Martínez, J., Martín-García, R., 2021. Scouring by rafted ice and cryogenic patterned ground preserved in a Palaeoproterozoic equatorial proglacial lagoon succession, eastern India, Nuna supercontinent. Marine and Petroleum Geology 123, 104766. https://doi.org/10.1016/j.marpetgeo.2020.104766.

Rogov, M., Ershova, V., Vereshchagin, O., Vasileva, K., Mikhailova, K., Krylov, A., 2021. Database of global glendonite and ikaite records throughout the Phanerozoic. Earth System Science Data 13, 343-356. https://doi.org/10.5194/essd-13-343-2021.

Romano, M., 2015. Reviewing the term uniformitarianism in modern Earth sciences. Earth-Science Reviews 148, 65-76. https://doi.org/10.1016/j.earscirev.2015.05.010.

Rosa, E.L.M., Isbell, J.L., 2021. Late Paleozoic glaciation, in: Alderton, D., Elias, S.A. (Eds.), Encyclopedia of Geology, second ed. Elsevier, Amsterdam, pp. 534-545. https://doi.org/10.1016/B978-0-08-102908-4.00063-1.

Rosa, E.L.M., Vesely, F.F., França, A.B., 2016. A review on late Paleozoic ice-related erosional landforms in the Paraná Basin: origin and paleogeographical implications. Brazilian Journal of Geology 46, 147-166. https://doi.org/10.1590/2317-4889201620160050.

Rosa, E.L.M., Vesely, F.F., Isbell, J.L., Kipper, F., Fedorchuk, N.D., Souza, P.A., 2019. Constraining the timing, kinematics and cyclicity of Mississippian-Early Pennsylvanian glaciations in the Paraná Basin, Brazil. Sedimentary Geology 384, 29-49. https://doi.org/10.1016/j.sedgeo.2019.03.001.

Rosa, E., Vesely, F., Isbell, J., Fedorchuk, N., 2021. As geleiras carboníferas no sul do Brasil. Boletim Paranaense de Geosciencias 78, 24-43. https://doi.org/10.5380/geo.v78i0.78669.

Rose, K.C., Ferraccioli, F., Jamieson, S.S.R., Bell, R.E., Corr, H., Creyts, T.T., Braaten, D., Jordan, T.A., Fretwell, P.T., Damaske, D., 2013. Early East Antarctic Ice Sheet growth recorded in the landscape of the Gamburtsev Subglacial Mountains. Earth and Planetary Science Letters 375, 1-12. https://doi.org/10.1016/j.epsl.2013.03.053.

Rothman, M.D., Mattio, L., Anderson, R.J., Bolton, J.J., 2017. A phylogeographic investigation of the kelp genus Laminaria (Laminariales, Phaeophyceae), with emphasis on the South Atlantic Ocean. Journal of Phycology 53, 778–789.

Rowe, C.D., Backeberg, N.R., 2011. Discussion on: reconstruction of the Ordovician Pakhuis ice sheet, South Africa by H.J. Blignault, J.N. Theron. South African Journal of Geology 114, 95-102. https://doi.org/10.2113/gssajg.114.1.95.

Runkel, A.C., Mackey, T.J., Cowan, C.C., Fox, D.L., 2010. Tropical shoreline ice in the late Cambrian: Implications for Earth´s climate between the Cambrian Explosion and the Great Ordovician Biodiversification Event, Geological Society of America Today 20, 4-10. https://doi.org/10.1130/GSATG84A.1.

Ryder, J.M., Thomson, B., 1986. Neoglaciation in the southern Coast Mountains of British Columbia: chronology prior to the late Neoglacial maximum. Canadian Journal of Earth Science 23, 273 -287.

Sandberg, C.G.S., 1928. The origin of the Dwyka Conglomerate of South Africa and other "glacial" deposits. Geological Magazine 65, 117-138.

Sanders, J.E., Cecioni, G.O., 1957. Discussion: "Flysch and Molasse". Bulletin of the American Association of Petroleum Geologists 41, 2136-2139.

Santos, P.R. dos, Rocha-Campos, A.C., Canuto, J.R., 1996. Patterns of late Palaeozoic deglaciation in the Paraná Basin, Brazil. Palaeogeography, Palaeoclimatology, Palaeoecology 125, 165-184.

Schatz, E.R., Mángano, M.G., Buatois, L.A., Limarino, C.O., 2011. Life in the Late Paleozoic ice age: Trace fossils from glacially influenced deposits in a Late Carboniferous fjord of western Argentina. Journal of Paleontology 85, 502-518. https://doi.org/10.1666/10-046.1.

Scheffler, K., Hoernes, S., Schwark. L: 2003. Global changes during Carboniferous–Permian glaciation of Gondwana: Linking polar and equatorial climate evolution by geochemical proxies. Geology 31, 605–608. https://doi.org/10.1130/0091-7613(2003)031<0605:GCDCGO>2.0.CO;2.

Schenk, P.E., 1965. Depositional environment of the Gowganda Formation (Precambrian) at the south end of Lake Timagami, Ontario. Journal of Sedimentary Petrology 35, 309-318.

Schenk, P.E., 1972. Possible Late Ordovician glaciation of Nova Scotia. Canadian Journal of Earth Sciences 9, 95-107.

Schermerhorn, L.J.G., 1970. Saharan ice. Geotimes 15, 7-8.

Schermerhorn, L.J.G., 1971. Upper Ordovician glaciation in Northwest Africa? Discussion. GSA Bulletin 82, 265-268.

Schermerhorn, L.J.G., 1974a. Late Precambrian mixtites: glacial and/or nonglacial? American Journal of Science 274, 673-824.

Schermerhorn, L.J.G., 1974b. No evidence for glacial origin of Late Precambrian tilloids in Angola. Nature 252, 114-115.

3763 Schermerhorn, L.J.G., 1975. Tectonic framework of Late Precambrian supposed glacials, in:
3764 Wright, A.E., Moseley, F. (Eds.), Ice Ages: Ancient and Modern. Seal House Press,
3765 Liverpool, pp. 241-274.

3766 Schermerhorn, L.J.G., 1976a. Reply. American Journal of Science 276, 375-384.

3767 Schermerhorn, L.J.G., 1976b. Reply. American Journal of Science 276, 1315-1324.

3768 Schermerhorn, L.J.G., 1977. Late Precambrian glacial climate and the Earth´s obliquity – a
3769 discussion. Geological Magazine 114, 57-64.

3770 Schermerhorn, L.J.G., 1981. Late Precambrian tilloids of northwest Angola, in: Hambrey,
3771 M.J., Harland, W.B. (Eds.), Earth´s Pre-Pleistocene Glacial Record. Cambridge University
3772 Press, Cambridge, pp. 158-161.

3773 Schermerhorn, L.J.G., Stanton, W.I., 1963. Tilloids in the West Congo Geosyncline.
3774 Quarterly Journal of the Geological Society of London 119, 201-241.

3775 Schieber, J., 1999. Microbial mats in terrigenous clastics: the challenge of identification in
3776 the rock record. Palaios 14, 3-12. https://doi.org/10.2307/3515357.

3777 Schieber, J., Southard, J., Thaisen, K., 2007. Accretion of mudstone beds from migrating
3778 floccule ripples. Science 318, 1760-1763. https://doi.org/10.1126/science.1147001.

Schieber, J., Southard, J.B., Kissling, P., Rossman, B., Ginsburg, R., 2013. Experimental deposition of carbonate mud from moving suspensions: importance of flocculation and implications for modern and ancient carbonate mud deposition. Journal of Sedimentary Research 83, 1025-1031. https://doi.org/10.2110/jsr.2013.77.

Schipper, C.I., Moussallam, Y., Curtis, A., Peters, N., Barnie, T., Bani, P., Jost, H.J., Hamilton, D., Aiuppa, A., Tamburello, G., Giudice, G., 2017. Isotopically ($\delta^{13}C$ and $\delta^{18}O$) heavy volcanic plumes from Central Andean volcanoes: a field study. Bulletin of Volcanology 79, 65. https://doi.10.1007/s00445-017-1146-4.

Schneebeli-Hermann, E., Kürschner, W.M., Kerp, H., Bomfleur, B, Hochuli, P.A., Bucher, H., Ware, D., Roohi, G., 2015.Vegetation history across the Permian-Triassic boundary in Pakistan (Amb section, Salt Range). Gondwana Research 27, 911-824. https://doi.org/10.1016/j.gr.2013.11.007.

Schneider, J.L., Fisher, R.V., 1998. Transport and emplacement mechanisms of large volcanic debris avalanches: evidence from the northwest sector of Cantal Volcano (France). Journal of Volcanology and Geothermal Research 83, 141–165.

Schwab, F.L., 1981. Late Precambrian tillites of the Appalachians, in: Hambrey, M.J., Harland, W.B. (Eds.), Earth´s Pre-Pleistocene Glacial Record. Cambridge University Press, Cambridge, pp. 751-755.

Schwarzbach, M., 1961. The climatic history of Europe and North America, in: Nairn, A.E.M. (Ed.), Descriptive Palaeoclimatology. Interscience Publ. Inc., New York, pp. 255-291.

Scotese, C.R., Song, H., Mills, B.J.W., van der Meer, D.G., 2021. Phanerozoic paleotemperatures: The earth´s changing climate during the last 540 million years. Earth-Science Reviews 215, 103503. https://doi.org/10.1016/j.earscirev.2021.103503.

Scott, K.M., 1966. Sedimentology and dispersal pattern of a Cretaceous flysch sequence, Patagonian Andes, Southern Chile. AAPG Bulletin 50, 72-107.

Scott, K.M., 1988a. Origin, Behavior and Sedimentology of Lahars and Lahar-runout Flows in the Toutle-Cowlitz River System. U.S. Geological Survey Professional Paper 1447A.

Scott, K.M., 1988b. Origin, behavior and sedimentology of prehistoric catastrophic lahars at Mount St. Helens, Washington, in: Clifton, H.E. (Ed.), Sedimentologic Consequences of Convulsive Geologic Events. Geological Society of America Special Paper 229, pp. 23-36.

Sensula, B., Böttger, T., Pazdur, A., Piotrowska, N., Wagner, R., 2006. Carbon and oxygen isotope composition of organic matter and carbonates in recent lacustrine sediments. Geochronometria 25, 77-94.

SEPM, 2021. Diagenesis and Porosity. http://www.sepmstrata.org/page.aspx?pageid=92 (accessed 2 January, 2021).

Servais, T. Cascales-Miñana, B., Cleal, C.J.,Gerrienne, P., Harper, D.A.T., Neumann, M., 2019. Revisiting the Great Ordovician Diversification of land plants: Recent data and perspectives. Palaeogeography, Palaeoclimatology, Palaeoecology 534, 109280. https://doi.org/10.1016/j.palaeo.2019.109280.

Seward, A.C., 1932. A Persian Sigillaria. Philosophical Transactions of the Royal Society of London. Series B, Containing Papers of a Biological Character 221, 377-390.

Shanmugam, G., 2002. Ten turbidite myths. Earth-Science Reviews 58, 311-341.

Shanmugam, G., 2012. Process-sedimentological challenges in distinguishing paleo-tsunami deposits. Natural Hazards 63, 5–30. https://doi.org/10.1007/s11069-011-9766-z.

Shanmugam, G., 2016. Submarine fans: a critical retrospective (1950-2015). Journal of Palaeogeography 5, 110-184.

Shanmugam, G., 2017a. The contourite problem, in: Mazumder, R. (Ed.), Sediment Provenance Influences on Compositional Change from Source to Sink. Elsevier Inc., pp. 183-254. https://doi.org/10.1016/B978-0-12-803386-9.00009-5.

Shanmugam, G., 2017b. Global case studies of soft-sediment deformation structures (SSDS): Definitions, classifications, advances, origins, and problems. Journal of Palaeogeography 6, 251-320. http://dx.doi.org/10.1016/j.jop.2017.06.004.

Shanmugam, G., 2019. Reply to discussions by Zavala (2019) and by Van Loon, Hüeneke, and Mulder (2019) on Shanmugam, G. (2018, Journal of Palaeogeography, 7 (3): 197–238): ´the hyperpycnite problem´. Journal of Palaeogeography 8, 31. https://doi.org/10.1186/s42501-019-0047-1.

Shanmugam, G., 2020. Gravity flows: Types, definitions, origins, identification markers, and problems. Journal of the Indian Association of Sedimentologists 37, 61-90. https://doi.org/10.51710/jias.v37i2.117.

Shanmugam, G., 2021a. Deep-water processes and deposits, in: Alderton, D., Elias, S.A. (Eds.), Encyclopedia of Geology, second ed., 2. Academic Press, United Kingdom, pp. 965-1009. https://doi.org/10.1016/B978-0-12-409548-9.12541-2.

Shanmugam, G., 2021b. Mass Transport, Gravity Flows, and Bottom Currents. Elsevier, 571 pp. https://doi.org/10.1016/C2019-0-03665-5.

Shanmugam, G., Lehtonen, L.R., Straume, T., Syvertsen, S.E., Hodgkinson, R.J., Skibej, M., 1994. Slump and debris-flow dominated upper slope facies in the Cretaceous of the Norwegian and northern North Seas (61-67°N): implications for sand distribution, AAPG Bulletin, 78, 910-937.

Sharp, M., 1982. Modification of clasts in lodgement tills by glacial erosion. Journal of Glaciology 28, 475-481.

Shepard, F.P., Dill, R.F., 1966. Submarine Canyons and Other Sea Valleys, Rand McNally, Chicago, 381 pp.

Shields, G.A., Strachan, R.A., Porter, S.M., Halverson, G.P., Macdonald, F.A., Plumb, K.A, Alvarenga, C.J. de, Banerjee, D.M., Bekker, A., Bleeker, W., Brasier, A., Chakraborty, P.P., Collins, A.S., Condie, K., Das, K., Rvans, D.A.D., Ernst, R., Fallick, A.E., Frimmel, H., Fuck, R.A., Hoffman, P.F., Kamber, B.S., Kuznetsov, A.B., Mitchell, R.N., Poiré, D.G., Poulton, S.W., Riding, R., Sharma, M., Storey, C., Stueeken, E., Tostevin, R., Turner, E., Xiao, S., Zhang, S., Zhou, Y., Zhu, M., 2022. A template for an improved rock-based subdivision of pre-Cryogenian time. Journal of the Geological Society 179, jgs2020-222. https://doi.org/10.1144/jgs2020-222.

Sial, A.N., Gaucher, C., Ferreira, V.P., Pereira, N.S., Cezario, J.S., Chiglino, L., Lima, H.M., 2015. Isotope and elemental chemostratigraphy, in, Ramkumar, M. (Ed.), Chemostratigraphy: Concepts, Techniques, and Applications. Elsevier, Amsterdam, pp.23-64. https://doi.org/10.1016/B978-0-12-419968-2.00002-9.

Silberfeld, T., Leigh, J.W., Verbruggen, H., Cruaud, C., de Reviers, B., Rousseau, F., 2010. A multi-locus time-calibrated phylogeny of the brown algae (Heterokonta, Ochrophyta, Phaeophyceae): Investigating the evolutionary nature of the “brown algal crown radiation”. Molecular Phylogenetics and Evolution 56, 659-674.

Siman-Tov, S., Stock, G.M., Brodsky, E.E., White, J.C., 2017. The coating layer of glacial polish. Geology 45, 987-990. https://doi.org/10.1130/G39281.1.

Simms, M.J., 2007. Uniquely extensive soft-sediment deformation in the Rhaetian of the UK: Evidence for earthquake or impact? Palaeogeography, Palaeoclimatology, Palaeoecology 244, 407–423.

Sloan, L.C., Barron, E.J., 1990. “Equable” climates during Earth history? Geology 18, 489-492.

Smith, D.G., 2019. Millennial-scale climate changes manifest Milankovitch combination tones and Hallstatt solar cycles in the Devonian greenhouse world: Comment. Geology 47, e488. https://doi.org/10.1130/G46475C.1.

Smith, D.G., Bailey, R.J., 2018a. Discussion on ´A 2.3 million year lacustrine record of orbital forcing from the Devonian of northern Scotland´. Journal of the Geological Society 173, 474- 488. Journal of the Geological Society 175, 561. https:/doi.org/10.1144/jgs2016-137.

Smith, D.G., Bailey, R.J., 2018b. Discussion: Howe, T.S., Corcoran, P.L., Longstaffe, F.J., Webb, E.A, Pratt, R.G., 2016. Climatic cycles recorded in glacially influenced rhythmites of the Gowganda Formation, Huronian Supergroup, Precambrian Research, 286, 269-280. Precambrian Research 316, 324-326. https://doi.org/10.1016/j.precamres.2017.04.022.

Smith, G.L.B., Eriksson, K.A., 1979. A fluvioglacial and glaciolacustrine deltaic depositional model for Permo-Carboniferous coals of the Northeastern Karoo Basin, South Africa. Palaeogeography, Palaeoclimatology, Palaeoecology 27, 67-84.

Smith, N.D., Ashley, G., 1985. Proglacial lacustrine environment, in: Ashley, C.M., Shaw, J., Smith, N.D. (Eds.), Glacial Sedimentary Environments. SEPM Short Course Notes 16, pp. 135-216. https://doi.org/10.2110/scn.85.02.0135.

Smith, N.D., Phillips, A.C., Powell, R.D., 1990. Tidal drawdown: A mechanism for producing cyclic sediment laminations in glaciomarine deltas. Geology 18, 10-13.

Sobiesiak, M.S., Kneller, B., Alsop, G.I., Milana, J.P., 2016. Inclusion of substrate blocks within a mass transport deposit: A case study from Cerro Bola, Argentina, in: Lamarche, G., Mountjoy, J., Bull, S., Hubble, T., Krastel, S., Lane, E., Micallef, A., Moscardelli, L., Mueller, C., Pecher, I., Woelz, S. (Eds.), Submarine Mass Movements and Their Consequences. Springer International Publ,. Switzerland, pp. 487-496.

Sobiesiak, M.S., Kneller, B., Alsop, G.I., Milana, J.P., 2018. Styles of basal interaction beneath mass transport deposits. Marine and Petroleum Geology 98, 629–639. https://doi.org/10.1016/j.marpetgeo.2018.08.028.

Sokołowski, R.J., Wysota, W., 2020. Differentiation of subglacial conditions on soft and hard bed settings and implications for ice sheet dynamics: a case study from north.central Poland. International Journal of Earth Sciences 109, 2699–2717. https://doi.org/10.1007/s00531-020-01920-x.

Soreghan, G.S., Sweet, D.S., Heavens, N.G., 2014. Upland glaciation in tropical Pangaea: Geologic evidence and implications for Late Paleozoic climate modeling. Journal of Geology 122, 137-163. https://doi.org/10.1086/675255.

Soutter, E.L., Kane, I.A., Huuse, M., 2018. Giant submarine landslide triggered by Paleocene mantle plume activity in the North Atlantic. Geology 46, 511–514. https://doi.org/10.1130/G40308.1.

Spiekermann, R., Jasper, A., Benício, J.R.W., Guerra-Sommer, M., Ricardi-Branco, F.S., Uhl, D., 2020. Late Palaeozoic lycopsid macrofossils from the Paraná Basin, South America – an overview of current knowledge. Journal of South American Earth Sciences 101, 102615. https://doi.org/10.1016/j.jsames.2020.102615.

Srivastava, A.K., Agnihotri, D., 2010. Dilemma of late Palaeozoic mixed floras in Gondwana. Palaeogeography, Palaeoclimatology, Palaeoecology 298, 54–69. https://doi.org/10.1016/j.palaeo.2010.05.028.

Stalker, A.M., 1975. The Large Interdrift Bedrock Blocks of the Canadian Prairies. Geological Survey of Canada, Paper 75-1, Part A, 421-422.

Stalker, A.M., 1976. Megablocks, or the Enormous Erratics of the Albertan Prairies. Geological Survey of Canada, Paper 76-1C, 185-188.

Stavrakis, N., 1986. Sedimentary environments and facies of the Orange Free State coalfield, in: Anhaeusser, C.R., Maske, S. (Eds.), Mineral Deposits of Southern Africa vols. I and II. Geological Society of South Africa, Johannesburg, pp. 1939–1952.

Stavrakis, N., Smyth, M., 1991. Clastic sedimentary environments and organic petrology of coals in the Orange Free State, South Africa. International Journal of Coal Geology 18, 1-16.

Stein, R.A., Sheldon, N.D., Smith, S.Y., 2021. C_3 plant carbon isotope discrimination does not respond to CO_2 concentration on decadal to centennial timescales. New Phytologist 229, 2576-2585. https://doi.org/10.1111/nph.17030.

Sterren, A.F., Cisterna, G.A., Rustán, J.J., Vaccari, N.E., Balseiro, D., Ezpeleta, M., Prestianni, C., 2021. New invertebrate peri-glacial faunal assemblages in the Agua de Lucho Formation, Río Blanco Basin, Argentina. The most complete marine fossil record of the early Mississippian in South America. Journal of South American Earth Sciences 106, 103078. https://doi.org/10.1016/j.jsames.2020.103078.

Stevenson, C.J., Talling, P.J., Sumner, E.J., Masson, D.G., Frenz, M., Wynn, R.B., 2014. On how thin submarine flows transported large volumes of sand for hundreds of kilometres across a flat basin plain without eroding the sea floor. Sedimentology 61, 1982-2019. https://doi.org/10.1111/sed.12125.

Stock, J.D., Dietrich, W.E., 2006. Erosion of steepland valleys by debris flows. GSA Bulletin 118, 1125-1148.

Stokes, C.R., 2018. Geomorphology under ice streams: Moving from form to process. Earth Surface Processes and Landforms 43, 85-123. https://doi.org/10.1002/esp.4259.

Stoopes, G.R., Sheridan, M.F., 1992. Giant debris avalanches from the Colima Volcanic Complex, Mexico: Implications for long-runout landslides (> 100 km) and hazard assessment. Geology 20, 299-302.

3947 Stratten, T., Humphreys, A.J.B., 1974. Extensive glacial pavement of Dwyka age near
3948 Douglas, Cape Province. South African Journal of Science 70, 44-45.

3949 Studer, B., 1827. Remarques geógnostiques sur quelques parties de la chaîne septentrionale
3950 des Alpes. Annales Des Sciences Naturelles, Paris 11, 1-47.

3951 Sugden, D.E., John, B.S., 1982. Glaciers and Landscape. Edward Arnold, London, p. 161.

3952 Sutherland, B.R., Barrett, K.J., Gingras , M.K., 2015. Clay settling in fresh and salt water.
3953 Environmental Fluid Mechanics 15, 147-160. https://doi.org/10.1007/s10652-014-9365-0.

3954 Syvitski, J.P.M., Shaw, J., 1995. Sedimentology and geomorphology of fjords, in: Perillo,
3955 G.M.E. (Ed.), Geomorphology and Sedimentology of Estuaries. Developments in
3956 Sedimentology 53, Elsevier Science B.V., Amsterdam, pp. 113-178.
3957 https://doi.org/10.1016/S0070-4571(05)80025-1.

3958 Tachibana, T., 2013. Lonestones as indicators of tsunami deposits in deep-sea sedimentary
3959 rocks of the Miocene Morozaki Group, central Japan. Sedimentary Geology 289, 62-73.

3960 Takasaki, R., Fiorillo, A.R., Kobayashi, Y., McCarthy, P.J., 2019. The first definite
3961 Lambeosaurine bone from the Liscomb Bonebed of the Upper Cretaceous Prince Creek
3962 Formation, Alaska, United States. Scientific Reports 9, 5384.
3963 https://doi.org/10.1038/s41598-019-41325-8.

Talling, P.J., Wynn, R.B., Masson, D.G., Frenz, M., Cronin, B.T., Schiebel, R., Akhmetzhanov, A.M., Dallmeier-Tiessen, S., Benetti, S., Weaver, P.P.E., Georgiopoulou, A., Zühlsdorff, C., Amy, L.A., 2007. Onset of submarine debris flow deposition far from original giant landslide. Nature 450, 541-544.

Talling, P.J., Masson, D.G., Sumner, E.J., Malgesini, G., 2012. Subaqueous sediment density flows: depositional processes and deposit types. Sedimentology 59, 1937-2003.

Talling, P.J., Allin, J., Armitage, D.A. et al., and 27 more authors, 2015. Key future directions for research on turbidity currents and their deposits. Journal of Sedimentary Research 85, 153-169. https://doi.org/10.2110/jsr.2015.03.

Tavener-Smith, T., Mason, T.R., 1983. A late Dwyka (early Permian) varvite sequence near Isandlwana, Zululand, South Africa. Palaeogeography, Palaeoclimatology, Palaeoecology 41, 233-249.

Tedesco, J., Cagliari, J., Aquino, C.D., 2020. Late Paleozoic Ice-Age rhythmites in the southernmost Paraná Basin: A sedimentological and paleoenvironmental analysis. Journal of Sedimentary Research 90, 969–979. https://doi.org/10.2110/jsr.2020.54.

Taylor, T.N., Taylor, N.R., Cúneo, N.R., 1992. The present is not the key to the past: a polar forest from the Permian of Antarctica. Science 257, 1675-1677.

Thiel, M., Gutow, L., 2005. The ecology of rafting in the marine environment. I. The floating substrata, in: Gibson, R.N., Atkinson, R.J.A., Gordon, J.D.M. (Eds.), Oceanography and Marine Biology: An Annual Review 42, pp. 181–264.

Thomas, G.S.P., Connell, R.J., 1985. Iceberg drop, dump and grounding structures from Pleistocene glacio-lacustrine sediments, Scotland. Journal of Sedimentary Petrology 55, 243-249. https://doi.org/10.1306/212F8689-2B24-11D7-8648000102C1865D.

Thompson, N.D., 2009. Distinct Element Numerical Modelling of Volcanic Debris Avalanche Emplacement Geomechanics (Ph.D. Thesis). Bournemouth University, Bournemouth.

Thompson, N., Matthew R., Bennett, M.D. Petford, N., 2010. Development of characteristic volcanic debris avalanche deposit structures: New insight from distinct element simulations. Journal of Volcanology and Geothermal Research 192, 191-200.

Tian, X., Gao, Y., Li, Z., Zavala, C., Chen, Z., Huang, Y., Yu, E., Wang, C., 2021. Fine grained gravity flow deposits and their depositional processes: A case study from the Cretaceous Nenjiang Formation, Songliao Basin, NE China. Geological Journal 56, 1496-1509. https://doi.org/10.1002/gj.4017.

Tinkler, K.J., 1993. Fluvially sculpted rock bedforms in Twenty Mile Creek, Niagara Peninsula, Ontario. Canadian Journal of Earth Sciences 30, 945-953. https://doi.org/10.1139/e93-079.

Tripathy, G., Goswami, S., Das, P.P., 2021. Late Permian species diversity of the genus Glossopteris in and around Himgir, Ib River Basin, Odisha, India, with a clue on palaeoclimate and palaeoenvironment. Arabian Journal of Geosciences 14, 703. https://doi.org/10.1007/s12517-021-07019-0.

Trompette, R., 1981. Late Precambrian tillites of the Volta Basin and the Dahomeyides Orogenic Belt (Benin, Ghana, Niger, Togo and Upper-Volta), in: Hambrey, M.J., Harland, W.B. (Eds.), Earth´s Pre-Pleistocene Glacial Record. Cambridge University Press, Cambridge, pp. 135-139.

Trosdtorf Jr. I., Rocha-Campos, A.C., Santos, P.R. dos, Tomio, A., 2005a. Origin of Late Paleozoic, multiple, glacially striated surfaces in northern Paraná Basin (Brazil): Some implications for the dynamics of the Paraná glacial lobe. Sedimentary Geology 181, 59-71. https://doi.org/10.1016/j.sedgeo.2005.07.006.

Trosdtorf, I., Assine, M.L., Vesely, F.F., Rocha-Campos, A.C., Santos, P.R. dos, Tomio, A., 2005b. Glacially striated, soft sediment surfaces on late Paleozoic tillite at São Luiz do Purunã, PR. Anais da Academia Brasileira de Ciências 77, 367–378.

Tucholke, B.E., 1992. Massive submarine rockslide in the rift-valley wall of the Mid-Atlantic Ridge. Geology 20, 129-132.

Ui, T., 1989. Discrimination between debris avalanche and other volcaniclastic deposits, in: Latter, J.H. (Ed.), Volcanic Hazards. Springer, Berlin, pp. 201-209.

4019 Vachtman, D., Mitchell, N.C., Gawthorpe, R., 2013. Morphologic signatures in submarine
4020 canyons and gullies, central USA Atlantic continental margins. Marine and Petroleum
4021 Geology 41, 250-263. https://doi.org/10.1016/j.marpetgeo.2012.02.005.

4022 Valdez Buso, V., Milana, J.P., di Pasquo, M., Aburto, J.E., 2021. The glacial paleovalley of
4023 Vichigasta: Paleogeomorphological and sedimentological evidence for a large continental
4024 ice-sheet for the mid-Carboniferous over central Argentina. Journal of South American Earth
4025 Sciences 106, 103066. https://doi.org/10.1016/j.jsames.2020.103066.

4026 van der Vegt, P., Janszen, A., Moscariello, A., 2012. Tunnel valleys: current knowledge and
4027 future perspectives, in: Huuse, M., Redfern, J., Le Heron, D.P., Dixon, R. J., Moscariello, A.,
4028 Craig, J. (Eds.), Glaciogenic Reservoirs and Hydrocarbon Systems. Geological Society,
4029 London, Special Publications 368. https://doi.org/10.1144/SP368.13.

4030 van der Meer, J.J.M., Menzies, J., Rose, J., 2003. Subglacial till: the deforming glacier bed,
4031 Quaternary Science Reviews 22, 1659-1685.
4032 https://doi.org/10.1016/S0277-3791(03)00141-0

4033 Van Houten, F.B., 1957. Appraisal of Ridgway and Gunnison “Tillites,” Southwestern
4034 Colorado. Bulletin of the Geological Society of America 66, 383-388.

4035 Vandyk, T.M., Kettler, C., Davies, B.J., Shields, G.A., Candy, I., Le Heron, D.P., 2021.
4036 Reassessing classic evidence for warm-based Cryogenian ice on the western Laurentian
4037 margin: The “striated pavement” of the Mineral Fork Formation, USA. Precambrian Research
4038 363, 106345. https://doi.org/10.1016/j.precamres.2021.106345.

Vellutini, P., Vicat, J.-P., 1983. Sur L´Origine Des Formation Conglomératiques de Base du Geosynclinal Ouest-Congolien (Gabon, Congo, Zaire, Angola). Precambrian Research 23, 87-101.

Ventra, D., Clarke, L.E., 2018. Geology and geomorphology of alluvial and fluvial fans: current progress and research perspectives, in: Ventra, D., Clarke, L.E. (Eds.), Geology and Geomorphology of Alluvial and Fluvial Fans: Terrestrial and Planetary Perspectives. Geological Society, London, Special Publications 440, pp. 1–21. https://doi.org/10.1144/SP440.16.

Veroslavsky, G., Rossello, E.A., López-Gamundí, O., de Santa Ana, H., Perinotto, A.J., 2021. Late Paleozoic tectono-sedimentary evolution of eastern Chaco-Paraná Basin (Uruguay, Brazil, Argentina and Paraguay). Journal of South American Earth Sciences 106, 102991. https://doi.org/10.1016/j.jsames.2020.102991.

Vesely, F.F., Assine, M.L., 2014. Ice-keel scour marks in the geological record: evidence from Carboniferous soft-sediment striated surfaces in the Paraná Basin, southern Brazil. Journal of Sedimentary Research 84, 26–39. https://doi.org/10.2110/jsr.2014.4.

Vesely, F.F., Rodrigues, M.C.N.L, Rosa, E.L.M., Amato, J.A., Trzaskos, B., Isbell, J.L., Fedorchuk, N.D., 2018. Recurrent emplacement of non-glacial diamictite during the late Paleozoic ice age. Geology 46, 615-618. https://doi.org/10.1130/G45011.1.

Vesely, F.F., Assine, M.L., França, A.B., Paim, P.S.G., Rostirolla, S.P., 2021. Tunnel-valley fills in the Paraná Basin and their implications for the extent of late Paleozoic glaciation in

4059 SW Gondwana. Journal of South American Earth Sciences 106, 102969.
4060 https://doi.org/10.1016/j.jsames.2020.102969.

4061 Visser, J.N.J., 1981. Carboniferous topography and glaciation in the North-Western part of
4062 the Karoo Basin, South Africa. Annals of the Geological Survey of South Africa 15, 13-24.

4063 Visser, J.N.J., 1982. Upper Carboniferous glacial sedimentation in the Karoo Basin near
4064 Prieska, South Africa. Palaeogeography, Palaeoclimatology, Palaeoecology 38, 63-92.

4065 Visser, J.N.J., 1983a. The problems of recognizing ancient subaqueous debris flow deposits
4066 in glacial sequences. Transactions of the Geological Society of South Africa 86, 127-135.

4067 Visser, J.N.J., 1983b. Glacial marine sedimentation in the Late Paleozoic Karoo Basin,
4068 Southern Africa, in: Molnia, B.F. (Ed.), Glacial-Marine Sedimentation. Plenum Press, New
4069 York, pp. 667-701.

4070 Visser, J.N.J., 1987. The palaeogeography of part of southwestern Gondwana during the
4071 Permo-Carboniferous glaciation. Palaeogeography, Palaeoclimatology, Palaeoecology 61,
4072 205-219.

4073 Visser, J.N.J., 1988. A Permo-Carboniferous tunnel valley system east of Barklay West,
4074 Northern Cape Province. South African Journal of Geology 91, 350-357.

Visser, J.N.J., 1989a. The Permo-Carboniferous Dwyka Formation of Southern Africa: deposition by a predominantly subpolar marine ice sheet. Palaeogeography, Palaeoclimatology, Palaeoecology 70, 377-391.

Visser, J.N.J., 1989b. Stone orientation in basal glaciogenic diamictite: four examples from the Permo-Carboniferous Dwyka Formation, South Africa. Journal of Sedimentary Petrology 59, 935-943.

Visser, J.N.J., 1996. A Late Carboniferous subaqueous glacial valley fill complex: Fluctuations in meltwater output and sediment flux. South African Journal of Geology 99, 285-291.

Visser, J.N.J., 1997. Deglaciation sequences in the Permo-Carboniferous Karoo and Kalahari basins of southern Africa: a tool in the analysis of cyclic glaciomarine basin fills. Sedimentology 44, 507-521.

Visser, J.N.J., Hall, K.J., 1985. Boulder beds in the glaciogenic Permo-Carboniferous Dwyka Formation in South Africa. Sedimentology 32, 281-294. https://doi.org/10.1111/j.1365-3091.1985.tb00510.x.

Visser, J.N.J., Kingsley, C.S., 1982. Upper Carboniferous glacial valley sedimentation in the Karoo Basin, Orange Free State. Transactions of the Geological Society of South Africa 85, 71-79.

Visser, J.N.J., Loock, J.C., 1982. An investigation of the basal Dwyka tillite in the southern part of the Karoo Basin, South Africa. Transactions of the Geological Society of South Africa 85, 179-187.

Visser, J.N.J., Loock, J.C., 1988. Sedimentary facies of the Dwyka Formation associated with the Nooitgedacht Glacial Pavements, Barkly West District. South African Journal of Geology 91, 38-48.

Visser, J.N.J., Colliston, W.P., Terblanche, J.C., 1984. The origin of soft-sediment deformation structures in Permo-Carboniferous glacial and proglacial beds, South Africa. Journal of Sedimentary Petrology 54, 1183-1196.

Visser, J.N.J., Loock, J.C., Colliston, W.P., 1987. Subaqueous outwash fan and esker sandstones in the Permo-Carboniferous Dwyka Formation of South Africa. Journal of Sedimentary Petrology 57, 467-478.

Visser, J.N.J., van Niekerk, B.N., van der Merwe, S.W., 1997. Sediment transport of the late Palaeozoic glacial Dwyka Group in the southwestern Karoo Basin. South African Journal of Geology 100, 223-236.

Volkheimer, W., 1969. Palaeoclimatic Evolution in Argentina and Relations with Other Regions of Gondwana, in: Amos, A.J. (Ed.), Gondwana Stratigraphy. IUGS Symposium in Buenos Aires 1967, UNESCO, pp. 551-587.

Von Brunn, V., 1977. A furrowed intratillite pavement in the Dwyka Group of northern Natal. Transactions of the Geological Society of South Africa 80, 125-130.

Von Brunn, V., 1994. Glaciogenic deposits of the Permo-Carboniferous Dwyka Group in the eastern region of the Karoo Basin, South Africa, in: Deynoux, M., Miller, J.M.G., Domack, E.W., Eyles, N., Fairchild, I.J., Young, G.M. (Eds.), Earth´s Glacial Record, Cambridge University Press, Cambridge, pp. 60-69.

Von Brunn, V., 1996. The Dwyka Group in the northern part of Kwazulu/Natal, South Africa: sedimentation during late Palaeozoic deglaciation. Palaeogeography, Palaeoclimatology, Palaeoecology 125, 141-163.

Von Brunn, V., Stratten, T., 1981. Late Paleozoic tillites of the Karoo Basin of South Africa, in: Hambrey, M.J., Harland, W.B. (Eds.), Earth´s Pre-Pleistocene Glacial Record. Cambridge University Press, Cambridge, pp. 71-79.

Von Gaertner, H.R.1943. Bemerkungen über den Tillite von Bigganiargga am Varangerfjord, Geologische Rundschau, 34, 226-231. (Quoted by Bjørlykke, K. 1967. The Eocambrian “Reusch Moraine” at Bigganjargga and the Geology Around Varangerfjord; Northern Norway. Norges Geologiske Undersøkelse 251, Oslo, 18-44.)

Waitt, R.B., 1989. Swift snowmelt and floods (lahars) caused by great pyroclastic surge at Mount St Helens volcano, Washington, 18 May 1980. Bulletin of Volcanology 52, 138-157.

Walters, J.C., 1978. Polygonal Patterned Ground in Central New Jersey. Quaternary Research 10, 42-54.

Walton, A.W., Palmer, B.A., 1988. Lahar facies of the Mount Dutton Formation (Oligocene-Miocene) in the Marysvale Volcanic Field, Southwestern Utah. GSA Bulletin 100, 1078-1091.

Waters, J.M., Craw, D., 2017. Large kelp-rafted rocks as potential dropstones in the Southern Ocean. Marine Geology 391, 13-19.

Watt, S.F.L., Talling, P.J., Vardy, M.E., Masson, D.G., Henstock, T.J., Hühnerbach, V., Minshull, T.A., Urlaub, M., Lebas, E., Le Friant, A., Berndt, C., Crutchley, G.J. , Karstens, J., 2012. Widespread and progressive seafloor-sediment failure following volcanic debris avalanche emplacement: landslide dynamics and timing offshore Montserrat, Lesser Antilles. Marine Geology 323, 69–94.

Whipple, K.X., Hancock, G.S., Anderson, R.S., 2000. River incision into bedrock: Mechanics and relative efficacy of plucking, abrasion and cavitation. GSA Bulletin 112, 490-503. https://doi.org/10.1130/0016-7606(2000)112<490:RIIBMA>2.0.CO;2.

White, W.M., 2015. Isotope geochemistry. John Wiley and Sons, Ltd., Chichester, pp. 277-363.

Whiteside, J.H., Lindström, S., Irmis, R.B., Glasspool, I.J., Schaller, M.F., Dunlavey, M., Nesbitt, S.J., Smith, N.D., Turner, A.H., 2015. Extreme ecosystem instability suppressed

4148 tropical dinosaur dominance for 30 million years. PNAS 112, 7909-7913.
4149 https://doi.org/10.1073/pnas.1505252112.

4150 Wilf, P., Little, S.A., Iglesias, A., Del Carmen Zamaloa, M., Gandolfo, M.A., Cúneo, N.R.,
4151 Johnson, K.R., 2009. Papuacedrus (Cupressaceae) in Eocene Patagonia: a new fossil link to
4152 Australasian rainforests. American Journal of Botany 96, 2031-2047.

4153 Williams, G.E., 2005. Subglacial meltwater channels and glaciofluvial deposits in the
4154 Kimberley Basin, Western Australia: 1.8 Ga low-latitude glaciation coeval with continental
4155 assembly. Journal of the Geological Society 162, 111-124.

4156 Wilson, H.H., 1969. Late Cretaceous eugeosynclinal sedimentation, gravity tectonics, and
4157 ophiolite emplacement in Oman Mountains, Southeast Arabia. AAPG Bulletin 53, 626-671.

4158 Wilson, J.P., White, J.D., Montañez, I.P., DiMichele, W.A., McElwain, J.C., Poulsen, C.J.,
4159 Hren, M.T., 2020. Carboniferous plant physiology breaks the mold. New Phytologist 227,
4160 667-679. https://doi.org/10.1111/nph.16460.

4161 Winterer, E.L., 1964. Late Precambrian pebbly mudstone in Normandy, France: tillite or
4162 tilloid?, in: Nairn, A.E.M. (Ed.), Problems in Palaeoclimatology. John Wiley and Sons,
4163 London, pp. 159-178.

4164 Winterer, E.L., von der Borch, C.C., 1968. Striated pebbles in a mudflow deposit, South
4165 Australia. Palaeogeography, Palaeoclimatology, Palaeoecology 5, 205-211.

Wobus, C.W., Crosby, B.T., Whipple, K.X., 2006. Hanging valleys in fluvial systems: Controls on occurrence and implications for landscape evolution. Journal of Geophys. Research 111, F02017. https://doi.org/10.1029/2005JF000406.

Wohlfarth, B., 2013. A Review of Early Weichselian Climate (MIS 5d-a) in Europe. Technical Report TR-13-03, Svensk Kärnbränslehantering AB, Stockholm. https://skb.se/upload/publications/pdf/TR-13-03.pdf.

Wolfe, J.A., 1977. Paleogene Floras from the Gulf of Alaska Region. U.S. Geological Survey Professional Paper 997. https://doi.org/10.3133/pp997.

Woodcock, N.H., 1979. Sizes of submarine slides and their significance. Journal of Structural Geology 1, 137–142.

Woodworth-Lynas, C.M.T., 1992. The Geology of Ice Scour (Ph.D. thesis). University of Wales, Bangor.

Woodworth-Lynas, C.M.T., 1996. Ice scour as an indicator of glaciolacustrine environments, in: Menzies, J. (Ed.), Past Glacial Environments: Sediments, Forms and Techniques. Butterworth Heinemann, Oxford, pp. 161-178.

Woodworth-Lynas, C.M.T., Dowdeswell, J.A., 1994. Soft-sediment striated surfaces and massive diamicton facies produced by floating ice, in: Deynoux, M., Miller, J.M.G., Domack, E.W., Eyles, N., Fairchild, I.J., Young, G.M. (Eds.), Earth´s Glacial Record. Cambridge University Press, Cambridge, pp. 241-259. https://doi.org/10.1017/CBO9780511628900.019.

Woodworth-Lynas, C.M.T., Guigné, J.Y., 1990. Iceberg scours in the geological record: examples from glacial Lake Agassiz, in: Dowdeswell, J.A., Scource, J.D. (Eds.), Glacimarine Environments: Processes and Sediments. Geological Society, London, Spec. Publ. 53, pp. 217-223.

Woodworth-Lynas, C.M.T., Simms, A., Rendell, C.M., 1985. Iceberg grounding and scouring on the Labrador Continental Shelf. Cold Regions Science and Technology 10, 163-186.

Woolfe, K.J., 1994. Cycles of erosion and deposition during the Permo-Carboniferous glaciation in the Transantarctic Mountains. Antarctic Science 6, 93-104.

Wright, R., Anderson, J.B., Fisco, P.P., 1983. Distribution and association of sediment gravity flow deposits and glacial/glacial-marine sediments around the continental margin of Antarctica, in: Molnia, B.F. (Ed.), Glacial-Marine Sedimentation. Plenum Press, New York, pp. 265-300.

Yang, B., Shi, G.R., Lee, S., Luo, M., 2018. Co-occurrence patterns of ice-rafted dropstones and brachiopods in the Middle Permian Wandrawandian Siltstone of the southern Sydney Basin (southeastern Australia) and palaeoecological implications. Journal of the Geological Society 175, 850-864. https://doi.org/10.1144/jgs2018-010.

Yassin, M.A., Abdullatif, O.M., 2017. Chemostratigraphic and sedimentologic evolution of Wajid Group (Wajid Sandstone): An outcrop analog study from the Cambrian to Permian, SW Saudi Arabia. Journal of African Earth Sciences 126, 159-175.

Yawar, Z., Schieber, J., 2017. On the origin of silt laminae in laminated shales. Sedimentary Geology 360, 22-34.

Ye, Q., Tong, J., Xiao, S., Zhu, S., An, Z., Tian, L., Hu, J., 2015. The survival of benthic macroscopic phototrophs on a Neoproterozoic snowball Earth. Geology 43, 507–510. https://doi.org/10.1130/G36640.1.

Yehle, L.A., 1954. Soil tongues and their confusion with certain indicators of periglacial climate. American Journal of Science 252, 532-546.

Yincan., Y. et al., 2017. Marine Geo-Hazards in China. China Ocean Press, Elsevier Inc., pp. 193-194. https://doi.org/10.1016/B978-0-12-812726-1.00006-1.

Youbi, N., Ernst, R.E., Mitchell, R.N., Boumehdi, M.A., Moume, W.E., Lahna, A.A., Bensalah, M.K., Söderlund, U., Doblas, M., Tassinari, C.C.G., 2021. Preliminary appraisal of a correlation between glaciations and large igneous provinces over the past 720 million years, in: Ernst, R.E., Dickson, A.J., Bekker, A (Eds.), Large Igneous Provinces: A Driver of Global Environmental and Biotic Changes. Geophysical Monograph 255, The American Geophysical Union and John Wiley and Sons, Inc., pp. 169-190. https://doi.org/10.1002/9781119507444.ch8.

Young, G.M., 1981a. The Early Proterozoic Gowganda Formation, Ontario, Canada, in: Hambrey, M.J., Harland, W.B. (Eds.), Earth´s Pre-Pleistocene Glacial Record. Cambridge University Press, Cambridge, pp. 807-812.

Young, G.M., 1981b. Diamictites of the Early Proterozoic Ramsay Lake and Bruce Formations, north shore of Lake Huron, Ontario, Canada, in: Hambrey, M.J., Harland, W.B. (Eds.), Earth´s Pre-Pleistocene Glacial Record. Cambridge University Press, Cambridge, pp. 813-816.

Young, G.M., 2013. Precambrian supercontinents, glaciations, atmospheric oxygenation, metazoan evolution and an impact that may have changed the second half of Earth history. Geoscience Frontiers 4, 247-261.

Young, G.M., Minter, W.E.L., Theron, J.N., 2004a. Geochemistry and palaeogeography of upper Ordovician glaciogenic sedimentary rocks in the Table Mountain Group, South Africa. Palaeogeography, Palaeoclimatology, Palaeoecology 214, 323–345.

Young, G.M., Shaw, C,S.J., Fedo, C.M., 2004b. New evidence favouring an endogenic origin for supposed impact breccias in Huronian (Paleoproterozoic) sedimentary rocks. Precambrian Research 133, 63-74. https://doi.org/10.1016/j.precamres.2004.03.013.

Zaki, A.S., Giegengack, R., 2016. Inverted topography in the southeastern part of the Western Desert of Egypt. Journal of African Earth Sciences 121, 56-61. https://doi.org/10.1016/j.jafrearsci.2016.05.020.

Zaki, A.S., Pain, C.F., Edgett, K.E., Giegengack, R., 2018. Inverted stream channels in the Western Desert of Egypt: Synergistic remote, field observations and laboratory analysis on Earth with applications to Mars. Icarus 309, 105-124. https://doi.org/10.1016/j.icarus.2018.03.001.

4243 Zaki, A.S., Giegengack, R., Castelltort, S., 2020. Inverted channels in the Eastern Sahara –
4244 distribution, formation, and interpretation to enable reconstruction of paleodrainage
4245 networks, in: Herget, J., Fontana, A. (Eds.), Palaeohydrology, Geography of the Physical
4246 Environment. Springer, Cham, pp. 117-134. https://doi.org/10.1007/978-3-030-23315-0_6.

4247 Zaki, A.S., Pain, C.F., Edgett, K.E., Castelltort, S., 2021. Global inventories of inverted
4248 stream channels on Earth and Mars. Earth-Science Reviews 216, 103561.
4249 https://doi.org/10.1016/j.earscirev.2021.103561.

4250 Zalasiewicz, J., Taylor, L., 2001. Deep-basin dropstones in the early Silurian of Wales: a clue
4251 to penecontemporaneous, near-shore algal forests. Proceedings of the Geologists' Association
4252 112, 63-66. https://doi.org/10.1016/S0016-7878(01)80050-X.

4253 Zavala, C., 2019. The new knowledge is written on sedimentary rocks – a comment on
4254 Shanmugam´s paper ´The hyperpycnite problem´. Journal of Palaeogeography 8, 23.
4255 https://doi.org/10.1186/s42501-019-0037-3.

4256 Zavala, C., 2020. Hyperpycnal (over density) flows and deposits. Journal of Palaeogeography
4257 9, 17. https://doi.org/10.1186/s42501-020-00065-x.

4258 Zavala, C., Arcuri, M., 2016. Intrabasinal and extrabasinal turbidites: origin and distinctive
4259 characteristics. Sedimentary Geology 337, 36–54.
4260 https://doi.org/10.1016/j.sedgeo.2016.03.008.

Zecchin, M., Catuneanu, O., Rebesco, M., 2015. High-resolution sequence stratigraphy of clastic shelves IV: High-latitude settings. Marine and Petroleum Geology 68A, 427-437. https://doi.org/10.1016/j.marpetgeo.2015.09.004.

Zimmermann, U., Tait, J., Crowley, Q.G., Pashley, V., Straathof, G., 2011. The Witputs diamictite in southern Namibia and associated rocks: constraints for a global glaciation? International Journal of Earth Sciences, 100, 511-526. https://doi.org/10.1007/s00531-010-0621-3.

Supplementary material: Tables

Place and/or environment	Percentage striated clasts	Interpretation or comment	Reference
Sediment gravity flow	19 of 19 clasts were striated.	One chert and the rest softer sedimentary clasts.	Winterer, 1964.
Sediment gravity flow	Almost 50%.	Ca. 1% of the grains were larger than sand, so one would not expect to find many striated clasts, even if all the striated clasts were sedimentary.	Winterer and von der Borch, 1968.
Tills and "tillites"	1-5% or 10-20%.		Anderson, 1983; Schermerhorn, 1974a.
Carboniferous "glacial" conglomerate	15-20% striated.		Anderson, 1983.
Late Paleozoic, "glaciogenic"	48% striated.	Mostly sub-parallel but also scattered.	Rocha-Campos and Santos, 1981.
Paleoproterozoic "glaciogenic"	Rare striations, and a few clasts that display facets.	Conglomerate above grooved soft sand surfaces.	Williams, 2005.
Carboniferous, "glaciogenic"	5-20% and up to 80%.		Visser, 1982; Hall and Visser, 1984; Visser et al., 1987.

East Antarctica, continental shelf	12% striated.		Anderson, 1983.
Ross Sea shelf area	60% striated or faceted; in redeposited conglomerate 21% were striated and 4% faceted.		Hall, 1989.
Antarctic shelf, McMurdo Sound	57% striated, 80% faceted.		Hall, 1989.
Many different Quaternary	0.1% - 80%, mostly 10-40%.		Atkins, 2003, 2004.

Table S1. Striations on clasts from different environments.

Location in ancient "glacial" environments	Structure, comment	Reference
Very common in pre-Pleistocene diamictites from all ages, worldwide (a, b and c from the list, and these are all displayed by most of these striated surfaces that is referred to).	Soft sediment striations and surfaces, within or on top of sediments, including within "tillites." Striations/grooves on all bedrock surfaces are commonly perfectly parallel.	Bigarella et al., 1967; Lindsay, 1970a; Schermerhorn, 1970, 1971; Fairbridge, 1971; Deynoux and Trompette, 1976; Frakes, 1979; Visser and Loock, 1982; Visser, 1983b; Visser et al., 1987, Deynoux and Ghienne, 2004; Le Heron et al., 2005, 2010, 2018a, 2018b, 2019b, 2020; Keller et al., 2011; Vesely and Assine, 2014, list of 17 places; Rosa et al., 2016, 2019; Molén, 2017; Alonso-Muruaga et al., 2018; Assine et al., 2018; Dietrich and Hofmann, 2019; Caputo and Santos, 2020; Isbell et al., 2021; López-Gamundí et al., 2021; Molén and Smit, 2022.
Common (as described in list, letter d).	Striations and grooves superimposed, stacked, on many beds above each other, commonly in soft sand.	Frakes and Crowell, 1969, 1970; Lindsay, 1970a; Flint, 1975; Deynoux and Trompette, 1976; Von Brunn, 1977; Biju-Duval et al., 1981; Moncrieff and Hambrey, 1988; Visser and Loock, 1988; Visser, 1988, 1989b; Deynoux and Ghienne, 2004; Le Heron et al., 2004, 2005, 2006, 2010, 2018b, 2020; Keller et al., 2011; Vesely and Assine, 2014; Assine et al., 2018; Caputo and Santos, 2020; Molén and Smit, 2022.

South Africa, LPIA (a, b, c, d and e in list.)	Sediment strings turn into grooves or striations. Three of four studied striated surfaces did not display any diamictites in the surrounding areas.	Molén and Smit, 2022.
Brazil, LPIA (a, b, c and f).	Many striated surfaces, the largest covers 2500 m^2. Displaying soft sediment slickensides from sliding (similar to Isbell et al., 2001), flutes and grooved tops of diamictites, sand slumps (interpreted to be from "icebergs"; but compare to Molén and Smit, 2022) and "anastomosing shear planes," inside diamictite or at surfaces.	Rosa et al., 2019.
Brazil, LPIA (a, b, c, d and e).	In one or more triple stacked striated surfaces: Straight, parallel, bypass zones, stacked, small sand flows cover striations, ripples next to striations. Interpreted to be a tidal water glacier.	Trosdtorf et al., 2005a, 2005b.
China (a, b, c, d.)	Bifurcating striae	Le Heron et al., 2018b, 2019a; Chen et al., 2020; compare to Molén and Smit, 2022.
Botswana, LPIA (c in list).	The "original ground moraine" is interpreted to have been "stripped off" from striated surface before mudflows were deposited.	Frakes and Crowell, 1970.
Antarctica, Permian (b, d, e in list).	Soft sediment surfaces are grooved or striated only if a thin veneer of sorted sediment is lying directly on top of the surfaces. At places where the sorted sediment disappear the striations also disappear.	Lindsay, 1970a.

South Africa, LPIA and Sahara, Ordovician (a, b, c, d and e in list).	1) Striations continued unbroken from the top of a "tillite" into the striations on the surface below. 2) Striations passed from lava to a triple stacked soft sediment surface. 3) Thin beds of sand, mud or laminated sediment directly overlying striated surface. 4) Stratigraphy is: Grooved "tillite" surface, mudstone, "tillite." 5) Soft sediment surface cut in ripple laminated siltstone. 6) Fossil plants between striated surface and "tillite." 7) A soft sediment surface, draped with mudrock displaying crustacean track ways, which transforms upwards to diamictite. Comment: All these structures may form by SGFs, but not below glaciers.	1) Flint, 1961. 2) Visser, 1988. 3) Visser, 1988; Visser and Loock, 1988; Deynoux and Ghienne, 2004 (Sahara, Ordovician). 4) Von Brunn, 1977. 5) Visser, 1983b. 6) du Toit, 1926; Sandberg, 1928. 7) Von Brunn, 1996.
Ethiopia, LPIA (b, c and e).	Traction carpet on a polished surface, stacked striated surfaces (but this was not recognized in article, their Fig. 6A.)	Bussert, 2010.
Argentina (b, d).	Intertill and intratill soft sediment surfaces, occasionally tectonic and glacial striations on the same surfaces.	González and Glasser, 2008.
South America in 1-2) LPIA and 3) Upper Precambrian (a, c, g).	1) Striations display the same direction as foliation in underlying gneiss. 2) Slickensides pass straight into the striations on a surface. 3) A 180 000 m^2 surface show parallel "glacial" grooves which occasionally exhibit "overhanging" walls. Comment: Appear to be at least partly tectonic.	1-2) Frakes and Crowell, 1969. 3) Isotta et al., 1969; Frakes, 1979.

Cameroon, Neoproterozoic (a, b, c, d).	Stacked (“staircase”), no glaciogenic deposits, on siltstone and limestone.	Caron et al., 2011.
Sahara, Saudi Arabia, Ordovician (a, b, c, d).	1) Abundance of striations and grooves in spite of the fact that there are very few clasts in the “tillite.” 2) At right angles or oblique to grooves; there are in places minor ripples. 3) Striations within current rippled and laminated sandstone. Comment: Would be possible if the origin is by SGF.	1) Schermerhorn, 1970, 1971. 2) Fairbridge, 1971, 1979. 3) Le Heron et al., 2004.
Saudi Arabia, Ordovician.	One picture shows striations that are very irregular. Comment: These display similarities to striations made by volcanic flows or tectonic movements (e.g., Pierson et al., 1990, Rainbird 1993, Glicken 1996, Eyles and Boyce 1998, Atkins 2003).	Keller et al., 2011, their Fig 12e.
West Africa, Late Precambrian (e).	One 1 cm layer of sandstone with ripple-marks is interposed in between the “tillite” and the striated surface. Comment: This can be suspected from deposition of debris flows in water.	Trompette, 1981.
Canada, Gowganda Fm, Paleoproterozoic (g).	Striated surfaces and boulders are probably of tectonic origin.	Bielenstein and Eisbacher, 1969; Harker and Giegengack, 1989; Miall, 1985.
Canada and South America, Precambrian.	Occasionally the “tillite” is stratified immediately above the surfaces. Comment: This indicates deposition from SGFs.	Schenk, 1965; Isotta et al., 1969.

Australia, Paleoproterozoic.	Comment: Some believe that these surfaces are tectonic, others that they are partially tectonic and partially glacial.	Daily et al., 1973; Coats and Preiss, 1987.
Australia, Late Proterozoic (c).	Grooves etc. in soft sediment sand are interpreted to be formed by meltwater or glaciers. Conglomerate deposited on top of the sand display the same transport direction as the grooves. No evidence of any other glaciogenic proxies. Comment: Except for a few examples, similar grooves do not form by meltwater and glaciers, but all may be from SGFs.	Williams, 2005.
Chile, Cretaceous.	Surface/contact zone exhibit both striations and ripple-marks. Comment: Has been reinterpreted as formed by turbidity currents or mudflows.	Cecioni, 1957, 1981; Sanders and Cecioni, 1957; Scott, 1966.
Norway, Late Proterozoic.	2 mm push up rinds around striations, recently weathered out clasts, mud-flake imprints. Comment: 1) The evidence suggests a soft surface. Point 2-4 below are explanations based on a glaciogenic interpretation. 2). "... the striated platform (...) is c. 150 Ma older than the overlying diamictite." 3) Quick melting and "instantaneous" lithification at a temperature > 1000°C. 4) A piece of till dropped from an iceberg and landed on top of the striations.	1) Molén, 2017. 2) Rice and Hofmann, 2000. 3) Bestmann et al., 2006. 4) Mentioned by Bjørlykke, 1967; as interpreted by von Gaertner, 1943.
Worldwide.	Glaciogenic striations. Displaying changing vertically and horizontally movement directions.	Not clearly documented before the Pleistocene.

Table S2. Striated surfaces/pavements which are all commonly interpreted to be from glaciation. All these surfaces conform well with an origin from mass transport, mainly from cohesive SGFs, but not with a glaciogenic origin. The table is not documenting every single occurrence of any surface structure from all mentioned areas, because then it would be very extensive. Some striated surfaces are referred to in more than one row, if many features are documented. The letters, a-g, are the criteria described in the list in section 2.5.

Place	Age	1/3-2/3 penetration	Small size of dropstones (cm)	Small compared to other sediments size of dropst	Clasts within single bed	Correlation between clast on and sediment thickness es	Fabrics transport in	Faltering horizontal movements of sediments	Push structures of currents next to clast	Sediment thickens next to clasts	Dilation out much penetrated	Reference and/or lasts but not around
		a	b	b	c	d	e	f	f, g	f, g	f, g	
Brazil	LPIA	N	<1 to 40	Y	Y					Y	Y	1
Argen- tina	LPIA	N			Y			Y		Y	Y	2
Ethiopia	LPIA	N	Often cm		Y					Y	Y	3
Malaysia	LPIA	N	0.5-20							Y	Y	4
S-Africa, Namibia	LPIA	N	>2-5, but > meter	Y	Y					Y	Y	5
Brazil	Dev	N	2							Y		6
China	Cam	N	Few cm				Y		Y	Y	Y	7
China	Neo	N	Y	Y							Y	8
Namibia	Neo	N	Y (N)	Y (N)	Y	Y		Y		Y	Y	9
Namibia	Neo	N			Y			Y	Y	Y	Y	10
Namibia	Neo	N	Y		Y					Y	Y	11
Namibia	Neo	N	< 2	Y	Y			Y		Y	Y	12
Scotland	Neo	N	3.5-9		Y		Y			Y	Y	13
Canada	Neo	N	most 1-4	Y	Y	Y		Y	Y	Y	Y	14

Tasma-nia	Neo	N	most cm	Y							Y	15
India	Pal	N	Few cm			Y						16

Table S3. The table document examples of areas displaying clasts from pre-Pleistocene formations which had been interpreted as glaciogenic dropstones in the papers which are referred to, or in the majority of published papers describing the same formation. Lonestones from sedimentary sequences which have been fully explained as from SGFs, even if there may be some different opinions, are not in the table. Often reports of dropstones only mention just that word. In other reports only superficial similarities between dropstones and observed clast are mentioned, and commonly there are no detailed descriptions of the clasts which are interpreted to be dropstones. Therefore, it is difficult to find extensive data for this table, and some interpretations may be conjectural, only because too little data have been documented in the original reports. In the table appearances of dropstones which may not be mentioned in the original publication, but which are evident from published photographs, are tabulated.

Examples of appearances of dropstones and sedimentary structures displayed around these clasts, from each research area, are documented in the different columns of the table. Not all lonestones from each area display all the apperances documented (which would be impossible), but may be predominant examples. The letters a-g in the columns refers to the descriptions in the list of features, with comments (section 2.13.3.). There may be clasts in the research areas which may display appearances that are compatible with any kind of transport, but the tabulated structures are those better compatible with transport by SGFs but less common or highly implausible from simple rafting in slowly moving or standing water. The data in the table do not show examples of exceptions of single or a few clasts which may have been deposited by any agent, if there is an abundance of clasts. Instead, the documented clasts

display the structures which may be in majority, or are otherwise reported in the referred articles, or possible only are photographed as typical for the area or formation. Therefore the table is partly conjectural and does not display definite documentation from each area. And further, the documentation from the different research areas does not include all data which may be of relevance, e.g., not the difference between the clast size of dropstones compared to clast size in other sediments, or other features which could be documented in the table, because such data is seldom published.

Despite the shortcomings in the documentation from different research areas, the sedimentary structures in the table are more or less incompatible with an interpretation of simple rafting by ice or any other rafting agent. It is possible to draw the conclusion that too many clasts have been reported as dropstones even if the full evidence for this interpretation is not available. In conclusion, the data in the table are as well documented as the descriptions provided in the original reports and therefore may be possible to use in evaluation of different interpretations.

Dev = Devonian.

Cam = Cambrian.

Neo = Neoproterozoic.

Pal = Paleoproterozoic.

N = Not documented as present. (Within paranthesis = exceptions.)

Y = Documented, present.

No sign = not mentioned or shown in the original publications.

References: 1. Aquino et al, 2016; Vesley et al., 2018, 2021; Tedesco et al., 2020. 2. Schatz et al., 2011; Valdez Buso et al., 2021. 3. Bussert, 2014. 4. Baioumy, et al., 2020. 5. Commonly 2-5 cm, rarely up to one meter, but in massive “glaciomarine” diamictites they may be a few meters. Visser, 1982, 1983b; Visser and Kingsley, 1982; Tavener-Smith and Mason, 1983; Haldorsen et al., 2001; Isbell et al., 2021. 6. Caputo and Santos, 2020. 7. Le Heron et al., 2018b. 8. Chen et al., 2021. 9. Hoffman and Halversen, 2008; Hoffman et al., 2021 (Ghaub). 10. Domack and Hoffman, 2011 (Ghaub). 11. Bechstädt et al., 2018 (Ghaub). 12. Hoffman and Halversen, 2008; Le Heron et al., 2021a (Chuos); see also Martin et al., 1985. 13. Hartley et al., 2020. 14. Molén, 2021. 15. Hoffman et al., 2009. 16. Rodríguez-López et al., 2021.